

Chulalongkorn University

## Chula Digital Collections

---

Chulalongkorn University Theses and Dissertations (Chula ETD)

---

2022

### Simulation study on co2 enhanced oil recovery for offshore area in Thailand

Pariwat Wongsriraksa  
*Faculty of Engineering*

Follow this and additional works at: <https://digital.car.chula.ac.th/chulaetd>



Part of the [Geological Engineering Commons](#), [Mining Engineering Commons](#), and the [Petroleum Engineering Commons](#)

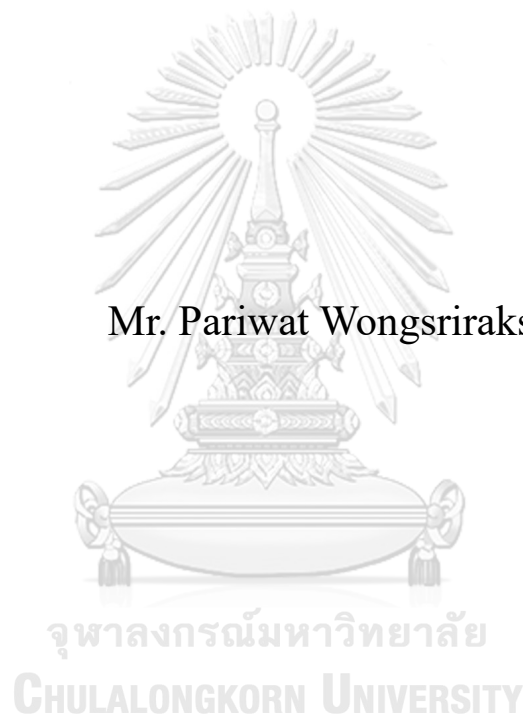
---

#### Recommended Citation

Wongsriraksa, Pariwat, "Simulation study on co2 enhanced oil recovery for offshore area in Thailand" (2022). *Chulalongkorn University Theses and Dissertations (Chula ETD)*. 5885.  
<https://digital.car.chula.ac.th/chulaetd/5885>

This Thesis is brought to you for free and open access by Chula Digital Collections. It has been accepted for inclusion in Chulalongkorn University Theses and Dissertations (Chula ETD) by an authorized administrator of Chula Digital Collections. For more information, please contact [ChulaDC@car.chula.ac.th](mailto:ChulaDC@car.chula.ac.th).

# SIMULATION STUDY ON CO<sub>2</sub> ENHANCED OIL RECOVERY FOR OFFSHORE AREA IN THAILAND



Mr. Pariwat Wongsriraksa

A Thesis Submitted in Partial Fulfillment of the Requirements  
for the Degree of Master of Engineering in Georesources and Petroleum  
Engineering  
Department of Mining and Petroleum Engineering  
FACULTY OF ENGINEERING  
Chulalongkorn University  
Academic Year 2022  
Copyright of Chulalongkorn University

การศึกษาการจำลองการเพิ่มการผลิตน้ำมัน โดยใช้คาร์บอนไดออกไซด์สำหรับพื้นที่นอกชายฝั่งใน  
ประเทศไทย



นายปรีวัฒน์ วงษ์ศรีรักษา

วิทยานิพนธ์นี้เป็นส่วนหนึ่งของการศึกษาตามหลักสูตรปริญญาวิศวกรรมศาสตรมหาบัณฑิต  
สาขาวิชาวิศวกรรมทรัพยากรธรณีและปิโตรเลียม ภาควิชาวิศวกรรมเหมืองแร่และปิโตรเลียม  
คณะวิศวกรรมศาสตร์ จุฬาลงกรณ์มหาวิทยาลัย  
ปีการศึกษา 2565  
ลิขสิทธิ์ของจุฬาลงกรณ์มหาวิทยาลัย

Thesis Title	SIMULATION STUDY ON CO <sub>2</sub> ENHANCED OIL RECOVERY FOR OFFSHORE AREA IN THAILAND
By	Mr. Pariwat Wongsriraksa
Field of Study	Georesources and Petroleum Engineering
Thesis Advisor	Associate Professor KREANGKRAI MANEEINTR, Ph.D.

---

Accepted by the FACULTY OF ENGINEERING, Chulalongkorn University  
in Partial Fulfillment of the Requirement for the Master of Engineering

..... Dean of the FACULTY OF  
ENGINEERING  
(Professor SUPOT TEACHAVORASINSKUN, D.Eng.)

THESIS COMMITTEE

..... Chairman  
(THOTSAPHON CHAIANANSUTCHARIT, Ph.D.)  
..... Thesis Advisor  
(Associate Professor KREANGKRAI MANEEINTR, Ph.D.)  
..... External Examiner  
(Witsarut Thungsuntonkhun, Ph.D.)



จุฬาลงกรณ์มหาวิทยาลัย  
CHULALONGKORN UNIVERSITY

ปริญญ์ วงษ์ศรีรักษา : การศึกษาการจำลองการเพิ่มการผลิตน้ำมันโดยใช้คาร์บอนไดออกไซด์สำหรับพื้นที่นอกชายฝั่งใน  
ประเทศไทย. ( SIMULATION STUDY ON CO<sub>2</sub> ENHANCED OIL RECOVERY  
FOR OFFSHORE AREA IN THAILAND) อ.ที่ปรึกษาหลัก : รศ. ดร.เกรียงไกร มณีอินทร์

เชื้อเพลิงฟอสซิลถูกนำมาใช้กันอย่างแพร่หลายทั่วโลก ทำให้เกิดก๊าซคาร์บอนไดออกไซด์ ซึ่งเป็นหนึ่งในสาเหตุหลักของการเปลี่ยนแปลงสภาพภูมิอากาศและภาวะโลกร้อน เทคโนโลยีหนึ่งที่ใช้ได้จริงเพื่อลดการปล่อย ก๊าซคาร์บอนไดออกไซด์คือ การดักจับ การใช้ประโยชน์ และการกักเก็บคาร์บอน (ซีซียูเอส) ซึ่งรวมถึงการใช้ ก๊าซคาร์บอนไดออกไซด์สำหรับการผลิตน้ำมันเพิ่ม (ซีโอทูอีโออาร์) และการกักเก็บในแหล่งกักเก็บทางธรณีวิทยา ในเมืองไทย แหล่งกักเก็บทางธรณีวิทยาที่มีศักยภาพสำหรับการเพิ่มการผลิตน้ำมันโดยใช้คาร์บอนไดออกไซด์ก็มี เนื่องจากคุณสมบัติของน้ำมันดิบ ความลึกของแหล่งกักเก็บ และความอืดของน้ำมัน โดยเฉพาะในอ่าวไทย อย่างไรก็ตามบริเวณอ่าวไทยที่มีอุณหภูมิสูงขึ้น เป็นผลให้ความดันต่ำสุดที่ทำให้คาร์บอนไดออกไซด์ละลายได้ (เอ็มเอ็มที) เพิ่มขึ้น ดังนั้น การศึกษานี้จึงเป็นกระบวนการละลายก๊าซคาร์บอนไดออกไซด์บางส่วน โดยที่ผ่านมาการศึกษาในเรื่องการเพิ่มการผลิตน้ำมันโดยใช้คาร์บอนไดออกไซด์ ในประเทศไทยไม่ค่อยมีการศึกษาเท่าที่ควรจึงทำให้การกำหนดตัวแปรที่เหมาะสมทำได้ลำบาก รวมถึง อัตราการฉีดของของไหล และความดันของแหล่งกักเก็บขณะ ที่ทำการอัดฉีดสำหรับกระบวนการเพิ่มการผลิตน้ำมัน โดยใช้คาร์บอนไดออกไซด์ การศึกษานี้มีวัตถุประสงค์เพื่อประเมินความเป็นไปได้ของ การเพิ่มการผลิตน้ำมันโดยใช้คาร์บอนไดออกไซด์ในแหล่งกักเก็บน้ำมันเบา ในพื้นที่นอกชายฝั่งโดยประยุกต์ใช้ข้อมูลจริงจากพื้นที่เพื่อสร้างเป็นแบบจำลองแหล่งกักเก็บ 3 มิติแบบวิวิธพันธ์ และใช้ในการจำลองการเพิ่มการผลิตน้ำมันโดยใช้คาร์บอนไดออกไซด์การศึกษานี้ใช้เทคโนโลยีการเพิ่มการผลิตน้ำมันโดยใช้คาร์บอนไดออกไซด์สองแบบคือ การอัดฉีดคาร์บอนไดออกไซด์เพียงอย่างเดียว และการอัดฉีดคาร์บอนไดออกไซด์สลับกับน้ำ (ดับบลิวเอจี) ภายใน 24 ปีของการผลิต ความดันที่ทำให้แหล่งกักเก็บแตกถูกคำนวณและถูกพิจารณาเพื่อป้องกันการแตกของแหล่งกักเก็บขณะทำการอัดฉีดของเหลวแทนที่ โดยทั้งสองตัวแปรหลักที่ศึกษาคืออัตราการอัดฉีดและความดันของแหล่งกักเก็บขณะ ที่ทำการอัดฉีด

ผลของการศึกษาแสดงให้เห็นว่า การอัดฉีดคาร์บอนไดออกไซด์สลับกับน้ำที่มีอัตราการอัดฉีดคาร์บอนไดออกไซด์สูงสุดที่ 0.8 ล้านลูกบาศก์ฟุตมาตรฐานต่อวัน และน้ำที่ 500 บาร์เรลของถังเก็บ/วัน และที่ความดันของแหล่งกักเก็บขณะทำการอัดฉีดที่ 90% ของความดันที่ทำให้แหล่งกักเก็บแตกสามารถผลิตน้ำมันดิบได้สูงสุด โดยมีค่าตัวแปรที่ใช้บังคับอัตราส่วนของน้ำมันดิบที่สามารถนำขึ้นมาใช้ได้ 48.1% และมีการผลิตน้ำมันดิบรวมสูงสุดที่ 550,497 บาร์เรลของถังเก็บ อย่างไรก็ตาม การผลิตน้ำมันดิบรวมของเทคโนโลยีการอัดฉีดคาร์บอนไดออกไซด์สลับกับน้ำดังกล่าวส่งผลให้มีการผลิตน้ำมันออกมาด้วยเป็นจำนวนมาก ในทางตรงข้าม การอัดฉีดคาร์บอนไดออกไซด์เพียงอย่างเดียว ที่อัตราสูงสุดที่ 0.8 ล้านลูกบาศก์ฟุตมาตรฐานต่อวัน และที่ความดันของแหล่งกักเก็บขณะทำการอัดฉีดที่ 90% ของความดันที่ทำให้แหล่งกักเก็บแตกสามารถผลิตน้ำมันดิบที่ค่าตัวแปรที่ใช้บังคับอัตราส่วนของน้ำมันดิบที่สามารถนำขึ้นมาใช้ได้ 43.1% และการผลิตน้ำมันทั้งหมดที่ 492,893 บาร์เรลของถังเก็บ แต่น้ำที่ผลิตได้กลับลดลงตามอัตราการผลิต สุดท้ายนี้ แม้ว่าพื้นที่ที่ทำการศึกษานี้มีอุณหภูมิใต้พื้นดินที่สูง เป็นเหตุให้กระบวนการผลิตเป็นแบบที่มีการละลายคาร์บอนไดออกไซด์เพียงบางส่วน แต่ผลของการศึกษานี้สามารถนำไปสู่การใช้ประโยชน์จากคาร์บอนไดออกไซด์จากแหล่งผลิตเพื่อการผลิตน้ำมันเพิ่มมากขึ้นและเพื่อกักเก็บคาร์บอนในพื้นที่ที่มีศักยภาพเพื่อทำให้ประเทศไทยเข้าถึงความเป็นกลางของคาร์บอนได้ในอนาคต

สาขาวิชา วิศวกรรมทรัพยากรธรณีและปิโตรเลียม  
ปีการศึกษา 2565

ลายมือชื่อนิสิต .....  
ลายมือชื่อ อ.ที่ปรึกษาหลัก .....

# # 6470807221 : MAJOR GEORESOURCES AND PETROLEUM ENGINEERING

KEYWORD: ENHANCED OIL RECOVERY / CO<sub>2</sub> FLOODING / WAG /  
HETEROGENEOUS / OIL RECOVERY FACTOR / CO<sub>2</sub> UTILIZATION /  
THE GULF OF THAILAND / SIMULATION

Pariwat Wongsriraksa : SIMULATION STUDY ON CO<sub>2</sub> ENHANCED OIL  
RECOVERY FOR OFFSHORE AREA IN THAILAND. Advisor: Assoc. Prof.  
KREANGKRAI MANEEINTR, Ph.D.

Fossil fuels are widely used all over the world. It generates carbon dioxide (CO<sub>2</sub>) which is one of the main causes for climate change and global warming. One practical technology to reduce CO<sub>2</sub> emission is carbon capture, utilization, and storage (CCUS) which includes the use of CO<sub>2</sub> for enhanced oil recovery (CO<sub>2</sub>EOR) and storage in the geological reservoir. In Thailand, there are some potential geological reservoirs for CO<sub>2</sub>EOR due to crude properties, depth of the reservoir and oil saturation, especially in the Gulf of Thailand. However, the high temperatures gradient in the Gulf of Thailand can lead to higher minimum miscibility pressure (MMP). Consequently, this study becomes partial CO<sub>2</sub> miscible process. Previous studies on this issue in Thailand are rarely available and it becomes more difficult to determine appropriate parameters including injection rate and operating pressure for the CO<sub>2</sub>EOR processes. This study aims to evaluate the possibility of CO<sub>2</sub>EOR in the presuming light oil reservoir in the offshore area by applying the real data from the area, a 3-D heterogeneous reservoir model is created and used in the CO<sub>2</sub>EOR simulations. This study uses two CO<sub>2</sub>EOR technologies which are CO<sub>2</sub> flooding and water alternating gas (WAG) within 24 years of production. The fracture pressure is calculated and considered to prevent the reservoir fracture whilst injecting displacing fluid. The two main parameters studied are the injection rate and operating pressure.

The results present that WAG method with the highest injection rate of both CO<sub>2</sub> at 0.8 MMSCF/day and water at 500 STB/day as well as operating pressure at 90% of fracture pressure can produce oil with the highest recovery factor at 48.1% and total oil production at 550,497 STB. However, the highest total oil production comes with the high amount of produced water. On the other hands, CO<sub>2</sub> flooding with the highest CO<sub>2</sub> injection rate at 0.8 MMSCF/day and the highest operating pressure at 90% of fracture pressure produces oil with lower recovery factor at 43.1% and total oil production at 492,893 STB but the produced water declines along with the production rate. Lastly, although this study area has high temperature which causes the process to be partially CO<sub>2</sub> miscible, the results of the study can contribute to utilize CO<sub>2</sub> from the source for more oil production and to store carbon for the potential site to reach Thailand's carbon neutrality in the future.

Field of Study:	Georesources and Petroleum Engineering	Student's Signature .....
Academic Year:	2022	Advisor's Signature .....

## ACKNOWLEDGEMENTS

I appreciate to my thesis advisor Associate Professor Dr. Kreangkrai Maneeintr of the Department of Mining and Petroleum Engineering, Chulalongkorn university for his excellent support, valuable guidance, useful direction and supportive encouragement from the beginning until the accomplishment the goals of this study. Without all of his support and assist, I could not accomplish the goals of this study. In addition, I am grateful to the chairperson Dr. Thotsaphon Chaianansucharit and external committee member Dr. Witsarut Thungsuntongkhun for their most kindly comments, recommendations and encouragement.

I am grateful to Dr. Sarawut Kaewtathip Director General , Dr. Supalak Parn-anurak Deputy Director General and its scholarship committee of the Department of Mineral Fuels, Minister of Energy to give me a full scholarship for study in Master degree of Mining and Petroleum Engineering, Faculty of Engineering, Chulalongkorn university as well as the supporting data in the gulf of Thailand for this study. Moreover, I appreciate to Mr. Warakorn Brahmopala Inspector General of the Minister of Energy to have me a chance to apply the scholarship, an excellent drive and a great advising.

Finally, I extend gratitude to my family, especially my wife, my daughter and my parents for supporting and encouragement. Thank you to all who are not mentioned but involved in this study.

จุฬาลงกรณ์มหาวิทยาลัย  
CHULALONGKORN UNIVERSITY

Pariwat Wongsriraksa

## TABLE OF CONTENTS

	Page
ABSTRACT (THAI) .....	iii
ABSTRACT (ENGLISH) .....	iv
ACKNOWLEDGEMENTS .....	v
TABLE OF CONTENTS .....	vi
LIST OF FIGURES .....	1
LIST OF TABLES .....	4
LIST OF ABBREVIATIONS .....	5
CHAPTER 1 .....	7
INTRODUCTION .....	7
1.1 Background .....	7
1.2 Sources of Carbon Dioxide (CO <sub>2</sub> ) .....	9
1.3 Enhance Oil Recovery Method .....	10
1.4 Study area .....	18
1.5 Research Objective .....	19
CHAPTER 2 .....	20
THEORIES AND LITERATURE REVIEW .....	20
2.1 Carbon Dioxide (CO <sub>2</sub> ) Properties .....	20
2.1.1 Supercritical CO <sub>2</sub> .....	20
2.1.2 Viscosity of CO <sub>2</sub> .....	21
2.2 CO <sub>2</sub> Enhance Oil Recovery .....	22
2.2.1 CO <sub>2</sub> Flooding Enhance Oil Recovery mechanism .....	22
2.2.2 Water Alternating Gas (WAG) .....	26
2.2.3 CO <sub>2</sub> Enhance Oil Recovery Projects .....	28
2.3 CO <sub>2</sub> Trapping Mechanism .....	32



2.3.1 Structural or stratigraphic trapping.....	33
2.3.2 Residual trapping.....	33
2.3.3 Solubility trapping.....	33
2.3.4 Mineral trapping .....	34
2.4 Pressure.....	34
2.4.1 Fracture pressure .....	34
2.4.2 Minimum miscibility pressure (MMP).....	37
2.5 CO <sub>2</sub> storage capacity .....	42
2.6 Determination of Candidate Wells for CO <sub>2</sub> Enhance Oil Recovery.....	45
2.7 Literature Review .....	46
CHAPTER 3 .....	52
SIMULATION .....	52
3.1 Reservoir simulation program .....	52
3.2 Geological data in the Gulf of Thailand .....	52
3.2.1 Crude oil composition and PVT properties .....	54
3.3 Simulation Model .....	55
3.3.1 Heterogenous reservoir model.....	56
3.3.2 CO <sub>2</sub> injection condition at wellhead.....	58
3.3.3 Well completion.....	59
3.4 Research methodology .....	59
CHAPTER 4 .....	63
RESULTS AND DISCUSSION.....	63
4.1 Reservoir depletion.....	64
4.2 Simulation results of CO <sub>2</sub> EOR.....	67
4.2.1 Results of CO <sub>2</sub> flooding technology .....	68
4.2.2 Result of water alternating gas (WAG) technology.....	77
4.2.3 CO <sub>2</sub> flooding and WAG comparison .....	87
4.3 Fluid movement in heterogeneous reservoir .....	91
4.3.1 The results in on 2-D cross-section .....	91

4.3.2 The results on 3-D reservoir model .....	97
CHAPTER 5 .....	100
CONCLUSIONS AND RECOMMENDATION .....	100
5.1 Conclusions .....	100
5.2 Recommendation .....	101
REFERENCES .....	102
VITA .....	110



## LIST OF FIGURES

Figure 1.1 Atmospheric CO <sub>2</sub> Level at Mauna Loa Observatory, Hawaii, USA (Nasa, 2022) .....	7
Figure 1.2 Global greenhouse gas emissions by Gas (EPA, 2022).....	8
Figure 1.3 Global CO <sub>2</sub> Emissions from fossil fuel combustion and some industrial processes (EPA, 2022) .....	8
Figure 1.4 The Carbon Dioxide (CO <sub>2</sub> ) emissions from electricity and heat production by fuel and share by fuel, 2000 – 2021 (IEA, 2022).....	10
Figure 1.5 Cyclic steam stimulation (CCS) (Thomas, 2008).....	12
Figure 1.6 Carbon Dioxide (CO <sub>2</sub> ) flooding (Buchanan et al, 2008).....	14
Figure 1.7 Enhanced oil recovery (EOR) method .....	17
Figure 2.1 Carbon dioxide phase diagram (Voormeij and Simandl, 2003) .....	21
Figure 2.2 Variation of CO <sub>2</sub> viscosity as a function of temperature and pressure (Bachu, 2013).....	22
Figure 2.3 The CO <sub>2</sub> miscible process showing the transition zone between the injector and production well (Verma, 2015) .....	26
Figure 2.4 The WAG schematic (Nunez-Lopez and Moskal, 2019).....	27
Figure 2.5 Overburden gradient and depth cross (Kananithikorn and Songsaeng, 2021) .....	36
Figure 2.6 The back – calculated Poisson’s ratio and depth (Kananithikorn and Songsaeng, 2021).....	36
Figure 3.1 Major tectonic subdivisions in Thailand (Charusiri and Pum-Im, 2009) .....	53
Figure 3.2 The calculated result of PVT property curve.....	55
Figure 3.3 X, Y and Z direction distance in this study .....	56
Figure 3.4 Porosity distribution in 3D model .....	57
Figure 3.5 Permeability distribution in 3D model .....	58
Figure 3.6 Working flow chart of methodology of this study.....	62
Figure 4.1 Total original oil in place in this study .....	63
Figure 4.2 Profile of reservoir pressure .....	64

Figure 4.3	Total oil production in primary recovery stage .....	65
Figure 4.4	Recovery factor in primary recovery stage .....	65
Figure 4.5	Oil production rate per day in primary recovery stage .....	66
Figure 4.6	Water production rate per day in primary recovery stage .....	66
Figure 4.7	The water cut in primary recovery stage .....	66
Figure 4.8	Total oil production of CO <sub>2</sub> flooding for case 1 to 6 .....	70
Figure 4.9	Recovery factor of CO <sub>2</sub> flooding for Case 1 to 6 .....	70
Figure 4.10	Remaining oil in place of CO <sub>2</sub> flooding for Case 1 to 6 .....	71
Figure 4.11	Oil production rate of CO <sub>2</sub> flooding for Case 1 to 6 .....	72
Figure 4.12	Water production rate of CO <sub>2</sub> flooding for Case 1 to 6 .....	73
Figure 4.13	Water cut of CO <sub>2</sub> flooding for Case 1 to 6 .....	73
Figure 4.14	Reservoir pressure of CO <sub>2</sub> flooding (case 1 to 6) .....	74
Figure 4.15	Total CO <sub>2</sub> injection of CO <sub>2</sub> flooding cases .....	75
Figure 4.16	Gas oil ratio (GORs) of CO <sub>2</sub> flooding cases .....	76
Figure 4.17	Total oil production of WAG for Case 7 to 14 .....	78
Figure 4.18	Recovery factor of WAG for Case 7 to 14 .....	79
Figure 4.19	Remaining oil in place of WAG for Case 7 to 14 .....	79
Figure 4.20	Oil production rate of WAG for Case 7 to 14 .....	81
Figure 4.21	Water production rate of WAG for Case 7 to 14 .....	82
Figure 4.22	Water cut of WAG for Case 7 to 14 .....	82
Figure 4.23	Reservoir pressure of WAG for Case 7 to 14 .....	83
Figure 4.24	Total CO <sub>2</sub> injection of WAG cases .....	84
Figure 4.25	Total water injection of WAG cases .....	85
Figure 4.26	Gas oil ratio (GOR) of WAG cases .....	86
Figure 4.27	Top 3 ranking in recovery factor term including the best case of CO <sub>2</sub> flooding .....	88
Figure 4.28	Oil production rate of top 3 rank of recovery factor .....	89
Figure 4.29	Water production rate of top 3 rank of recovery factor .....	89
Figure 4.30	Water cut of top 3 rank of recovery factor .....	90

Figure 4.31 Reservoir pressure profile of top 3 rank of recovery factor .....	91
Figure 4.32 CO <sub>2</sub> movement on top view of reservoir of the CO <sub>2</sub> flooding for Case 6 .....	93
Figure 4.33 CO <sub>2</sub> movement inside view in 2-D cross-section of CO <sub>2</sub> flooding for Case 6.....	94
Figure 4.34 CO <sub>2</sub> movement on top view of reservoir of the WAG for Case 14 .....	95
Figure 4.35 CO <sub>2</sub> and water movement inside view in 2-D cross-section of WAG for Case 14.....	96
Figure 4.36 CO <sub>2</sub> movement in 3-D reservoir model CO <sub>2</sub> flooding case 6 .....	97
Figure 4.37 CO <sub>2</sub> and water movement in 3-D reservoir model WAG case 14 .....	98



## LIST OF TABLES

Table 2.1 CO <sub>2</sub> geological storage trapping mechanisms (Zhong et al, 2018).....	32
Table 2.2 Summary of MMP (MPa) and relative error predicted by experimental and different empirical correlation (Li et al, 2021) .....	42
Table 2.3 Technical Screening Guidelines for CO <sub>2</sub> Flooding (Meyer, 2007) .....	46
Table 3.1 Fundamental reservoir data in offshore area in the Gulf of Thailand .....	54
Table 3.2 The oil compositions .....	55
Table 3.3 Using reservoir properties for model construction .....	57
Table 3.4 The studied parameter .....	61
Table 4.1 Results of oil production at the end of primary production .....	67
Table 4.2 Production data at the end of primary production.....	67
Table 4.3 Studied cases .....	68
Table 4.4 CO <sub>2</sub> flooding technology cases .....	69
Table 4.5 Total oil production and recovery factor at the end of simulation of CO <sub>2</sub> flooding for 24 years .....	69
Table 4.6 Remaining oil in place from CO <sub>2</sub> flooding case .....	72
Table 4.7 Total CO <sub>2</sub> injection volume of CO <sub>2</sub> flooding cases .....	75
Table 4.8 WAG technology cases .....	77
Table 4.9 Total production and recovery factor at the end of simulation of WAG for 24 years .....	78
Table 4.10 Remaining oil in place volume of WAG case .....	80
Table 4.11 The total CO <sub>2</sub> and water injection volume of WAG cases .....	84
Table 4.12 Total oil production and recovery factor .....	87

## LIST OF ABBREVIATIONS

°API	Degree American Petroleum Institute
ASP	Alkali Surfactant Polymer
BBL	Barrel
BHFP	Bottom Hole Flowing Pressure
°C	Degree Celsius
CMP	Conference of the Parties serving as the meeting of the Parties to the Kyoto Protocol
CO <sub>2</sub> EOR	Carbon Dioxide Enhanced Oil Recovery
COP	Conference of the Parties
CCUS	Carbon Capture Utilization and Storage
CH <sub>4</sub>	Methane
C <sub>3</sub> H <sub>8</sub>	Propane
C <sub>4</sub> H <sub>10</sub>	Pentane
Cp	Centipoise
CSS	Cyclic Steam Stimulation
DMF	Department of Mineral Fuels
EOR	Enhanced Oil Recovery
EPA	Environmental Protection Agency
°F	Degree Fahrenheit
GHG	Greenhouse Gas
FCM	First Contact Miscible
FT	Feet
GOR	Gas Oil Ratio
Gt	Gigaton
H <sub>2</sub>	Hydrogen
HC	Hydrocarbon Gas
HCO <sub>3</sub> <sup>-</sup>	Bicarbonate Ion
HCPV	Hydrocarbon Pore Volume
H <sub>2</sub> S	Hydrogen Sulfide
IEA	International Energy Agency

IFT	Interfacial Tension
IPCC	Intergovernmental Panel on Climate Change
°K	Degree Kelvin
Kg/m <sup>3</sup>	Kilogram per Cubic Meter
LWD	Logging While Drilling
M	Thousand (1,000 of petroleum unit)
m	Meter
MCM	Multiple Contacts Miscible
mD	Millidarcy
MEOR	Microbial Enhanced Oil Recovery
MMP	Minimum Miscibility Pressure
Mpa	Megapascal
N <sub>2</sub>	Nitrogen
NETL	National Energy Technology Laboratory
OBV	Overburden pressure
OOIP	Original Oil in place
psi	Pound per square inch
PV	Pore Volume
PVT	Pressure-Volume-Temperature
PWD	Pressure While Drilling
RF	Recovery Factor
SACROC	Scurry Area Canyon Reef Operators Committee
SCF	Standard Cubic Feet
SCF/STB	Standard Cubic Feet per Stock Tank Barrel
STB	Stock Tank Barrel
STOIP	Stock Tank Oil Initially in place
SWAG	Simultaneous Water Alternating Gas
TVDSS	True Vertical Depth Subsea
WAG	Water Alternating Gas



## CHAPTER 1

### INTRODUCTION

#### 1.1 Background

Since the 18<sup>th</sup> century, the human activities have raised the amount of atmospheric carbon dioxide (CO<sub>2</sub>) from 365 ppm in 2002 to greater than 400 ppm in 2022 (Nasa, 2022). CO<sub>2</sub> is considered as the noticeable heat-trapping gas to the global warming (Abeydeera et al., 2019), which comes from the extraction and burning of fossil fuels such as oil, natural gas and coal, from wildfires, and from volcanic eruptions (Nasa, 2022). For this reason, CO<sub>2</sub> can create the climate change and global warming. Figure 1.1 illustrates atmospheric CO<sub>2</sub> levels measured at Mauna Loa Observatory, Hawaii, in recent years, with natural, seasonal changes removed.

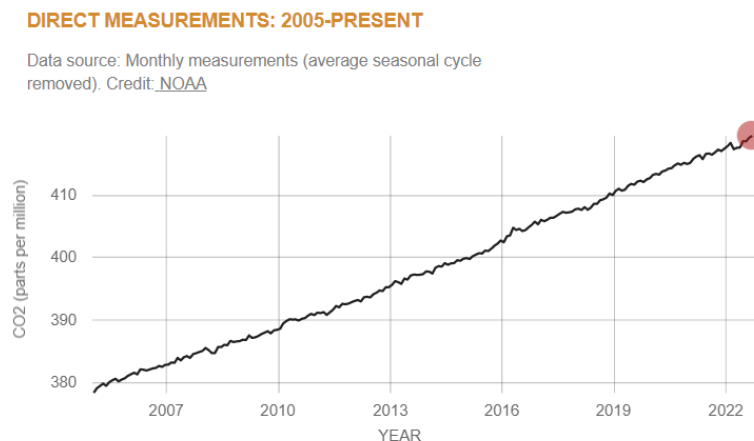


Figure 1.1 Atmospheric CO<sub>2</sub> Level at Mauna Loa Observatory, Hawaii, USA  
(Nasa, 2022)

The prime cause of global climate change has received significant global attention, which is Greenhouse gases. CO<sub>2</sub> is considered to be the one among these greenhouse gases. At the global scale, CO<sub>2</sub> is a primary source (65% of global greenhouse gas emission) which comes from industrial process and the fossil fuel. Figure 1.2 represents global greenhouse gas emission by gas (EPA, 2022).

Research in 2014 found that China is the top CO<sub>2</sub> emitters (30%), the United States (15%), the EU (9%), India (7%), the Russian Federation (5%), Japan (4%) and others (30%) as displayed in Figure 1.3. The data include the emission of CO<sub>2</sub> from fossil fuel, cement manufacturing and flared gas (EPA, 2022).

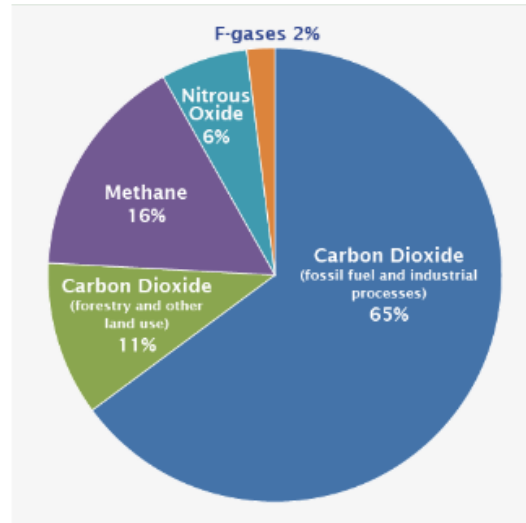


Figure 1.2 Global greenhouse gas emissions by Gas (EPA, 2022)

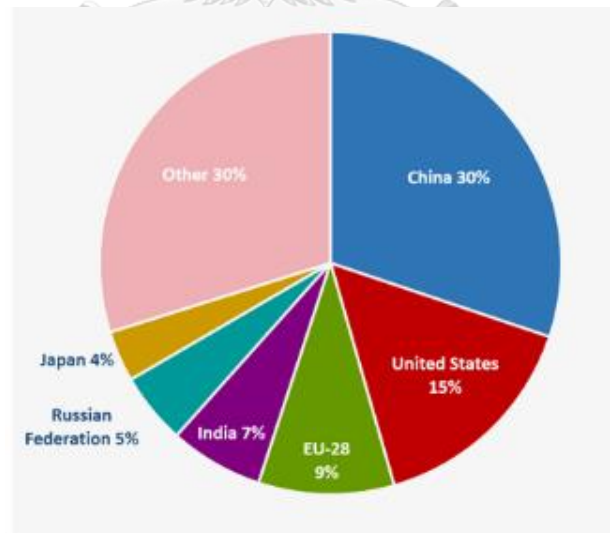


Figure 1.3 Global CO<sub>2</sub> Emissions from fossil fuel combustion and some industrial processes (EPA, 2022)

To reducing CO<sub>2</sub> emission, Thailand announced that Thailand's targeted mitigation of greenhouse gas emission and joining other states to keep global temperature rise below 1.5 degree Celsius to deal with the climate crisis and aimed to reach carbon neutrality by 2050, and net zero greenhouse gas emissions by or before 2065 at the world leader's summit of the twenty-sixth session of the conference of the parties to the United Nations framework convention on climate Change (COP 26), the sixteenth session of the conference of the parties to the Kyoto Protocol (CMP 16) and the third session of the conference of the parties to the Paris Agreement (CMA 3) at Glasgow, Scotland (United nation, 2021).

Carbon neutrality is defined as a means of production where the total output of CO<sub>2</sub> during any production is neutral. When subject is carbon neutral, it does not mean that the production process does not emit any greenhouse gas, it indicates that the overall output is equal to zero by using on other offsets such as carbon credit which is a good tool to be put in place to provide carbon offsetting (Counterbalanced) (Becker et al, 2020).

## **1.2 Sources of Carbon Dioxide (CO<sub>2</sub>)**

The huge amounts of carbon are stored in the Earth's crust as natural gas, oil and coal. If not for the human mining activities, this carbon would not be recycled back into the atmosphere for millennium (Sabine and Feely, 2003). CO<sub>2</sub> emissions principally come from burning solid and liquid fuels, but the use of solid fuels and natural gas is increasing much faster than that of liquid fuels or oil. The energy industries and other large facilities mainly use solid fuel and gas whereas oil is mostly used for transportation (Freund, 2013). Other human activities (cement industry), also significantly contribute of CO<sub>2</sub> quantities into the atmosphere every year.

The largest increase in CO<sub>2</sub> emissions by sector in 2021 took place in electricity and heat production. From this information, the global increase in emissions since the use of all fossil fuels increased to help meet electricity demand growth at 46% and close to 14.6 Gt of CO<sub>2</sub> emissions. From coal power plants, the CO<sub>2</sub> emissions rise to 10.5 Gt, which is 800 Mt above their 2020 level and more than 200 Mt above their

previous peak in 2018 (IEA, 2022). Figure 1.4 illustrates CO<sub>2</sub> emissions from electricity and heat production by fuel and share by fuel, 2000 – 2021.

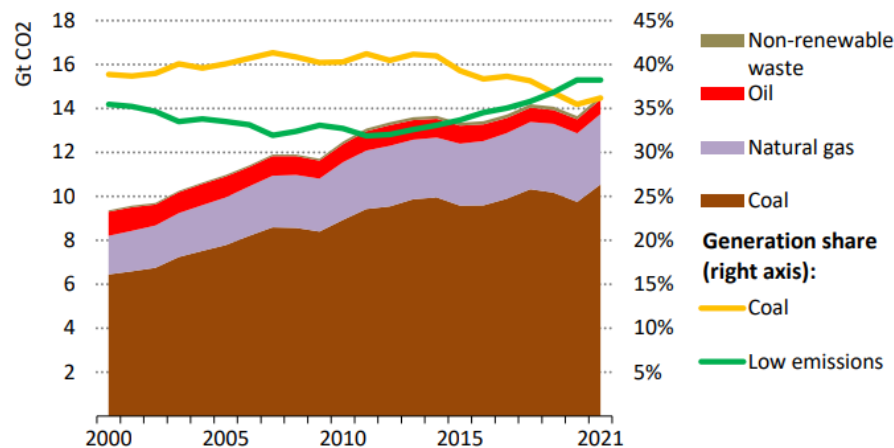


Figure 1.4 The Carbon Dioxide (CO<sub>2</sub>) emissions from electricity and heat production by fuel and share by fuel, 2000 – 2021 (IEA, 2022)

### 1.3 Enhance Oil Recovery Method

There are two or three recovery stages in the oilfield development. The first stage is a primary recovery. Natural drive mechanisms is the main mechanism to produce crude oil by the process of gas cap expansion, dissolved gas expansion and aquifer influx which supported by the reservoir's natural drive. After crude oil is extracted from reservoir for some period of time, reservoir pressure and oil production rate decline. In order to prolong the duration of the primary recovery stage, the pressure maintenance and artificial lifting techniques are operated.

The second stage is a secondary recovery. Water is the most favorable material to be injected into the reservoir via the injection well because of less cost. Water injection is not only to maintain reservoir pressure but also to displace oil toward producing wells. Producing the remaining oil in reservoir requires more advanced, complex and high-price technologies. For this reason, the most reservoirs were relinquished at this second stage.

In case of the remaining of crude oil is economic, other techniques will be performed after the secondary recovery which is called a tertiary recovery. An enhance oil recovery (EOR) is considered a tertiary stage. However, it can be applied at any stages of the petroleum field development. Crude oil is extracted by the injection of a substantial which is not initially present in the reservoir (Nunez-Lopez and Moskal, 2019). Numerous EOR methods have been widely applied with vary in the degrees of success, for light crude oil, heavy crude oil recovery as well as tar sands (Thomas, 2008).

### 1. Thermal methods

Thermal method is best appropriate for heavy crude oil in the range of 10 and 20° API and tar sands at less than or equal to 20° API. This method provides heat into the reservoir and vaporize some of the crude oil. The major mechanisms comprise of a large viscosity reduction and consequently mobility ratio. Other mechanisms, for instance, rock and fluid expansion, visbreaking and steam distillation may also be exhibited. Many techniques are grouped into thermal methods as presented below:

#### 1) Cyclic steam stimulation (CSS)

CSS is a single well process and consists of three stages. For the initial stage, steam injection is continuously injected into well around one month. Then, the single well is shut in for a few days for the purpose of heat distribution, denoted as soak. For the third stage, the well is resumed on production (Thomas, 2008). An oil production rate speedily raises to a high production rate, stays at that high level for a short time and finally declines over several months. The cycles of CSS are repeated when oil production rate becomes unprofitable. CSS is particularly attractive because it has quick payout. Figure 1.5 illustrates the CCS stages.

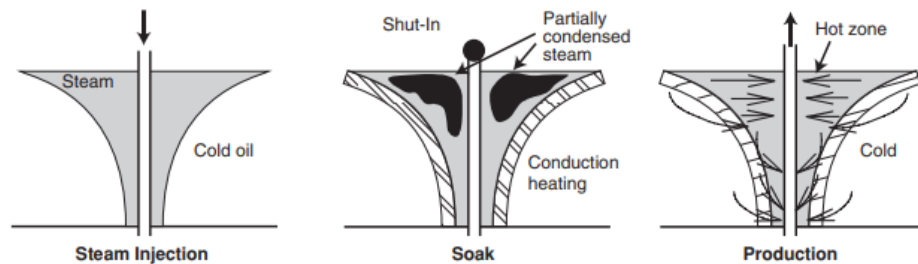


Figure 1.5 Cyclic steam stimulation (CCS) (Thomas, 2008)

## 2) Steamflooding

This method has a pattern like waterflooding drive. Its efficiency depends on the geology and pattern size. Steam is continuously injected into injection well and slowly set up a steam zone. Crude oil is mobilized as a result of oil viscosity reduction. The disadvantage of the steamflooding is the override and excessive heat loss of the steam.

## 3) In-situ combustion

The In-situ combustion or fire flooding is generated by injected air or oxygen ( $O_2$ ) into the reservoir to burn a portion of the in-place oil for heat generating at very high temperature which in the range of 450 to 600°C. The heat is generated in a narrow zone and causes high oil viscosity reduction where happens close to the combustion zone. The high thermal efficiency happens when the small heat loss occurs at the underburden or overburden as well as no heat loss at surface or wellbore. In some cases, the gas or water is used along with air to improve heat recovery as an additive. The produced toxic gas and severe corrosion as well as gravity override are problems of the in-situ combustion. The In-situ combustion has been applied in many places around the world especially in heavy crude oil field, however, very few projects have been worthy. There are 3 main variation of the in-situ combustion methods which includes:

- Forward combustion, ignition takes place close to the injection well and heated zone moves along with the air flow direction.
- Reverse combustion, ignition happens close to the production well and heated zone moves in opposite of the air flow direction. The Reverse combustion is

unsuccessful in the many fields due to the consumption of oxygen ( $O_2$ ) in the air before reaching to production well.

- High pressure air injection, there is no ignition in this process. This method involves low temperature oxidation of the in-place oil and is applied in several light crude oil reservoirs in the state (Thomas, 2008).

## 2. Non-thermal methods

The methods are the most appropriated for light crude oils with oil viscosity at less than 100 cp (Thomas, 2008). In some cases, this method is applicable to moderately viscous oils at lesser than 2000 cp, which are inappropriate for the thermal methods. There are two major mechanisms in non-thermal methods are to lower the interfacial tension (IFT) and to improve the mobility ratio. The three major types under are miscible, chemical and immiscible gas injection in non-thermal methods. Several miscible methods have been economically successful. A few chemical methods are also remarkable.

### 1) Miscible flooding

The miscible flooding is using the miscible displacing fluid with the reservoir crude oil either at first contact miscibility (FCM) or after multiple contacts miscibility (MCM). A narrow transition zone or a mixing zone develops between the displacing fluid (solvent) and the displaced fluid (oil), inducing a displacement of a piston-like. The transition zone or a mixing zone and the solvent profile spread as the miscible flood advances. The interfacial tension (IFT) is reduced to very low in the miscible flooding. The several miscible flooding processes are including enriched gas drive, high pressure gas ( $CO_2$  or  $N_2$ ) injection, vaporizing gas drive and miscible slug process.

- Carbon dioxide ( $CO_2$ ) miscible is a method that has been increasing in last decade years due to the potentiality of  $CO_2$  sequestration propose (Thomas, 2008). Apart from environmental purposes,  $CO_2$  is a unique displacing fluid because  $CO_2$  has relatively low minimum miscibility pressures (MMP) with a wide range of crude oils property.  $CO_2$  displaces and extracts heavier fractions ( $C_5$ - $C_{30}$ ) from the reservoir crude oil and progresses miscibility after multiple contacts miscibility (MCM). The

method is appropriate to light and medium light crude oils with gravity greater than 30° API in shallow reservoirs at low temperatures (Thomas, 2008). Many CO<sub>2</sub> injection projects are designed in use for this process, especially the water alternating gas (WAG) technology which CO<sub>2</sub> and water are alternated in slugs until the required CO<sub>2</sub> slug size is reached to about 20% HCPV (Thomas, 2008). This process approaches to reduce the instable viscosity. The availability, cost and the essential infrastructure of CO<sub>2</sub> are the major factors in the possibility of the process. The problem can come from an asphaltene precipitation in some cases. Figure 1.6 represents the CO<sub>2</sub> flooding process.

- Nitrogen gas or N<sub>2</sub> miscible is similar in principle to CO<sub>2</sub> miscible method and involved mechanism to accomplish the miscibility. However, N<sub>2</sub> has higher minimum miscibility pressures (MMP) than CO<sub>2</sub>. This method is suitable to light and medium light crude oils at greater than 30° of API, in deep reservoirs with moderate temperatures.

- Miscible slug process is a type of single contact miscibility process. An agent, for instance, propane (C<sub>3</sub>H<sub>8</sub>) or pentane (C<sub>4</sub>H<sub>10</sub>), is injected into injection well in a slug form (4-5% HCPV). The miscible slug drives in placed crude oil by using an injected gas, for instance, methane (CH<sub>4</sub>) or nitrogen (N<sub>2</sub>) or water. This miscible slug method is suitable many types of reservoirs such as sandstone, carbonate reservoirs. The inherent disadvantages is the gravity segregation in miscible flooding. The instable viscosity can be dominant and causes poor displacement efficiency.

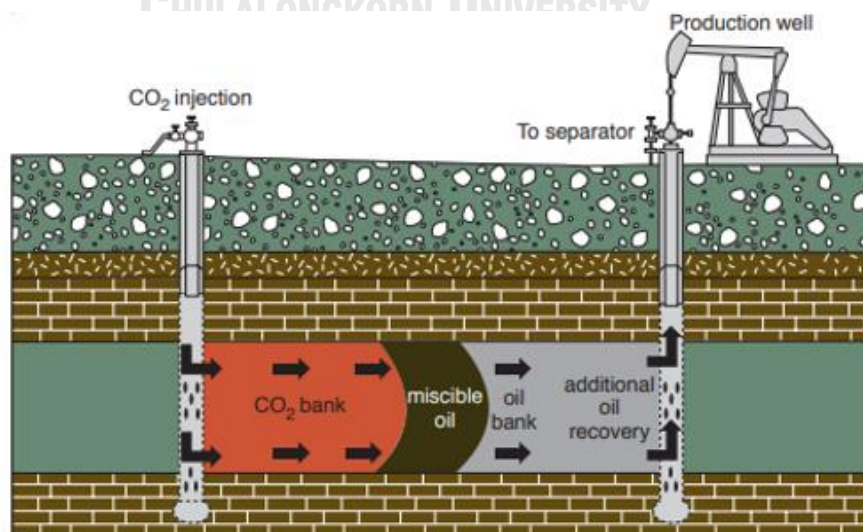


Figure 1.6 Carbon Dioxide (CO<sub>2</sub>) flooding (Buchanan et al, 2008)



- Enriched gas drive is a type of multiple contacts miscibility (MCM) process and involves the continuous injection of a gas, for instance, flue gas or nitrogen ( $N_2$ ), natural gas, enriched with low carbon fractions ( $C_2$ - $C_4$ ) into the injection well. At the reasonably high pressures, these fractions condense into the reservoir crude oil and develop a mixing zone. The miscibility will be accomplished after the multiple contacts miscibility (MCM) between the reservoir oil and the injected gas. An increase in oil phase volume and decrease in viscosity difference can also be providing the mechanisms towards increased oil recovery. The limitation of this method is the reservoir depth which is greater than 6000 ft due to the required the minimum miscible pressure or MMP.

- Vaporizing gas drive is an another multiple contact miscibility (MCM) process and requires flue gas or nitrogen ( $N_2$ ), natural gas continuous injection under high pressure. Under this condition, the lighter carbon fractions ( $C_2$ - $C_6$ ) are vaporized from the reservoir crude oil into the injected gas. A Mixing zone improves and the miscibility will be accomplished after multiple contacts miscibility (MCM). The limitation of the process is that the crude oil compositions must have adequately high amount of the lighter carbon fraction ( $C_2$ - $C_6$ ) to improve miscibility and the injection pressure must be lower than the reservoir saturation pressure to allow vaporization of the light crude oil fractions. The limitation of this method is the strength of reservoir pressure to withstand the high injection pressures.

## 2) Chemical Flooding

This method applies a chemical formulation to be a displacing fluid, that develops a mobility ratio reduction and/or a capillary number increment. The major chemical flooding methods are alkaline flooding, polymer flooding, micellar flooding, surfactant flooding, and alkali-surfactant-polymer or ASP flooding.

- Alkaline flooding, the alkaline chemical is an aqueous solution which injected into reservoir in a form of slug. The carbonate or orthosilicate of sodium and hydroxide are normally used as a alkaline chemical. The alkaline chemical process reacts with the crude oil acid components and produces the in-situ surfactant. The interfacial tension (IFT) reduction is the main mechanism of enhance oil recovery

process. Spontaneous emulsification may also occur. Dropping of entrainment and/or drop entrapment may take place relying on the formed of emulsion type which may be a cause of improve or diminish the recovery. A large number of Alkalies are required in the case of wettability alternating. The process of Alkaline flooding is complicated to design because of the diverse reactions that occurs between the reservoir fluids and rocks and the alkaline chemical.

- Polymer flooding or water-soluble polyacrylamides uses polymers and polysaccharides which are productive in enhancing mobility ratio and decreasing permeability contrast. In most cases, this method is utilized as a slug process (20-40% PV) and is driven by applying diluted brine. The concentration of polymer is in between 200 and 2000 ppm. The major limitations consist in polymer degradation and the disappear of polymer to the reservoir and loss of injectivity in some case. In the past, failure of polymer floods is the too late applying of polymer in the waterflood while the low mobile oil saturation. To be more effective in this method, the earlier apply of polymer during a waterflood at the breakthrough of water.

- Micellar flooding has been more productive in many fields than other chemical flooding methods. The main elements of this flooding process are a polymer slug and a microemulsion slug (micellar slug). These two slugs use brine to be a driving mechanism. Microemulsions are oil-water dispersions with small drop size distributions and stabilized surfactant. The microemulsions can be miscible with both crude oil and water. The high cost of chemicals, the high initial expense, the small well spacing requirement and the delay of considerable response are the disadvantages of micellar flooding. Moreover, the high salinity, clay content and temperature as well as geology in many candidate oil fields are inappropriate for the micellar flooding application.

- Surfactant flooding is productive in lowering interfacial tension (IFT) between reservoir oil and water. Petroleum sulfonates and some other commercial surfactants are regularly utilized. The polymer slug is injected before an aqueous surfactant slug, and the two chemical slugs are driven by using brine. The main reason failure of the surfactant flooding is the immoderate surfactant loss to the reservoir. In some case, the surfactant reaction and adsorption with the rock mineral are severe. Moreover, the treatment and disposal of emulsions are troublesome.

### 3) Other Methods

- Microbial EOR (MEOR), microbes react well with a carbon source in oil reservoir, for instance, oil and produce surfactant, biomass and gases such as  $\text{CH}_4$ ,  $\text{N}_2$ ,  $\text{CO}_2$ , and  $\text{H}_2$ , slimes or polymers and certain organic acids. The interfacial tension (IFT) reduction, viscosity reduction, improved mobility ratio, emulsification, wettability alteration, selective plugging, oil swelling and increased reservoir pressure because of the formation of gases are the oil recovery mechanism. An permeability increment can result from the acids formed.

- Foam flooding is a non-Newtonian fluid and complex with properties and attributes dominated by many factors. Foam is a liquid dispersion that contain surfactant in a gas, for instance,  $\text{CO}_2$ , air,  $\text{N}_2$ , steam or natural gas. The gas simultaneous injection and the surfactant solution are injected into the crude oil reservoir generates in place foam. Foam arranges breaks and re-forms in the pore throats while fluids advance in the porous medium. The exist of crude oil restrains the foam formation, therefore it is not efficient in mobilizing remaining oil in the reservoir. Foam mobility is lower than that of gas or steam and it acts as a viscous fluid. Foam has been applied as a mobility control agent or blocking agent, with steam and  $\text{CO}_2$  in some candidate reservoirs. Figure 1.7 illustrates the overall of EOR methods.

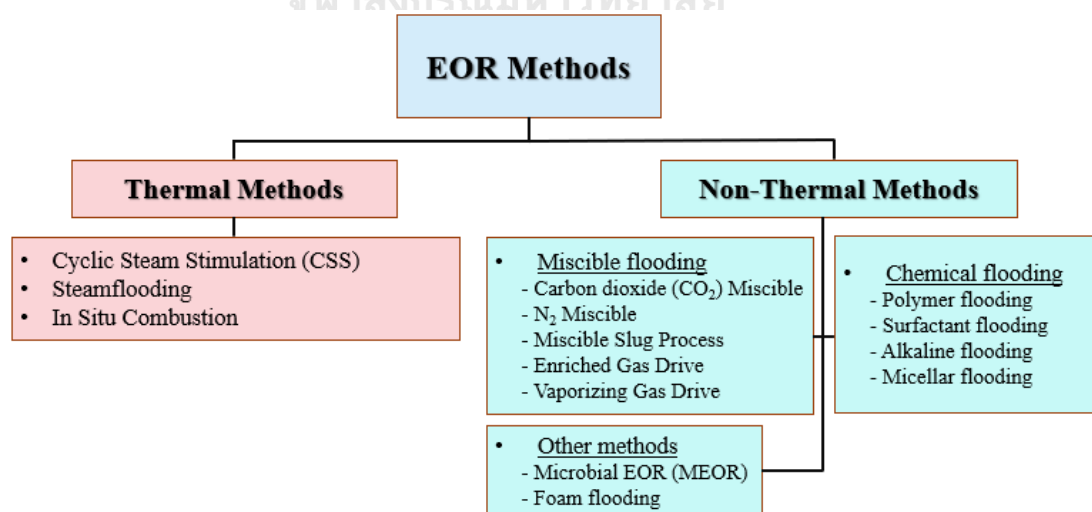


Figure 1.7 Enhanced oil recovery (EOR) method

#### 1.4 Study area

Pattani basin is an important oil and gas accumulation basin in the Gulf of Thailand, its geological faults are reflected thousands of small subdivision reservoirs which is one of the most complicated systems in the world (Attavithamthorn et al, 2013). Porosity and permeability decrease with burial depth increment. Reservoir porosity ranges from less than 10% to more than 30% and reservoir permeability ranges from a couple millidarcies to a couple of Darcies. In fluvial sandstone reservoirs in the Gulf of Thailand, grain size distribution leans to be coarse downward with moderate to high vertical heterogeneity ranging from 0.3 to 0.95. The range of reservoir fluid is in range from free gas to black oil. In the south part of the basin, the main free gas reservoirs are located whilst the black oil reservoirs are mainly located in the north part of the basin. In general, all main reservoirs contain light oil of 40 to 50° API and 400 scf/stb Gas oil ratio (GOR). However, some reservoirs compose of heavy oil of 10-20° API and 100-200 scf/stb GOR. In the case of geothermal gradient in Pattani basin is relatively high at 3°F per 100 ft. The great depth of reservoirs reaches to high reservoir temperatures ranging from 200°F at 4000 ftTVDSS to 350°F at 9000 ftTVDSS (Attavithamthorn et al, 2013).

As the decline production rate in mature fields, operators are attempting to prolong its field life and maximize the full potential of their asset. Moreover, the operators are trying to adopt technology to maximize its production rate before ending of its concession.

Waterflooding is the current base recovery method operated in Pattani basin. Gas flooding EOR is considered to be assuring process as high reservoir temperatures in Pattani basin rule out other EOR candidate processes, for instance, chemical flooding EOR. A reservoir potential estimation in Pattani basin when exploited with natural gas and CO<sub>2</sub> injection is yet to be done (Attavithamthorn et al, 2013).

## 1.5 Research Objective

1) To evaluate the possibility of carbon dioxide enhanced oil recovery (CO<sub>2</sub>EOR) in the presuming light oil reservoir in offshore area by using a simulation of the heterogeneity model.

2) To investigate the effects of WAG with CO<sub>2</sub> and CO<sub>2</sub> injection rate on oil production.

Scope of this research

ECLIPSE software is used to run reservoir simulation for CO<sub>2</sub>EOR. Input parameters of reservoir are based on offshore area in the Gulf of Thailand. The economic evaluation, geomechanics and geochemistry are not included in this research.

### Contribution of this research

The contributions of this study are to utilize CO<sub>2</sub> from the source for more oil production and for potential of carbon storage to reach Thailand's carbon neutrality in the future.

This study is separated into 5 chapters. Chapter 1 is an introduction which includes of CO<sub>2</sub> emission as well as sources of CO<sub>2</sub>, enhanced oil recovery methods and the objectives of this study. Chapter 2 summarizes the relevant theories of CO<sub>2</sub> including properties, pressure, CO<sub>2</sub> enhanced oil recovery as well as the literature review. Chapter 3 explains how to create the heterogeneous reservoir model, entire input data and operational conditions in ECLIPSE software. Chapter 4 presents the results and discussion of reservoir simulation and the comparison study of each studied parameter. Finally, chapter 5 is the conclusions of this study and recommendation for future studies are provided.

## CHAPTER 2

### THEORIES AND LITERATURE REVIEW

The chapter 2 presents the related basic knowledge of CO<sub>2</sub>EOR as well as literature review of related study and existing projects.

#### 2.1 Carbon Dioxide (CO<sub>2</sub>) Properties

CO<sub>2</sub> is a colorless, odorless, nonflammable gas with a slightly sour taste. CO<sub>2</sub> has small quantities in the atmosphere. Chemical compound of CO<sub>2</sub> consists of oxygen and carbon. CO<sub>2</sub> is a gas with density of approximately 1.98 kg/m<sup>3</sup> in normal pressure and temperature and denser than air (1.225 kg/m<sup>3</sup>). Molecular weight of CO<sub>2</sub> is 44.01. CO<sub>2</sub> is highly soluble in oil and soluble in water (Vishnyakov et al, 2020).

##### 2.1.1 Supercritical CO<sub>2</sub>

Depending on pressure and temperature, CO<sub>2</sub> can take on three separate phases. Phase diagram in Figure 2.1 illustrates the various phases including gas, liquid and supercritical form. CO<sub>2</sub> is in a supercritical phase at temperatures greater than 31.1°C and pressures greater than 1,070 psi or 7.38 MPa (critical point). Supercritical fluids differ quite significantly compared to the properties of real fluids. Supercritical fluids cannot be defined as a liquid or as a gas but as a substance in a state “supercritical state” (Budisa and Schulze-Makuch, 2014). Below these temperature and pressure conditions, CO<sub>2</sub> will be either gas or liquid. Depending on in situ temperature and pressure, CO<sub>2</sub> can be stored as a compressed gas or liquid, or in a supercritical (dense) phase (Voormeij and Simandl, 2003). If the temperature and pressure are both increased from the standard temperature and pressure to be at or above the critical point for CO<sub>2</sub>, it can adopt properties midway between a gas and a liquid.

The special properties of supercritical CO<sub>2</sub> are high solubility, high miscibility, high density, high diffusion rate, high dissolving power, and low toxicity (Budisa and Schulze-Makuch, 2014).

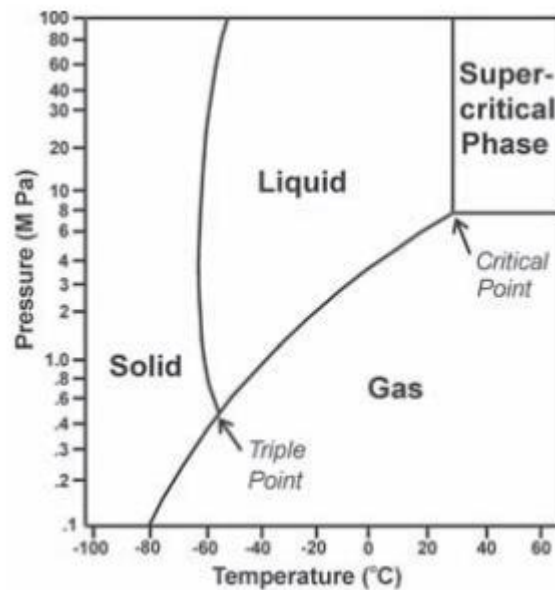


Figure 2.1 Carbon dioxide phase diagram (Voormeij and Simandl, 2003)

#### 2.1.2 Viscosity of CO<sub>2</sub>

CO<sub>2</sub> viscosities are reported in the liquid phase, near the critical region, and in the gas phase. CO<sub>2</sub> viscosity is much lower than oil and brine. The range of CO<sub>2</sub> viscosity in the region between 0.02 and 0.08 cP which is very low. The CO<sub>2</sub> viscosity has ten times lower than water viscosity (Vishnyakov et al, 2020). CO<sub>2</sub> viscosity is used to indicate the resistance properties of the fluid flow. Performance of CO<sub>2</sub> injection is dependent on CO<sub>2</sub> viscosity. In CO<sub>2</sub> liquid phase, viscosity reduces when temperature increases. Inversely, CO<sub>2</sub> viscosity increases when temperature increases for gas phase. The difference of viscosity depends on pressure and temperature as represents in Figure 2.2 (Bachu, 2003)

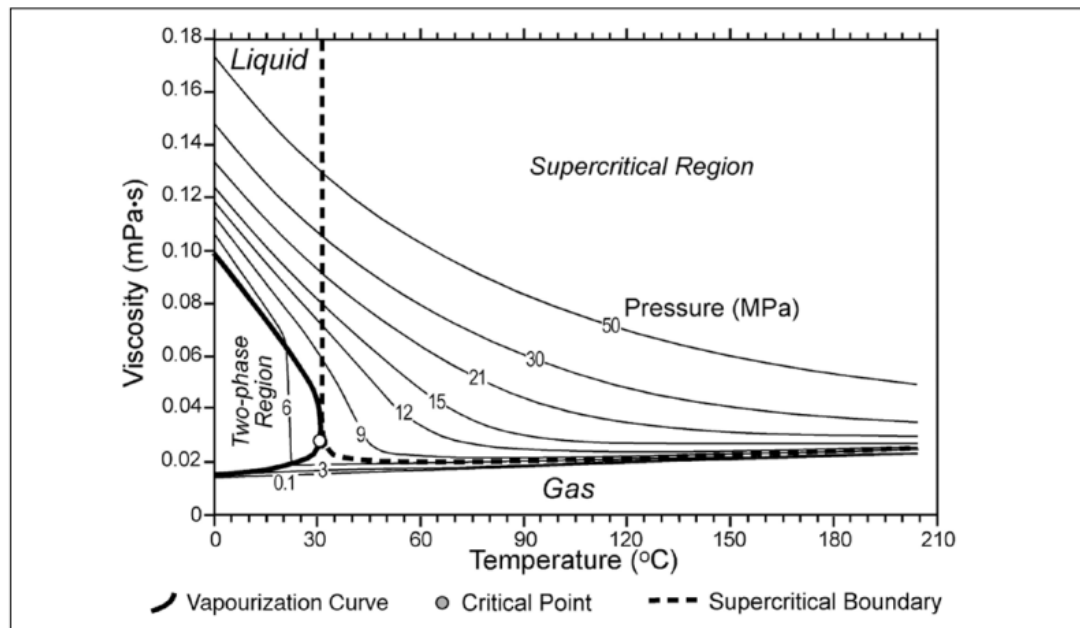


Figure 2.2 Variation of CO<sub>2</sub> viscosity as a function of temperature and pressure (Bachu, 2013)

## 2.2 CO<sub>2</sub> Enhance Oil Recovery

Gas injection is the oldest process in enhanced oil recovery (EOR) and it is currently steady increasing. The most of the carry out methods use of non-hydrocarbon gases, for instance CO<sub>2</sub>, Nitrogen (N<sub>2</sub>) and flue gas. In order to accomplish the miscibility with crude oil, an adequately high pressure is required to achieve miscibility. The unfavorable of the reservoir condition of the gas flooding causes a gas early breakthrough which causes the low of sweep efficiency. (Vishnyakov et al, 2020).

### 2.2.1 CO<sub>2</sub> Flooding Enhance Oil Recovery mechanism

CO<sub>2</sub> is highly soluble in oil and less soluble in water. The following properties are known which CO<sub>2</sub> uses in Enhanced Oil Recovery when CO<sub>2</sub> dissolves with reservoir liquids (Vishnyakov et al, 2020):

- 1) Decreasing in viscosity of crude oil and increase in viscosity of water.
- 2) Oil swelling and oil density reduction.
- 3) Multiple contact miscibility with hydrocarbon.
- 4) Acidic type interaction with the formation carbonates and clays.



### 5) Interfacial tension reduction.

#### Dissolution in water

CO<sub>2</sub> is much better miscible in water than hydrocarbon gases. However, a water salinity and temperature incremental decreases the miscibility of CO<sub>2</sub>. A raising in pressure has the reverse effect and the miscibility increasing. Under the reservoir conditions, the miscibility of gaseous is in range of 3–5% (Vishnyakov et al, 2020). The miscibility of CO<sub>2</sub> in water by 20-30% raises the viscosity of water. When CO<sub>2</sub> is dissolved in water, some carbonic acid is arranged. The carbonic acid etches carbonates and clays. This etching process opens and enlarges throats between formation grains and the permeability of sandstone rocks increases by 5-15% and carbonate rocks increases by 6-75%. The acidic environment also decreases swelling of clays. This dissolution in water has a significant effect on increasing reservoir permeability.

#### Dissolution in oil

At the suitable conditions, CO<sub>2</sub> has an outstanding miscibility in oil. Collate to water, crude oil can uptake more than 4-10 times of CO<sub>2</sub> at the appropriate conditions. This high miscibility also guarantees CO<sub>2</sub> significant transfer of CO<sub>2</sub> to oil from an aqueous solution in oil-water contact. This transfer decreases the interfacial tension (IFT) between water and oil, which causes the oil displacement to be miscible. The highest miscible of CO<sub>2</sub> and oil takes place when the pressure of completely dissolving is exceeded minimum miscibility pressure (MMP), regardless of the CO<sub>2</sub> concentration.

At high gas saturation pressure and temperature, the complete of miscibility pressure is significantly higher. At pressures below the miscibility pressure, CO<sub>2</sub> and oil isolate then forming gaseous and liquid phases. The gas phase is arranged by CO<sub>2</sub> with the light fractions of crude oil. The residual liquid oil is extracted and produced of crude oil light fractions. The oil viscosity is greatly decreased when CO<sub>2</sub> is completely miscible in it. Isolation of CO<sub>2</sub> and oil reaches to significant increment in

the reformed viscosity and oil density. This reformed crude oil is then left behind the front of propagating CO<sub>2</sub> slug.

Full miscibility of CO<sub>2</sub> and oil at the initial of CO<sub>2</sub> injection does not instantly occur. Whilst, in the oil displacement process, CO<sub>2</sub> is enriched with hydrocarbons in reservoir, and the displacement becomes gradually miscible. Hence, the miscible pressure for CO<sub>2</sub> is significantly lower than for hydrocarbon gases, nitrogen and flue gases. The oil swelling or volume increment with the dissolution of CO<sub>2</sub> has a substantial effect on enhance of oil recovery. When oil swelling takes place, a greatly decrease in the oil viscosity is observed.

Mechanism of the CO<sub>2</sub> flooding (Vishnyakov et al, 2020):

1) Mixing oil displacement under the miscible displacement

The oil is displaced by CO<sub>2</sub> is the same way as it is done by a conventional solvent. In this case, three zones in reservoir are constructed in the same direction of oil displacement: (1) CO<sub>2</sub> zone, (2) transition zone or mixing zone which compose of both CO<sub>2</sub> and oil (3) reservoir oil zone. Laboratory analysis on natural cores discloses that the displacement coefficient of the mixed displacement of oil by carbon dioxide can reach to 0.95 (Vishnyakov et al, 2020).

When injected CO<sub>2</sub> contacts reservoir crude oil, the dense CO<sub>2</sub> will begin to dissolve into crude oil. This dissolving does not instantaneously happen, but with time and the repeated multiple contact between the fluids. Crude oil and CO<sub>2</sub> can dissolve together to become a single phase. In the instance where CO<sub>2</sub> and oil completely dissolved, it is termed to miscible and CO<sub>2</sub> flooding are often referred to as miscibility flooding. In this miscibility effect is to cause the oil to slightly swell and the viscosity becomes less so that the miscible fluid flows within and through the reservoir pores more easily. The majority of CO<sub>2</sub>EOR projects perform in the fully miscible conditions, however an incomplete or partially miscible to completely immiscible CO<sub>2</sub> floods may also be performed and can be productive at enhancing oil production (Whittaker and Perkins, 2013).

## 2) Immiscible displacement

The light fractions of crude oil are dissolved in CO<sub>2</sub> and some CO<sub>2</sub> is dissolved in oil. Whilst CO<sub>2</sub> saturated in light fractions of oil displacement, oil enriched with CO<sub>2</sub> component isolation of oil occurs, and it is difficult to recover oil saturated with heavy components is formed and remained in the swiped zones.

CO<sub>2</sub> and oil do not form a single phase and is not miscible. However, the dissolved CO<sub>2</sub> in the crude oil causes oil swelling and the reduction of viscosity that both enhance sweep efficiency and help additional oil recovery. The hydrocarbon gases are the same to this process, CO<sub>2</sub> miscibility in crude oil significantly increases with pressure and decreases with temperature (Verma, 2015). CO<sub>2</sub> will be in a gaseous state regardless of the pressure at the reservoir temperatures above is higher than the critical level. In this condition, the field development result will be much less productive than in miscible displacement process because of the unfavorable ratio of oil and gas mobility which leads to low sweep efficiency (Vishnyakov et al, 2020).

## 3) Swelling effects

CO<sub>2</sub> injection decreases mobility of water and elevates in the mobility of oil. This process increases swipe efficiency by enhancing the displacement front stability. Moreover, oil volume swelling is the most important factors for crude oil displacement by injected CO<sub>2</sub>. The exact volume of oil expansion or swelling is a complex process of the light crude oil contents in the crude oil, reservoir temperature and pressure. Higher oil volume leads to artificial increase in oil saturation and in pore pressure. This effect improves to an productive displacement of remaining oil. The result of this process can cause the oil recovery coefficient may increase by 6-10% (Vishnyakov et al, 2020). Figure 2.3 illustrates the CO<sub>2</sub> miscible process illustrating the transition zone between the injector and production well.

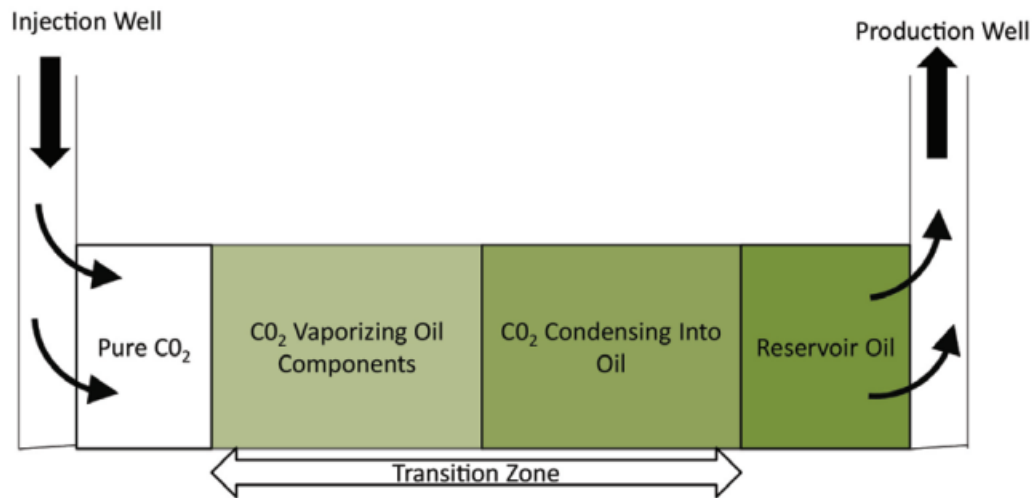


Figure 2.3 The CO<sub>2</sub> miscible process showing the transition zone between the injector and production well (Verma, 2015)

### 2.2.2 Water Alternating Gas (WAG)

In this method, hydrocarbon or inert gas is injected into the reservoir which contains remaining oil. The injected gas becomes miscible with the lighter components of the crude oil which decreases the viscosity of crude oil and increase the sweep efficiency in the presence of a chasing fluid, for instance, water or brine. The component exchanges processes between the injected gas and reservoir oil causes heavy and light compositions of crude oil in the reservoir which separately moves to the production side. Some of the injectants, for instance, CO<sub>2</sub>, assist to raise oil production by ways of reduction of oil viscosity, oil swelling and solution gas drive. Gas injection method can be extensively categorized as miscible and immiscible gas injection, counting on their miscibility with the crude oil at the reservoir conditions.

In an immiscible gas injection method, the CO<sub>2</sub> gas is injected at lower pressure into the reservoir. The miscible gas injection process can be extensively categorized as high pressure, enriched gas miscible displacement, miscible slug flooding and dry gas miscible displacement. A large difference in the mobility of gas and oil is observed in the event of the gas injection processes because of the dissimilar in the gas viscosity to the crude oil and water at the reservoir conditions. This results in an gas early breakthrough to the production well because of the high sweep CO<sub>2</sub> velocity (Bhatia et al, 2014).

Water and gas are alternately injected to control the gas sweep velocity. This technology is called as WAG injection process. An oil recovery by injection of WAG is due to the separation of gas to the top of reservoir and a gathering of water at the bottom of reservoir resulting in the recovery of crude oil. As the remaining oil after gas flooding is generally lower than water flooding process. Furthermore, the formation of three phase zones may result in lowering the remaining oil saturation. Therefore, WAG technology presents the potential for elevated microscopic displacement efficiency. Therefore, WAG technology can lead to enhanced oil recovery by combining better mobility control and contacting upswept zones and lead to enhance microscopic displacement. Several screening criteria are to be taken into consideration before the application of WAG technology for any field operation. The reservoir vertical permeability, the reservoir pay thickness, injection gas availability, formation type and mobility ratio are significant factors (Bhatia et al, 2014). The  $\text{CO}_2$  and water injection volume in WAG flooding process are major influence on the recovery factor, it should be appraised for the highest recovery (Verma, 2015).

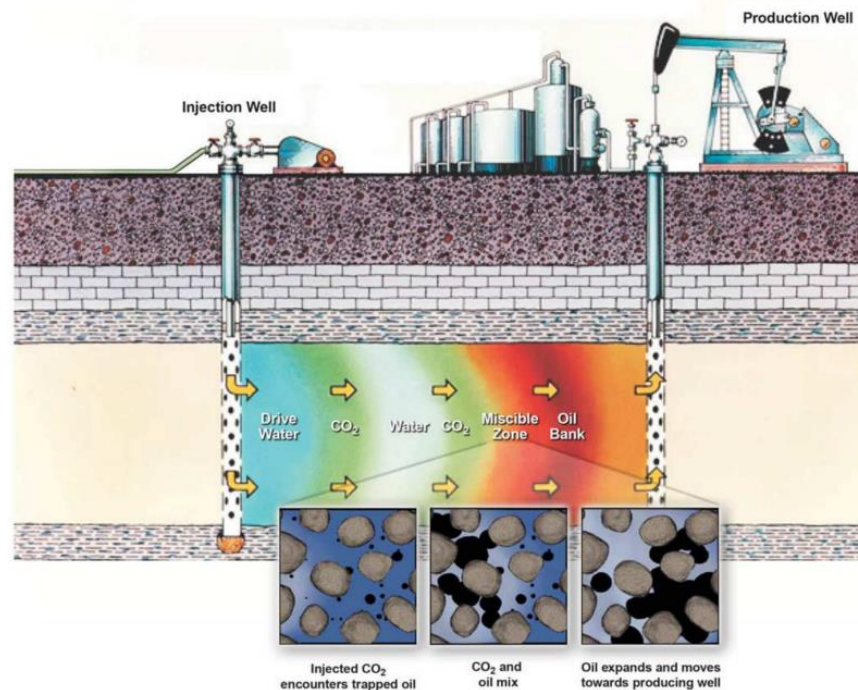


Figure 2.4 The WAG schematic (Nunez-Lopez and Moskal, 2019)

### 2.2.3 CO<sub>2</sub> Enhance Oil Recovery Projects

CO<sub>2</sub>EOR is set up technique in the U.S. and is the only oil recovery method that has presented any growth since the 1980s. As a matter of fact, CO<sub>2</sub>EOR now accounts for over 5% of the U.S. oil production (NETL, 2011). It can prolong the productive life of an existing oilfield by several years and it can lead to recover of millions of barrels of additional oil. The basic theory behind CO<sub>2</sub>EOR is the mutual miscibility of crude oil and CO<sub>2</sub> in the pressure and temperature geological reservoir conditions. For the appropriate conditions, injected CO<sub>2</sub> is able to dissolve and displace remaining oil which is trapped in rock pores. The oil wells are strategically designed to optimize the CO<sub>2</sub> areal sweep through the reservoir. As the injected CO<sub>2</sub> moves through the pore spaces in the rock, it encounters remaining crude oil. The crude oil is miscible with CO<sub>2</sub>, pressurized with CO<sub>2</sub>, easy mobilized due to oil viscosity reduction and forming a concentrated oil bank that is swept to designed producing wells. In this process, several operators are able to gain access to oil that would otherwise be left in the ground.

#### 1) CO<sub>2</sub> Pilot project in Dubai, UAE.

In 2009, the pilot project has three vertical wells including a CO<sub>2</sub> injection well, a monitor well and an oil producing well. The project has been operated for a year to accomplish a set of pre-defined objectives. During this period, an inclusive data obtaining program was performed and collected data from wells and reservoir performance were analyzed to address key uncertainties related to the miscible CO<sub>2</sub>EOR injection process. The reservoir pressure is above MMP of CO<sub>2</sub>. The injector well is perforated at lower zone and producer well is perforated in lower as well as upper zone. Well spacing is between 70 meters and the reservoir is a heterogeneous carbonate oil reservoir.

After 60 days of injection, the CO<sub>2</sub> breakthrough was observed at producer well due to wellhead pressure incremental, GOR and the percentage of CO<sub>2</sub> at the surface. Prior to the CO<sub>2</sub> breakthrough, the production rate increased gradually by 5-7 % and instantly dropped by 30-40% after the breakthrough (Basry et al., 2011).

## 2) CO<sub>2</sub>EOR project in Jilin province, China

This block is of a light crude oil reservoir with average permeability of 3.5 mD and single pay layer is thin. CO<sub>2</sub> flooding is considered to be a better technology for reservoirs with very low permeability (Huang et al, 2016). The bubble point pressure (1,060 psi) is far below MMP (3,321 psi). Therefore, the bubble point pressure effect on gas production is not significant. Water injection starts but the injectivity of water is poor; so, the company starts to inject CO<sub>2</sub> after that.

Whilst the CO<sub>2</sub> injection, the oil production rate of many producers significantly increased. For this project a systematic process has been implemented to the field monitoring and data analysis in order to appraise the miscibility effect of CO<sub>2</sub> flooding. The injection pressure and the bottom hole flowing pressure data from the producing wells are used for the reservoir pressure during CO<sub>2</sub> flooding evaluation, which can be a good indication for miscible or immiscible flooding modes. The produced gas and oil composition along with the oil production rate and CO<sub>2</sub> breakthrough timing are also used to analyze the mechanisms and performance of CO<sub>2</sub> flooding.

The field performance and miscibility effect of the CO<sub>2</sub> flooding pilot project carried out in H59 block have been estimated via detailed analysis of the formation pressure, production and injection data and the produced oil composition injection. The dynamic analysis of production has presented that a largely increase in oil production has been observed after CO<sub>2</sub> injection and the higher pressure in the bottom hole is sustained. The performance of the well can be extremely affected by early CO<sub>2</sub> breakthrough, which is attributed to the large injection volume, the fractures existed in the reservoir and the short well distance. Processes have to be taken to mitigate the CO<sub>2</sub> breakthrough in order to increase the CO<sub>2</sub> injection effect.

The analysis results and production response of the produced oil composition have revealed that an immiscible or near miscible flooding or partially miscible mode predominated in the field operation, although a high reservoir pressure is sustained at some stages during CO<sub>2</sub> injection. After the breakthrough of CO<sub>2</sub>, solution gas driving

plays an important role for oil production. It is essential to maintain the relatively high pressure of CO<sub>2</sub> flooding process, however, the high heterogeneity and low permeability nature of the reservoir has made very difficult process (Huang et al, 2016).

### 3) CO<sub>2</sub>EOR project in Daqing oil field, China

Daqing Oilfield is a supergiant oilfield comprised of Mesozoic continental sandstones. The first CO<sub>2</sub> project in China occurred in 1963 to slow the oil field steady decline. The results were optimistic and recommended that CO<sub>2</sub> flooding could raise production by 10 %. In year of 1990 to 1995, water alternating gas (WAG) with (CO<sub>2</sub>) injection was undertaken in Daqing, resulting in a 6 % raise in production. Daqing has extensively executed water flooding technology across the its oilfield reportedly with over 9,000 injector wells to compensated for production declines. With waterflooding also in decline, the attempts are decided to improve oil production by CO<sub>2</sub> flooding which was recommenced in 1999 (Hill et al., 2020).

### 4) CO<sub>2</sub>EOR project in Changqing Oilfield, China

This oilfield locates in the Shaanxi and Ningxia Provinces, North-Central China. It is China's third largest and perhaps most rapidly growing EOR project, also with conventional production reportedly in decline. The active waterflooding in an attempt to rebuild oil production. CO<sub>2</sub> injection has been carryout since the early 2000's. There is actively injecting a steady supply of 60 tons per day of liquid CO<sub>2</sub>, a 0.5 HCPV flood, transported by 3 trucks daily and buffered by abundant liquid CO<sub>2</sub> storage tanks at the field site. CO<sub>2</sub> produced with the oil is not recovered nor recycled at the site. The Jiyuan Block in Changqing oil field extracts out of the Triassic Yanchang Formation, a highly fractured continental sandstone at a depth of 3,000 m or 9,842 ft. The low-pressured reservoir is tight at 7 % of porosity or less with sub-millidarcy permeability at 8 mD. Hydraulic fracture stimulation has been operated to raise permeability to 7 mD at the field. In 2018, CO<sub>2</sub> has been injected in 9 wells with 36 producing wells formed in 9-spot patterns. CO<sub>2</sub> reports a total of approximately 376,000 tonnes had been injected with an equivalent to 315,000 tonnes of oil production (approximately 42,000 bbl). Flooding is miscible with MMP of 2,872 psi and a formation pressure of 2,857 psi. Reported recovery of CO<sub>2</sub> flooding was



evaluated at about 20 % relative to 10 % recovery from water flooding. A sequestration rate of 73 % is reported (Hill et al., 2020).

#### 5) CO<sub>2</sub> EOR project in Gulf Coast, Texas, Mississippi, Louisiana, U.S.

The Gulf Coast reservoirs are consisted in mostly Tertiary and Mesozoic marine-marginal fluvial and deltaic sandstones, such as the Cretaceous Tuscaloosa and Tertiary Frio Formations. They are sand-rich with Darcy-level permeabilities. The excellent injectivity is accompanied by an abundant natural and industrial CO<sub>2</sub> supply, available by supercritical pipeline that runs from Jackson dom, Mississippi to Houston Texas. The operators typically produce by direct CO<sub>2</sub> injection without the use of WAG. The young sediments with their high permeabilities probably do not represent useful analogs for China's EOR projects. However, the pipelines and surface facilities are instructive as they allow for the injection of optimal slugs of CO<sub>2</sub> over the lifetime of projects (Hill et al., 2020).

#### 6) CO<sub>2</sub> EOR project in Permian Basin, West Texas, U.S.

The Permian basin now the largest producing basin in the U.S., is largely a carbonate platform, with reservoirs producing from the Permian San Andres Formation, attended by some shallow marine to continental sandstones. CO<sub>2</sub> EOR storage projects are located in the carbonates of the San Andres. The carbonate producing intervals are identified by broad range of permeabilities but regularly in the range of 10 to 100 mD. Supercritical CO<sub>2</sub> carried to the basin comes from the natural sources (dome structure to the north in New Mexico and Colorado) and natural gas separation sources by pipeline. Since 1972, CO<sub>2</sub> has injected over 175 million tonnes, oil producing 30,000 bbls/day. For instance, Whiting North Ward Estes Field, with 18 % porosity and 15 mD permeability has a total of 816 producers and 816 injectors in line drive and 5-spot patterns produced by WAG technology. For carbonate reservoirs in the Permian Basin's geology, the remaining oil zones have been discovered in the carbonates of the San Andres and thought to result from secondary porosity generated during the dolomitization process (Hill et al., 2020).

### 7) CO<sub>2</sub>EOR project in The Rocky Mountains, Wyoming, Montana, U.S.

The EOR projects of Rocky Mountain are identified by Mesozoic and Paleozoic fluvial, marine and Aeolian clastic rock orders with lower permeability. Supercritical CO<sub>2</sub> comes from natural gas separation and natural sources (dome structures). In the Rocky Mountains, there are a wide range of reservoir conditions. The Salt Creek field is identified by moderate to high permeabilities and porosities. The near-miscible Paleozoic continental-marine transition sandstones of the Merit Lost Soldier Field in Wyoming and the miscible Rangeley Weber field of Colorado, which has been operated for CO<sub>2</sub> flooded for 30 years. The petrologic features of the Lost Soldier and Rangeley Weber fields are 7–13 % porosity, 10 mD permeability, 35° API gravity, and range of depth in between 1500 - 2100 m. However, leading to achievement in these projects are the volumes supercritical CO<sub>2</sub> supply by pipeline. Supercritical CO<sub>2</sub> from the Exxon Shute Creek natural gas separation plant floods the Lost Soldier field with a 60 % HCPV slug of WAG injection technology and produced CO<sub>2</sub> is recaptured at its separation and recycle facility (Hill et al., 2020).

## 2.3 CO<sub>2</sub> Trapping Mechanism

A geological formation must have the properties, for instance, injectivity, capacity, and restriction in terms of long-term CO<sub>2</sub> storage and safety. CO<sub>2</sub> can be stored in a geological formation by diverse methods through a variety of chemical and physical trapping mechanisms (Zhong et al, 2018). Table 2.2 represents CO<sub>2</sub> geological storage trapping mechanisms.

Table 2.1 CO<sub>2</sub> geological storage trapping mechanisms (Zhong et al, 2018)

Storage Mechanism	Trapping Type
Physical storage	Structural Trapping
	Residual Trapping
Chemical Storage	Solubility Trapping
	Mineral Trapping

Physical trapping of CO<sub>2</sub> takes place when CO<sub>2</sub> is stationary as a free gas or supercritical fluid and as a process, it depends on the storage volume availability. Whereas chemical trapping of CO<sub>2</sub> happens when CO<sub>2</sub> contact with any materials in underground storage sites or reservoir. The cap-rock integrity is vital to prevent the upward movement of supercritical CO<sub>2</sub> towards the surface (Zhong et al, 2018).

#### 2.3.1 Structural or stratigraphic trapping

This trapping mechanisms are the essential parts in the storage of CO<sub>2</sub> in a depleted hydrocarbon reservoir. The cap-rock integrity is vital to prevent the upward movement of supercritical CO<sub>2</sub> towards the surface (Zhong et al, 2018). Once CO<sub>2</sub> is injected, supercritical CO<sub>2</sub> can be more buoyant than other liquids that might be presented in the pore space. Therefore, CO<sub>2</sub> will percolate up through the more porous rocks until it reaches the top of the reservoir where it meets an impermeable layer of cap-rock. This is already used extensively by the natural gas storage industry.

#### 2.3.2 Residual trapping

Residual trapping methods the CO<sub>2</sub> left behind as residual or droplets in the pore spaces when the supercritical CO<sub>2</sub> is injected into the reservoir (Zhong et al, 2018). As the supercritical CO<sub>2</sub> is injected into the reservoir it displaces fluid. As it moves through the porous rock but some of the CO<sub>2</sub> will be left behind as disconnected - or residual - droplets in the pore spaces which are immobile, just like water in a sponge.

#### 2.3.3 Solubility trapping

The solubility trapping methods that CO<sub>2</sub> dissolves into the oil phase and/or aqueous in the reservoir, by which not only the decreasing oil viscosity as CO<sub>2</sub> miscible with oil but also brine can dissolve a large amount of CO<sub>2</sub> (Zhong et al, 2018). CO<sub>2</sub> dissolves in other fluids in its supercritical and gaseous state. This phase in the trapping process associates the CO<sub>2</sub> dissolving into the brine which presents in the porous rock. Brine containing CO<sub>2</sub> is denser than the surrounding fluids, so it will sink into the bottom of the rock formation over time, trapping the CO<sub>2</sub> even more firmly.

### 2.3.4 Mineral trapping

As CO<sub>2</sub> is dissolves in brine, it decomposes into H<sup>+</sup> and HCO<sub>3</sub><sup>-</sup> and forms a weak carbonic acid which can react with the minerals in the surrounding rock to form solid carbonate minerals ((Nghiem et al, 2009; Zhong et al, 2018). Mineral trapping is the safest form of trapping but it takes the longest duration among various CO<sub>2</sub> trapping mechanisms (Young et al., 2019)

## 2.4 Pressure

### 2.4.1 Fracture pressure

When CO<sub>2</sub> is injected into a permeable and porous reservoir rock, the CO<sub>2</sub> will be forced into pores at a pressure higher than the surrounding formation pressure. This injection pressure could lead to deformation of the reservoir rock or the seal rock, resulting in the opening of fractures or failure along a fault plane. For injecting CO<sub>2</sub> into the reservoir, the downhole injection pressure must be greater than the reservoir fluid pressure. However, increasing formation pressure may induce the fractures in the formation. Consequently, the injection pressure must be monitored to ensure that the injection pressure should not be exceeded that fracture pressure which is not exceed to 90% (IPCC, 2005).

The fracture pressure can be obtained from many researchers. One calculated by following Hubbert and Willis's equation is shown in equation 2.1 (Bourgoyne et al., 1987).

$$P_{ff} = \sigma_{min} + P_f \quad (2.1)$$

Where

$P_{ff}$	=	Formation fracture pressure
$P_f$	=	Formation pressure
$\sigma_{min}$	=	Minimum matrix stress

Furthermore, the fracture pressure calculation by following Eaton's (1969) equation is shown in equation 2.2 (Kananithikorn and Songsaeng, 2021).

$$\text{Fracture Pressure} = (\text{OBP} - P) \left( \frac{\gamma}{1-\gamma} \right) + P \quad (2.2)$$

Where            OBP = Overburden pressure  
                      P    = Pore pressure  
                       $\gamma$    = Poisson's ratio

From equation 2.2, an overburden pressure (OBP) is the vertical stress and it is a pressure from the weight of overlying formations including the rock layers and water column. The density log from drilled well in Pattani basin is used to identify the overburden gradient. The result is increasing from 0.93 psi/ft to 1 psi/ft in the interesting section between 5,000 ftTVDss to 9,000 ftTVDss. Figure 2.5 displays the overburden gradient and depth cross (Kananithikorn and Songsaeng, 2021).

Due to the limitation of actual Poisson's ratio in Pattani basin, the back – calculated Poisson's ratio ( $\gamma$ ) is from the maximum ECD while the lost circulation occurs and the formation pressure data of suspected lost circulation zone which assume mud only lost into sandstone. The equation of back – calculated Poisson's ratio ( $\gamma$ ) is shown in equation 2.3.

$$\gamma = \frac{\left( \frac{\text{Fracture Pressure} - P}{\text{OBP} - P} \right)}{1 + \left( \frac{\text{Fracture Pressure} - P}{\text{OBP} - P} \right)} \quad (2.3)$$

The back – calculated Poisson's ratio ( $\gamma$ ) is ranging from 0.36 to 0.44 and vary with depth (Kananithikorn and Songsaeng, 2021). Figure 2.6 illustrates the back – calculated Poisson's ratio and depth from different 2 platforms in Pattani basin indicate differently linear trend lines.



Figure 2.5 Overburden gradient and depth cross (Kananithikorn and Songsaeng, 2021)

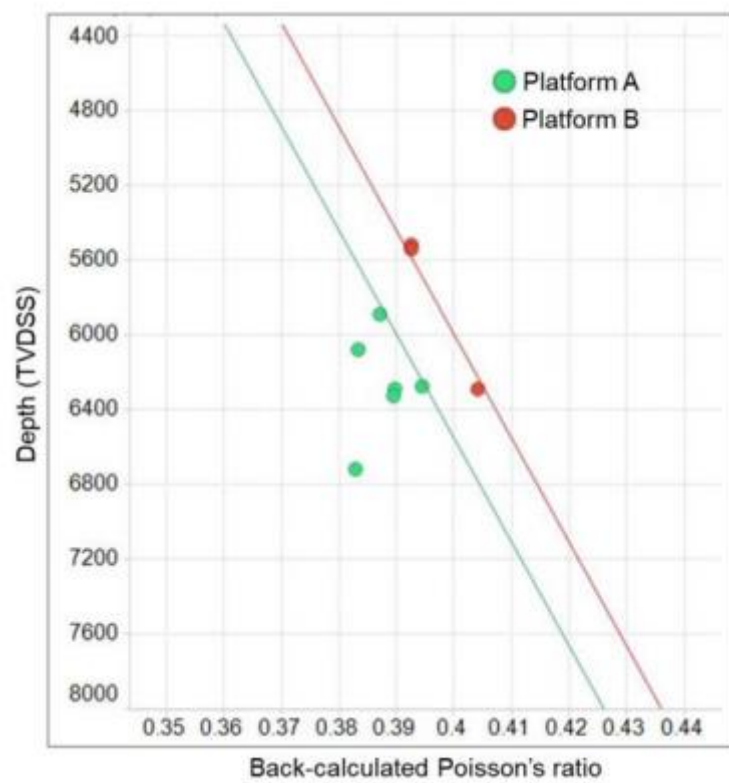


Figure 2.6 The back – calculated Poisson's ratio and depth (Kananithikorn and Songsaeng, 2021)

#### 2.4.2 Minimum miscibility pressure (MMP)

One of the vital parameters in carbon dioxide (CO<sub>2</sub>) miscible flooding technology is the minimum miscibility pressure (MMP). MMP is defined as the lowest pressure at which recovery of oil is (90–92%) at injection (1.2 PV) of CO<sub>2</sub> (Mansour, 2018). The MMP is considered as the lowest pressure at which CO<sub>2</sub> and oil are completely miscible. The MMP is specific for individual oil compositions and must be defined by performing laboratory analyses, for instance, using a slim tube apparatus or through a rising bubble experiment. The oil recovery mechanisms are normally designed to maintain the reservoir pressure above the MMP. If the reservoir pressure during the oil production is less than the MMP, the lighter components of hydrocarbon in the crude oil (lower molecular weight and generally lower viscosity) may be favorably produced (Whittaker and Perkins, 2013). The injected gas and crude oil in reservoir become a multi-contact miscibility (MCM) at a fixed temperature. MMP must be evaluated because every production field needs an appropriate plan to develop an injection and surface facilities environment before any field trial. Evaluation of reliable MMP need to be performed by traditional laboratory techniques, but it is time-consuming and very high-priced. Also, the MMP can depend on several literature MMP empirical correlations, but this method is not a suitable scheme because each MMP correlation relates to an individual formation condition (Mansour, 2018).

Theoretically, there is a minimum pressure level when CO<sub>2</sub> is injected into an oil reservoir. Below that MMP level CO<sub>2</sub> and oil is immiscible or partially miscible. The pressure increment leads to an increase in CO<sub>2</sub> density, which decreases the density difference between CO<sub>2</sub> and crude oil. As a result, the Interfacial tension (IFT) between CO<sub>2</sub> and crude oil disappears, and they will reach mutual solubility in each other. A large amount of research has been applied to determine the MMP parameter, and one could find various correlations and experimental processes as well, which are largely implemented for MMP prediction. The oil composition, reservoir temperature, and purity of injected gas are main factors affecting CO<sub>2</sub> and oil MMP (Moghadasi et al, 2018). Some affecting factors are condensed in detail below (Mansour, 2018).

- MMP does not change as methane presents in the reservoir.
- As the oil gravity becomes heavier as MMP increases. Consequently, production fields with heavy API are not appropriated for CO<sub>2</sub>EOR.
- MMP is higher with high reservoir temperature.
- MMP is inversely related to the reservoir crude oil's C<sub>5</sub> to C<sub>30</sub> summation.
- MMP does not require Methane to propane presence.

Generally, the low temperature reservoirs containing light crude oils have smaller CO<sub>2</sub> MMP. However, the impurity impacts are not general and depend on the type of components. Basically, the oil recovery is higher when CO<sub>2</sub> and crude oil are miscible. In fact, oil recovery rapidly raises as the pressure increases and then flattens out when MMP is accomplished with CO<sub>2</sub> injection (Moghadasi et al, 2018). There are two categories of miscible flooding, known as follows:

- 1) First contact miscibility (FCM): In this process crude oil and CO<sub>2</sub> are miscible in all proportions upon first contact, making a single homogenous solution.
- 2) Multiple contact miscibility (MCM): in general, crude oil and CO<sub>2</sub> are not fully miscible on the first contact. In fact, miscibility takes place dynamically upon multiple contacts within the reservoir.

There are various experimental means, equations of state, and empirical equations for evaluating MMP. One of widely accepted experimental methods is a slim tube experiment because it can repeat the interaction between gas and crude oil in a one dimensional porous medium. As a result, that slim-tube experiment can replicate crude oil and gas interaction in a one-dimensional porous medium. It remains the most reliable method of evaluating minimum miscibility pressure (Mansour, 2018).

The empirical correlations for estimating MMP provide fast and cheap alternatives to experimental methods. It is beneficial for quick screening reservoirs for potential CO<sub>2</sub> flooding. Several empirical correlations for estimating MMP have been calculated from regression data analysis of slim tube data. Generally, the empirical correlations for the predicting of MMP reservoir temperature, the (C<sub>2</sub>-C<sub>6</sub>) content of reservoir fluid, and API (oil gravity) as the input parameters. There are popular MMP



empirical correlations, for instance, Cronquist, Lee, Yelling and Metcalfe, Alston et al., Emera and Sarma (Mansour, 2018).

Cronquist empirical correlation is depended on the reservoir temperature, pentane plus (C<sub>5+</sub>) molecular weight, and volatile oil fraction as (CH<sub>4</sub> and N<sub>2</sub>) for MMP valuation as present in equation 2.4.

$$\text{MMP} = 0.11027 + (1.8T_R + 32)^y \quad (2.4)$$

Where  $y = 0.744206 + 0.0011038 \times \text{MWTC}_{5+} + 0.0015279X_{\text{vol}}$   
 $T_R$  = Reservoir temperature (°C)  
 $X_{\text{vol}}$  = Mole Fraction of volatile components (CH<sub>4</sub>+N<sub>2</sub>) in crude oil (mol%)

Remarks (1) The oil gravity (API) ranged from 23.7 to 44.8.  
 (2) The temperature ranged from 21.67 to 120.8°C.  
 (3) The experimental (MMP) ranged from 7.4 to 34.5 MPa.

Lee empirical correlation predicted a model to evaluate MMP using reservoir temperature as input data only by considering CO<sub>2</sub> vapor pressure, as shown in Equation 2.5. If any reservoir oil's bubble point pressure (P<sub>b</sub>) is more than MMP the P<sub>b</sub> takes as MMP. The P<sub>b</sub> can be collected from the constant mass study test.

$$\text{MMP} = 7.3924 \times 10^b \quad (2.5)$$

Where  $b = 2.772 - (1519 / (492 + 1.8T_R))$

Remarks (1) Based on equating MMP with CO<sub>2</sub> vapor pressure when  $T < \text{CO}_2$  critical temperature, while using the corresponding correlation when  $T \geq \text{CO}_2$  critical temperature.  
 (2) if  $\text{MMP} < P_b$ , P<sub>b</sub> is taken as MMP.

Yelling and Metcalfe empirical correlation (1980) proposed an empirical correlation for MMP at different reservoir temperatures by using the equation 2.6. This correlation is not relied on oil composition and is depended only on reservoir conditions. The empirical correlation of MMP of this method is varied from 15 to 19 Mpa approximately.

$$\text{MMP} = 12.6472 + 0.01553(1.8T_R + 32) + 1.24192 \times 10^{-4}(1.8T_R + 32)^2 - \frac{716.9427}{(1.8T_R + 32)} \quad (2.6)$$

Where  $T_R$  = Reservoir temperature ( $^{\circ}\text{C}$ )

Remarks (1) temperature limitations in range of 35.8 to 88.9 $^{\circ}\text{C}$ .

(2) if  $\text{MMP} < P_b$ ,  $P_b$  is taken as MMP.

Alston et. al., (1985) present an empirical correlation for MMP caused by gas solution in reservoir fluids. The MMP empirical correlation that is in Equation 2.7 are predicted depended on  $\text{CO}_2$  composition stream, light crude oil fraction ( $\text{CH}_4 + \text{N}_2$ ), reservoir temperature, pentane plus ( $\text{C}_{5+}$ ) molecular weight, and intermediate oil fraction ( $\text{C}_2$  to  $\text{C}_6$ ,  $\text{H}_2\text{S}$ , and  $\text{CO}_2$ ) as well as composition of the  $\text{CO}_2$  stream. Moreover, there is an impurity correction factor which need to be concerned for estimating MMP by contaminated or enriched carbon dioxide ( $\text{CO}_2$ ) stream.

$$P_{\text{CO}_2} = 1.25 * 10^{-7} (1.8T_R + 460)^{1.06} (M_{\text{C}_{5+}})^{1.78} \left( \frac{Y_{\text{VOL}}}{Y_{\text{INT}}} \right)^{0.316} \quad (2.7)$$

Where  $T_R$  = Reservoir temperature ( $^{\circ}\text{C}$ )

$M_{\text{C}_{5+}}$  = Molecular weight of  $M_{\text{C}_{5+}}$  in the crude oil (g/mol)

$Y_{\text{vol}}$  = volatile mole percent (mole%)

$Y_{\text{int}}$  = intermediate mole percent (mole%)

Remark if  $\text{MMP} < P_b$ ,  $P_b$  is taken as MMP.

Emera and Sarma (2005) present the genetic logarithm (GA) - depending on the correlation to MMP as shown in equation 2.8. The input data parameters that are depended on this correlation are ( $\text{C}_1$  and  $\text{N}_2$ ) volatiles ratio, reservoir temperature, intermediates components ( $\text{C}_2$ – $\text{C}_4$ ,  $\text{H}_2\text{S}$ , and  $\text{CO}_2$ ), pentane plus ( $\text{C}_{5+}$ ) molecular weight, and ( $\text{C}_2$ – $\text{C}_4$ ,  $\text{H}_2\text{S}$ , and  $\text{CO}_2$ ). This MMP empirical correlation was presented to be suitable for low permeability reservoirs, when ( $Y_{\text{vol}}/Y_{\text{int}} > 1$ ).

$$\text{MMP}_{\text{pure}} = 0.003 * T^{0.544} (MW_{\text{C}_{5+}})^{1.006} \left( \frac{Y_{\text{VOL}}}{Y_{\text{INT}}} \right)^{0.143} \quad (2.8)$$

Where  $M_{C5+}$  = Molecular weight of  $M_{C5+}$  in the crude oil (g/mol)  
 $Y_{vol}$  = volatile mole percent (mole%)  
 $Y_{int}$  = intermediate mole percent (mole%)

In most published empirical correlations, it is suggested that the calculated MMP should raise with the reservoir temperature, while some of them apply different parameters to address the effect of the oil compositions on MMP. Other empirical correlations predict  $CO_2$  MMP as a function of three variables; namely the mole fraction of a light component in the reservoir oil, temperature and molecular weight of plus fraction. Some studies have adopted different approach than those available in the literature which considered other PVT parameters, for instance, API,  $R_{si}$  and  $P_b$  that could contribute to the development of  $CO_2$  MMP predictions. The equation 2.9 is presented for another calculation of MMP (Khazam et al, 2016).

$$MMP_{CO_2} = 5578 + 10.37 * T + 0.929 * P_b + 10,220 * \frac{API}{R_{si}} - 166.3 * API - 8.71 * P_b * \frac{API}{R_{si}} \quad (2.9)$$

Where  $MMP_{CO_2}$  = Minimum miscibility pressure of  $CO_2$  solvent (psi)  
 $T$  = Reservoir temperature ( $^{\circ}F$ )  
 $P_b$  = Bubble point pressure (psi)  
 $R_{si}$  = Initial solution gas oil ratio (Scf/STB)  
 $API$  = Oil gravity ( $^{\circ}API$ )

For this study, the designed model characterizes a miscible state by calculating the crude oil atoms and ratio of  $CO_2$  that pass through the initial interface. The equation (2.10) is presented for calculation of MMP (Li et. al, 2021).

$$MMP_{CO_2} = 0.15T_R - 30.92 \quad (2.10)$$

Where  $MMP_{CO_2}$  = Minimum miscible pressure of  $CO_2$  (MPa)  
 $T_R$  = Reservoir temperature (Kelvin)

From this MMP calculation, it can be compared to the experimental results to check the predictive performance of the model. Yu et al. (2020) will be set to be as a benchmark. Table 2.2 shows the summary of MMP (MPa) and relative error predicted by experimental and different empirical correlations. The overall results can prove that even if only the influencing factor of  $T_R$  is considered, the model proposed has satisfactory prediction accuracy (Li et al, 2021).

Table 2.2 Summary of MMP (MPa) and relative error predicted by experimental and different empirical correlation (Li et al, 2021)

Model	Number of Parameters	Predicted MMP (MPa)	Relative Error (%)
Yu et al.	-	22.75	-
CO <sub>2</sub> (this study)	1	19.63	13.71
Crude Oil (this study)	1	20.81	8.53
Lee	1	20.84	8.32
Alston et al.	4	19.72	13.22
Shokir	8	20.03	11.89
Emera and Sarma	2	30.11	32.44
Cronquist	3	26.59	16.96
Glaser	2	27.60	21.41
Yellig and Metcalfe	1	16.55	27.18

Whenever the reservoir pressure is above an MMP but below the fractured pressure, in theoretically, the oil recoveries could be as high as 90% of the OOIP in the CO<sub>2</sub> swept region. However, the recoveries in most fields are generally lower because of the reservoir complexity in terms of lithology, fracture, structure, rock wettability, capillary pressure, gravity and oil viscosity, and permeability contrast between several zones in the reservoir (Verma, 2015).

## 2.5 CO<sub>2</sub> storage capacity

The aerial extent of the structures was identified from the location of spilling points from elevation contour lines and 3D cross-sections. Aquifer thickness was acquired from well data when present. Volumes are calculated by multiplying the aerial extent with the aquifer thickness, assuming an average thickness based on well data. For the efficiency factor a value of 2% was chosen. Average permeabilities and porosities of the aquifer are calculated from well data on the specific stratigraphic unit. The volume was calculated using the following equation 2.11, which is clearly a fixed percentage evaluation approach (Van der Meer and Yavuz, 2009):

$$\text{CO}_2 \text{ Storage capacity (kg)} = V_r * (N/G) * E * \phi * \rho \quad (2.11)$$

Where  $V_r$  = Bulk aquifer volume ( $\text{m}^3$ )  
 $N/G$  = Net to gross ratio (-)  
 $E$  = Efficiency factor (constant = 0.02)  
 $\Phi$  = Porosity (-)  
 $\rho$  =  $\text{CO}_2$  density at depth (Rotliegend =  $700 \text{ kg/m}^3$ , Triassic =  $650 \text{ kg/m}^3$ )

Estimation of  $\text{CO}_2$  storage ability are highly uncertain because of the data lacking. The most difficult aspect of calculating storage ability is the evaluate of volumetric storage efficiency. It depends on a number of factors, not just geological parameters, for instance, thickness and extent of an aquifer but also on petrophysical parameters, for instance, relative permeability. Furthermore, the storage efficiency depends on a range of factors which have opposing effects, that makes it difficult to draw up common rules. Physical properties in the reservoir also affect mass capacity evaluation. The density of  $\text{CO}_2$  relies on the temperature and pressure which may be uncertain. Especially, the temperature may not be exactly known in a saline aquifer. Consequently, a value of 2% is frequently used for regional evaluates in open aquifers. In specific sites, the value may be larger than this. For closed aquifers the value will be considerably smaller and depending on the aquifer size (Pickup, 2013).

The storage resource specific to petroleum reservoirs can be evaluated by using the recognized recovery production volumes converted to volumes at reservoir conditions ( $KR_{\text{RES}}$ ) values. To convert this subsurface volume of  $KR_{\text{RES}}$  to a storage resource, the total volume is reduced by a storage efficiency value. The storage efficiency distribution for the gas and crude oil reservoirs used for this resource evaluation will be the same as the buoyant storage efficiency values. The recognized recovery replacement storage resource ( $KRR_{\text{SR}}$ ) is determined by multiplying the  $KR_{\text{RES}}$  by the density of  $\text{CO}_2$  in equation 2.12 (Brennan et al., 2009).

$$KRR_{SR} = (KRR_{RES} * B_{SE}) * \rho_{CO_2} \quad (2.12)$$

Where  $B_{SE}$  = the storage efficiency of buoyant  $CO_2$  storage (fraction)  
 $\rho_{CO_2}$  = density of  $CO_2$  (Mass/Volume)  
 $KRR_{RES}$  = the known recovery corrected to a volume at subsurface conditions (volume) which can be calculated in equation 2.13.

$$KRR_{RES} = [(KRR_{OIL} + KRR_{NGL}) * FVF_{OIL}] + (KRR_{GAS} * FVF_{GAS}) \quad (2.13)$$

Where  $KRR_{OIL}$  = the known recovery of oil (Volume)  
 $KRR_{NGL}$  = the know recovery of natural gas liquids (Volume)  
 $FVF_{OIL}$  = the formation volume factor for oil and natural gas liquids (fraction)  
 $KRR_{GAS}$  = the known recovery of gas (volume)  
 $FVF_{GAS}$  = the formation volume factor for gas (fraction)

The storage capacity in a depleted gas or crude oil reservoir may be evaluated more precisely than saline aquifer because more information is available on the spread of the reservoir and the rock properties. Furthermore, hydrocarbon has been trapped in a particular formation over geological time periods confirming the presence of a caprock or seal. It is normally assumed that the volume of  $CO_2$  which may be stored in a reservoir is equal to the volume of hydrocarbon which has been produced, or will potentially be produced which can be calculated in equation 2.14 (Pickup, 2013).

$$V_{CO_2} = R_f * STOIP * B_O \quad (2.14)$$

Where  $V_{CO_2}$  = Volume of  $CO_2$   
 $R_f$  = Recovery factor  
 $B_O$  = Oil formation volume factor  
 $STOIP$  = stock tank oil initially in place

The  $CO_2$  volume which may be stored may also be directly calculated from the volume of the reservoir (Pickup, 2013) in equation 2.15 as:

$$V_{CO_2} = R_f * A * H * \phi * (1 - S_{wc}) \quad (2.15)$$

Where     A           =   Area of reservoir  
              H           =   Thickness of reservoir  
              S<sub>wc</sub>       =   Connate water saturation

optionally, the CO<sub>2</sub> volume which may be stored and may be estimated from produced and injected volumes. For an oil reservoir, the equation 2.16 may be used (Pickup, 2013):

$$V_{CO_2} = N_p B_o + (G_p - N_p R_s) B_g + W_p B_w - W_i B_w - G_i B_g \quad (2.16)$$

Where     N<sub>p</sub>       =   Volume of produced oil (measured at surface)  
              W       =   Volume of water produced or injected (in surface unit)  
              G       =   Volume of gas produced or injected (in surface unit)  
              R<sub>s</sub>       =   Dissolved gas ratio  
              B       =   Formation volume factor (Reservoir volume/Surface volume)

The subscripts w, g, i and p stand for water, gas, injected and produced, respectively.

## 2.6 Determination of Candidate Wells for CO<sub>2</sub> Enhance Oil Recovery

The study of the successful CO<sub>2</sub> EOR project is conducted by reviewing design and performance data in several wells. The different operational parameters will be used to determine the candidate wells that might highly produce of oil from CO<sub>2</sub> EOR technique.

The first commercial CO<sub>2</sub> EOR injection project was originated at SACROC (Scurry Area Canyon Reef Operators Committee) Unit of the Kelly-Snyder Field in Scurry County, West Texas U.S. and it has remained today as the world's largest miscible flooding project. From the result of the years of experience in CO<sub>2</sub>EOR laboratory, field pilot project and full-scale commercial operations, sufficient data has been acquired to develop technical screening criteria for potential CO<sub>2</sub> flooding

candidates. The technical screening guideline for CO<sub>2</sub> flooding shown in table 2.2 (Meyer, 2007).

Table 2.3 Technical Screening Guidelines for CO<sub>2</sub> Flooding (Meyer, 2007)

	Recommended	Current projects range
<b>Crude oil</b>		
(1) gravity, °API	>22	27 to 44
(2) Viscosity, cP	<10	0.3 to 6
Composition	High percentage of Intemediates (C5 to C12)	
<b>Reservoir</b>		
Oil saturation	>40	15-70
Formation type	Relatively thin Sandstone or carbonate	
Permeability	Not critical if sufficient rates can be applied	
Depth/Temperature	For miscible displacement, depth must be great enough to allow injection pressure greater than MMP, which increase with temperature and for heavier oils. Recommend depths of CO <sub>2</sub> floods of typical Permian basin oils is as follow:	
	<b>Gravity, °API</b>	<b>Depth Greater than (ft)</b>
<b>CO<sub>2</sub> misible</b>	>40	2,500
	32 to 39.3	2,800
	28 to 31.9	3,300
	22 to 27.9	4,000
<b>CO<sub>2</sub> immiscible</b>	13 to 21.9	1,800
	<13	Fails CO <sub>2</sub> Screening

Not all reservoirs are appropriate for CO<sub>2</sub>EOR and are screened depending on the factors, for instance, MMP, reservoir geology, oil gravity and viscosity to help identify the most likely candidates for miscible CO<sub>2</sub> flooding (Verma, 2015).

## 2.7 Literature Review

Abeydeera et al. (2019) worked on global research on carbon emissions and found that carbon mitigation opportunities and eventually accomplishing zero carbon emission target are some of the most popular research areas in the carbon emission research domain over the past 2 years.



Meyer (2007) prepares the background report for the American Petroleum Institute to summarize the Summary of Carbon Dioxide Enhanced Oil Recovery (CO<sub>2</sub>EOR) Injection Well Technology. He identifies the processes and operating practices that have been developed by the oil and gas industry for injecting CO<sub>2</sub> for EOR. These methods and practices have been specifically improved to use in CO<sub>2</sub>EOR. In the U.S. alone, the oil and gas industry operated over 13,000 CO<sub>2</sub>EOR wells, over 3,500 miles of high-pressure CO<sub>2</sub> pipelines, and has injected over 600 million tons of CO<sub>2</sub> (11 trillion standard cubic feet) and produces about 245,000 barrels of oil per day from CO<sub>2</sub>EOR projects. He also provided the technical screening guideline for miscible CO<sub>2</sub> flooding and immiscible CO<sub>2</sub> flooding from SACROC (Scurry Area Canyon Reef Operators Committee) Unit of the Kelly-Snyder Field in Scurry County, West Texas.

Budisa and Schulze-Makuch (2014) studied on CO<sub>2</sub> and concluded that in the supercritical phase, CO<sub>2</sub> is an aprotic agent miscible with a range of organic liquids and some bacteria and their enzymes are active in this solvent. Planetary environments with supercritical carbon dioxide exist under the seabed of the Earth.

Buchanan and Carr (2008) studied geologic sequestration of CO<sub>2</sub> in Kansas and found that the CO<sub>2</sub> increases in density and becomes a supercritical fluid under the great pressures that naturally exist at depth greater than 2,400 ft (800 m). The supercritical fluids take up less space and diffuse more easily through the pore spaces in rock formations than either gases or ordinary liquids.

Due to no actual fracturing data in Pattani Basin in the Gulf of Thailand. Kananithikorn and Songsaeng (2021) modified the Eaton equation by using the data from pressure while drilling (PWD) and formation pressure test data which are used to back-calculate for Poisson's ratio and identified a relationship with depth. This interpreted Poisson's ratio trend will be used to calculate for fracture pressure by incorporating with the estimated depletion pressure and depth that is expected to encounter in each planned well.

Li et al. (2021), worked on the prediction of MMP. Nowadays, there are several means to predict MMP, for instance, experimental measurement and computation methods. The former has been spready used because of their high precision. Even though, these experimental measurements have accurate techniques, they still suffer from some problems including time-consumption and operation cost. In addition, it is difficult for any experimental process to simulate the actual crude oil reservoir conditions completely; therefore, their results are highly influenced by the equipment. Li et al. developed on the molecular dynamics-based model to estimate MMP of CO<sub>2</sub> and oil system. Their process characterized the miscible state by calculating the ratio of both CO<sub>2</sub> and crude oil atoms that passed through the initial interface to their respective totals. These ratio values instantly dropped and fluctuated after a certain value with an increase in pressure at a fixed T<sub>R</sub> (reservoir temperature in Kelvin). The value is the MMP of T<sub>R</sub>. In comparison with conventional prediction approaches, the present work proposed a straightforward model to simulate the complex miscibility of CO<sub>2</sub> and crude oil, and the miscible principle was clarified at the molecular scale. Reservoir temperature (T<sub>R</sub>) and MMP had a linear relationship in their study and the slope was about 0.15 MPa/K, which are in agreement with theoretical analyses and literature results.

Nunez-Lopez and Moskal (2019) provides an overview of CO<sub>2</sub> EOR and its ability to reduce greenhouse gas (GHG) emissions. The results from a recent study, which express that all CO<sub>2</sub>EOR operations produce negative emission crude oil during the first several years of production, are analyzed in the context of the urgency of climate change mitigation. CO<sub>2</sub>EOR is the only commercially implemented carbon utilization option which provides large scale permanent storage for captured CO<sub>2</sub>.

Thomas (2008) examined the EOR technology which have been examined in the several oil field. Some of these fields have been commercially successful, while others are mainly of academic interest. This research found that the miscible CO<sub>2</sub> flooding technology has had considerable success for light crude oils, though the economics is not explicit at this stage.

Attavikamthorn et al. (2013) worked on the metamodeling of gas flooding EOR in Pattani Basin, in the Gulf of Thailand by creating parametric and non-parametric metamodels to evaluate the potential of gas flooding EOR using real data of Pattani Basin reservoir. Monte Carlo simulation are managed to verify the their parametric and non-parametric metamodels. The parametric metamodel is used to evaluate the potential of five gas injection technologies including (1) Standalone gas injection, (2) Single cycle WAG injection, (3) Double cycle WAG injection, (4) SWAG injection and (5) Single cycle WAG with gas followed by injection of water. The standalone gas injection provides a lower recovery factor compared to waterflooding which is the base recovery technology. Inversely, the gas flooding EOR methods which combine the injection of water, for instance, WAG and SWAG injection technology are promising gas flooding EOR methods for reservoirs of Pattani Basin, particularly when the injection fluid contains a high fraction of gas. The double cycle WAG injection technology provides the higher recoveries than the single Cycle WAG injection technology. Decreasing the percentage of injection water in SWAG technology tends to elevate the recovery factor. However, this results in the high gas injection volume.

Verma (2015) provided the basic technical information regarding the CO<sub>2</sub>EOR method, which was at the core of the evaluation methodology, to evaluate the technically recoverable crude oil within the production fields of the identified sedimentary basins of the U.S. The emphasis is on CO<sub>2</sub>EOR because this is currently one technology being considered as an ultimate long-term geologic storage solution for CO<sub>2</sub> owing to its economic profitability from incremental oil production offsetting the cost of carbon sequestration and he find that the target to maximize recovery; A miscible CO<sub>2</sub>EOR process is preferred over the immiscible one. For the CO<sub>2</sub>EOR process, CO<sub>2</sub> can be injected either as a continuous stream, water alternating gas (CO<sub>2</sub>), also known as WAG, or as tapering WAG. Because CO<sub>2</sub> and water injection volume in a WAG flood has a major influence on the recovery factor, it should be estimated for maximum recovery.

Bhatia et al. (2014) also worked on the experiment of the production performance of WAG injection process for enhanced oil recovery. The comparative study of different WAG injection process for the core sample obtain from the brown production field has been done. The single cycle WAG (with HC gas), five cycle WAG (with HC gas and CO<sub>2</sub>) and tapered WAG using HC gas have been experimentally investigated. At the end of his experiment, it is found that (1) The WAG injection process gives the mobility control of water and gas phases, better sweep control and improves the total HCPV recovery. Consequently, almost all the gas-injection techniques now are converted to the WAG injection technique. (2) The cycle numbers in the WAG injection methods affect the recovery of crude oil from the reservoir. The results present that for the same injecting fluid volume in single cycle and five cycle technique the incremental recovery of HCPV has been examined. (3) The tapering during the WAG injection technique helps to improve the recovery of the HCPV. Increasing WAG ratio during the process gives better incremental recovery than decreasing WAG ratio. (4) The tapered WAG process with decreasing WAG ratio does not present recovery after three cycles of WAG process. This limitations use of more cycles of WAG process as they are not profitably feasible. (5) The trapping of the gas presents the better effect on the crude oil recovery and water velocity through core pack. (6) Chasing water injection after WAG method helps to get the incremental crude oil recovery. (7) The CO<sub>2</sub> gas at temperature and pressure in reservoir conditions is close to supercritical behavior and thus helps to enhance the recovery of oil during WAG injection process. (8) Gas trapping constant for several variants of WAG is found within the range of 1.3 to 2.8. This shows better gas trapping phenomena in the WAG technology.

Huang et al. (2016) analyzed the pilot project of CO<sub>2</sub> flooding EOR in a low permeability reservoir in China oil field. To estimate the miscibility effect of CO<sub>2</sub> flooding technique, injection and production well data were analyzed, comprising of injection pressure, bottom hole flowing pressure (BHFP) of production wells, CO<sub>2</sub> breakthrough time and produced crude oil and gas compositions. The reservoir pressure distribution during CO<sub>2</sub> injection was figured out based on the injection pressure and BHFP using the Kriging interpolation method, and the varying miscible

region was illustrated in pressure contours. The analysis results presented that CO<sub>2</sub> injection can significantly elevate oil production, but the size of the miscible region can be highly decreased after early CO<sub>2</sub> breakthrough that can cause BHFP and oil production declining. In comparison with the experimental data of core flooding with CO<sub>2</sub> at different modes, the produced crude oil composition data point that CO<sub>2</sub> flooding in the production field is more likely in near miscible or immiscible modes, though the injection pressure is higher than the MMP, which can be attributed to unanticipated early CO<sub>2</sub> breakthrough and low permeability nature of the reservoir (Huang et al, 2016).

Although this study has met the technical screening guidelines for miscible CO<sub>2</sub> Flooding presented in Table 2.3, the calculation from equation (2.10) of this study indicates that the MMP<sub>CO2</sub> (4,101 psi) of this study is higher than both working pressure at 80% of fracture pressure (3,531 psi) and 90% of fracture pressure (3,973 psi). Consequently, this study is considered as the partial miscible CO<sub>2</sub> EOR. Furthermore, this study would distinguish CO<sub>2</sub>EOR in offshore area in the Gulf of Thailand using the reservoir simulation (ECLIPSE) with heterogeneous reservoir model. The heterogeneous reservoir model is used to obtain more understanding of how CO<sub>2</sub> extract the residual light oil after natural drive mechanism as well as WAG (Water-Alternating-Gas and CO<sub>2</sub>).

The CO<sub>2</sub>EOR in Thailand is uninviting and less study due to the high investment to build infrastructure to transport the CO<sub>2</sub> from its source to oil field as well as no attractive tax or legal for any operator. Despite, the fact that Thailand has many potential areas which include of lighter oil than other places. This study could provide the remarkable data for CO<sub>2</sub>EOR method, optimal of injection rate of CO<sub>2</sub> which impact to reservoir pressure as well as WAG-CO<sub>2</sub> favorable rate in the heterogeneous reservoir model in the future.

## **CHAPTER 3**

### **SIMULATION**

The area of this study is offshore area in the Gulf of Thailand. The data derive from the Department of Mineral Fuels (DMF), Ministry of Energy and from the published data in public domain. The interesting area is in the Gulf of Thailand due to light oil production and depth of well drilling are suitable for CO<sub>2</sub> flooding as well as the distance from CO<sub>2</sub> sources. From those data, the heterogeneous reservoir models will be created by using the values of porosity and permeability between the ranges of the measured data from the Gulf of Thailand.

#### **3.1 Reservoir simulation program**

The simulation will be run in this study by ECLIPSE software which is Schlumberger product. The ECLIPSE simulation is the one of the useful simulation programs on the global oil and gas market which covers the hydrocarbon reservoirs in the form of black oil, compositional model as well as thermal simulation. Furthermore, the ECLIPSE can interact with reservoir fluid properties simulation software such as PVTi. ECLIPSE 300 is designed for compositional hydrocarbon model and CO<sub>2</sub> simulation as well as thermal simulation (Schlumberger, 2020). Consequently, The ECLIPSE 300 will be mainly used for this study.

Besides the ECLIPSE software, MATHLAB, Prosper as well as PETREL will be run to completely fulfill the input data for necessary supporting the ECLIPSE software.

#### **3.2 Geological data in the Gulf of Thailand**

The data of offshore area in the Gulf of Thailand is obtained from Department of Mineral Fuels (DMF) and the published papers in the public domain.

The Gulf of Thailand has subdivided into 2 major sub-segments including Western Gulf and Eastern Gulf sub-segments, separated from each other by Ko Kra Ridge. The western sub-segment includes 9 graben type basins which comprises of Sakorn, Paknam, Hua Hin, Northwest, Western, Kra, Chumporn, Nakhon Srithammarat, and Songkhla basins. The eastern Sub-segment comprises of 2 major

basins, namely Pattani and Malay basins and one smaller basin which is the Khmer basin (Charusiri and Pum-Im, 2009). Figure 3.1 illustrates the major tectonic subdivisions in Thailand.

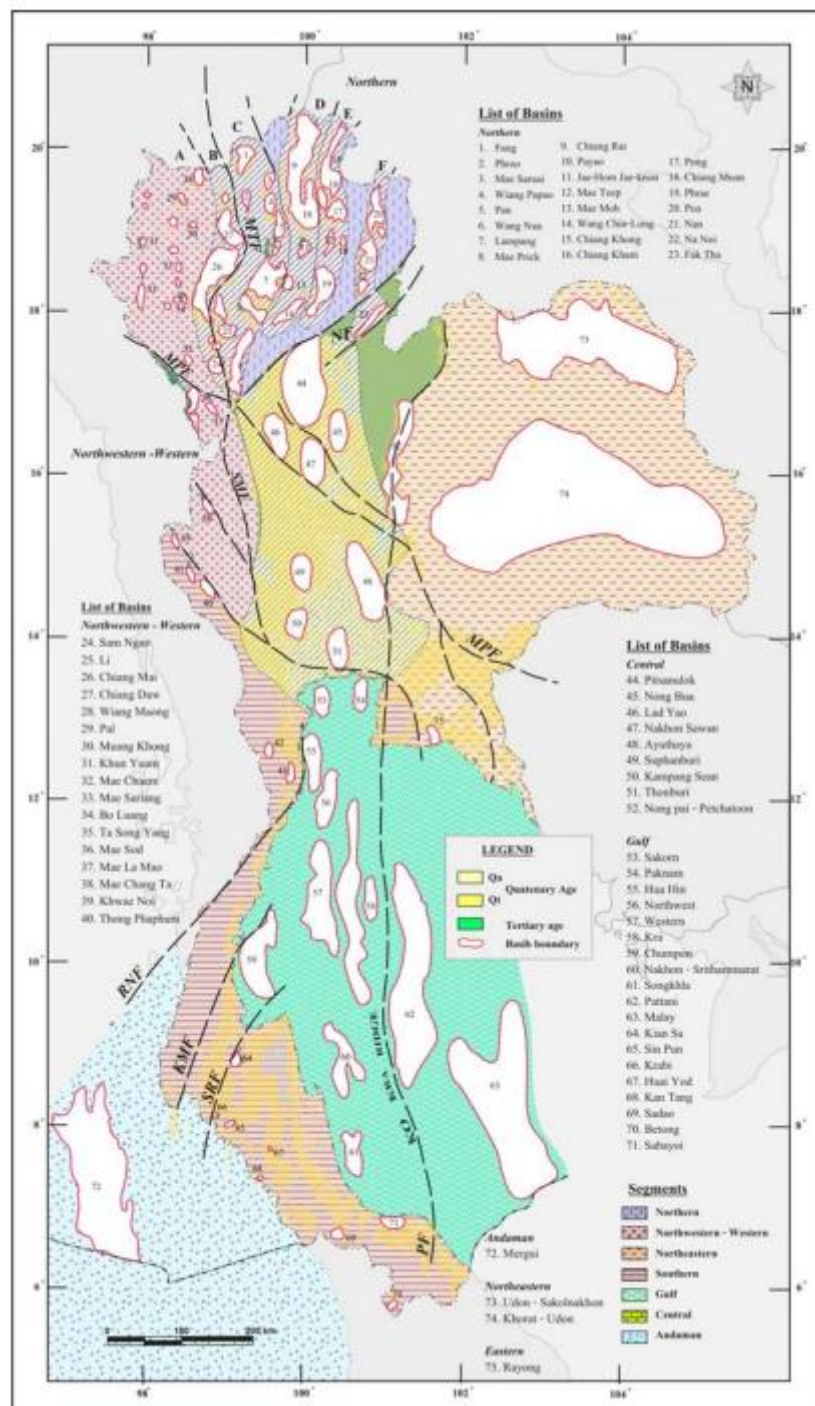


Figure 3.1 Major tectonic subdivisions in Thailand (Charusiri and Pum-Im, 2009)

For the Eastern Gulf Sub segment, its stratigraphy is denoted by the Pattani Basin, the largest basin in the Gulf of Thailand. Many of the basins represent in Figure 3.1 appear to lie at or close to the intersection of three major strike-slip faults, namely NE–SW, NW–SE and N–S trending faults. These faults have been proved by satellite-borne image interpretation (Charusiri and Pum-Im, 2009).

The actual fundamental reservoir data in offshore area in the Gulf of Thailand presented in Table 3.1 for this study which are obtained from DMF and public domain. A candidate reservoir is selected to create a simulated reservoir model for this study. This candidate reservoir data has met the technical screening guidelines for CO<sub>2</sub> flooding which are presented in Table 2.2. Although the hydrostatic pressure gradient is 0.433 psi/ft. in general, this study uses the real information pressure from logging tool which has a few higher-pressure gradients (0.51 psi/ft) than hydrostatic gradient.

Table 3.1 Fundamental reservoir data in offshore area in the Gulf of Thailand

Parameter	Value	Parameter	Value
TVD Depth (ft)	5,949-5,891	Initial Reservoir Pressure (psi)	3,023
Thickness (ft)	60	Initial Temperature (°F)	257
Porosity (fraction)	0.21-0.29	Median Porosity	0.23
Horizontal Permeability (mD)	76-717	Vertical Permeability (mD)	7.6-71.7
Rock Type	Sandstone	Fracture Pressure (psi)	4,414

### 3.2.1 Crude oil composition and PVT properties

The actual crude oil sample from exploration well in offshore area in the Gulf of Thailand is tested at the lab and reported to DMF which this study is obtained from. The lab test report gives the oil compositions and 39.6 °API gravity.

The Pressure-Volume-Temperature (PVT) properties of reservoir fluids are obtained from logging tools of the development well from both logging while drilling tools (LWD) and Wireline tools as well as core sample. The obtained data will be input into sub-ECLIPSE software which is PVTi to calculate the reservoir properties



such as bubble point pressure, critical temperature, critical pressure and related information to run in the ECLIPSE 300. Table 3.2 represents the crude oil composition in this study and Figure 3.2 represents the calculated results of PVT property curve after inputting the data into PVTi. The bubble point pressure is about 300 psi, so this reservoir is liquid phases including oil and water.

Table 3.2 The oil compositions

Hydrocarbon component	ZI (percent)	Weight fraction (percent)
C3	41.86	15.99
C8	32.72	30.33
C12	8.4	11.75
C15	7.17	12.79
C20	4.28	10.19
C25	2.67	7.98
C30	1.94	7.00
C35	0.96	3.97
Sum	100	100

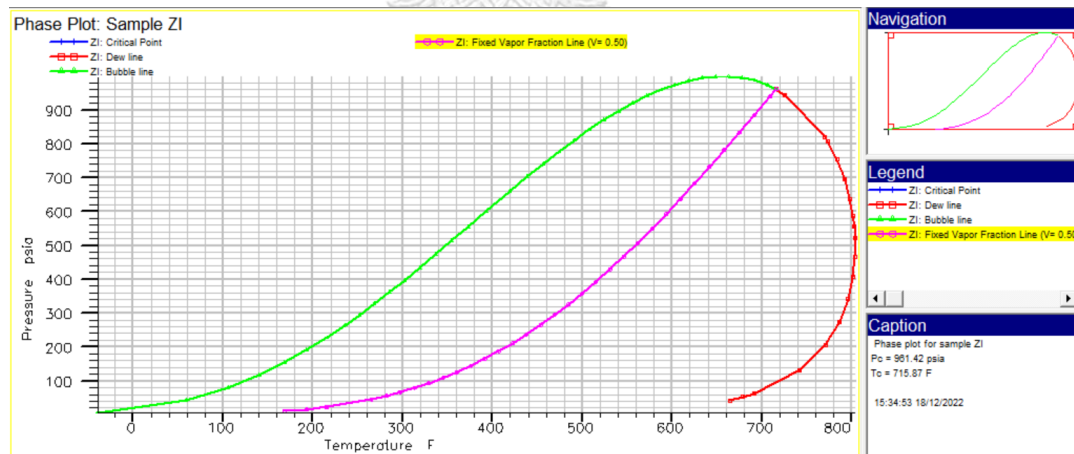


Figure 3.2 The calculated result of PVT property curve

### 3.3 Simulation Model

To simulate CO<sub>2</sub>EOR, the reservoir model set-up is required to be close to the real conditions. The reservoir model as well as all grids are created to be heterogeneous model with varying of both porosity and permeability. One injector and one producer are designed to locate at the corner of the reservoir model and the

distance between well is about 500 m. (1,640 ft). Consequently, X and Y direction distance will be 354 m (1,160 ft). Moreover, above and below of this reservoir is shale and the rock type of this reservoir is sandstone. Figure 3.3 represents X, Y and Z direction distance as well as location of Injection well and production well.

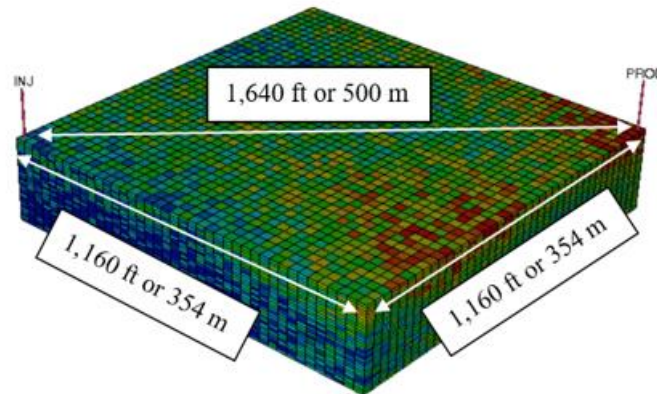


Figure 3.3 X, Y and Z direction distance in this study

### 3.3.1 Heterogenous reservoir model

Actual fundamental reservoir data in offshore area in the Gulf of Thailand from Table 3.1 will be used in this study. Each grid in the reservoir model is randomly set with the porosity data in range of 0.21-0.29 and the permeability data from 76-717 mD. The average values or medians of porosity and permeability are 0.23 and 146 mD respectively. The sandstone heterogeneous reservoir is modeled and summarized in Table 3.3 Figure 3.4 and Figure 3.5 illustrate the heterogeneous porosity distribution and permeability distribution in 3D model, respectively.

Table 3.3 Using reservoir properties for model construction

Parameter	Values	Unit
Grid dimension ( in X, Y, Z axis)	40 x 40 x 30	block
Grid size	29 x 29 x 2	ft
Reservoir size	1,160 x 1,160 x 60	ft <sup>3</sup>
Top of reservoir	5,891	ft
Reservoir thickness	60	ft
Porosity	0.21 - 0.29	fraction
Median porosity	0.23	fraction
Horizontal permeability	76 - 717	mD
Vertical permeability	0.1 * kh	mD
Median horizontal permeability	146	mD
Reservoir initial temperature	257	°F
Reservoir initial pressure	3,023	psi
Fracture pressure	4,414	psi
Working preesure at 90% of Fracture pressure	3,973	psi
Working preesure at 80% of Fracture pressure	3,531	psi
Rock type	Sandstone	

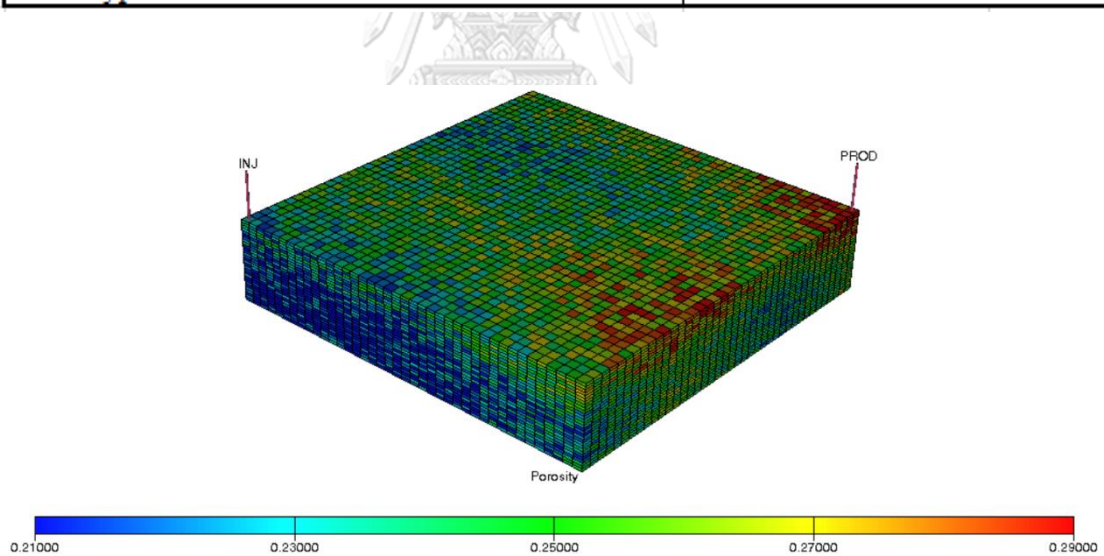


Figure 3.4 Porosity distribution in 3D model

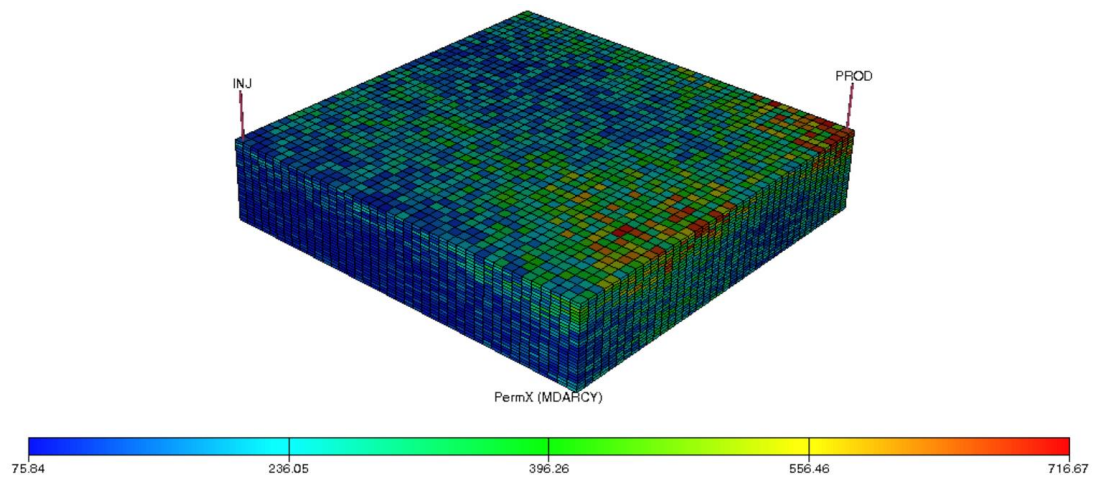


Figure 3.5 Permeability distribution in 3D model

### 3.3.2 CO<sub>2</sub> injection condition at wellhead

There are three possible CO<sub>2</sub> sources, (1) natural hydrocarbon gas reservoirs containing CO<sub>2</sub> as an impurity (Usually less than 25%), (2) industrial or anthropogenic sources with wide variation of CO<sub>2</sub> percentage in the effluent, and (3) natural CO<sub>2</sub> reservoirs. Relying on the CO<sub>2</sub> purity, the source gas would require processing in order to bring the concentration of CO<sub>2</sub> high enough (90 – 98%) for EOR, particularly for a miscible method (Verma, 2015). When CO<sub>2</sub> is supplied to CO<sub>2</sub>EOR projects, it is of high purity (>95% by volume) and in a supercritical dense phase state. At the wellhead, injected CO<sub>2</sub> is essentially consisted in a mixture of fresh pipeline supply and recycle from gas plant operations. Depending on the typical process used to recover CO<sub>2</sub> content is in the range 92 to 97% (Meyer, 2007).

Either anthropogenic CO<sub>2</sub> or geologically sourced CO<sub>2</sub> can be used in CO<sub>2</sub>EOR, although a requirement for CO<sub>2</sub> purity of higher than 95% is rule of thumb (Whittaker and Perkins, 2013). Consequently, the assumption of designed injected CO<sub>2</sub> is pure CO<sub>2</sub> (100% of CO<sub>2</sub>) in this study for the most efficiency of CO<sub>2</sub>EOR.

### 3.3.3 Well completion

Since the primary recovery stage is designed before starting of CO<sub>2</sub> injection process. The designed perforation zone is at the top part of reservoir due to the highest production of hydrocarbon expectation and the oil water contact distance. After the end of primary recovery process, the perforation zone is still kept at the top of reservoir for cost saving.

Moreover, the corrosion control is mandated for the well completion due to the mixing of water and CO<sub>2</sub>, especially in WAG process. The selected materials are based on their durability and corrosion resistance. The carbon steel casing and tubing are sensitive to corrosion. To mitigate corrosion in this study, the higher thickness and weight are based on the maximum potential burst and collapse pressure plus suitable safety factors. In deep zone, high pressure, high temperature environments, higher strength grades and corrosion resistant alloys will be used in well susceptible to CO<sub>2</sub> attack (Meyer, 2007). Consequently, the thicker wall thickness will be used and is being used in this study for casing and tubing, respectively.

## 3.4 Research methodology

The reservoir model is built by adding the input data obtained from Logging while drilling tools, wireline logging tools and core flooding. The production process starts from day one of production by the natural mechanism with artificial lift until pressure depression (around 4 years). The electrical submersible pump is applied for artificial lift technology in this study. After primary recovery, CO<sub>2</sub> flooding will be performed to extract more remaining oil in the reservoir for 20 years period. In order to compare with favorable of CO<sub>2</sub> flooding, the water alternating gas (WAG) technology will be applied for performing the simulation. Consequently, all simulation cases will be ended at 24 years after the first day of production.

The detail of the research methodology is presented below:

- 1) Prepare and collect data.
- 2) Perform literature review on CO<sub>2</sub>EOR, prepare the thesis proposal and study on ECLIPES program.

- 3) Set up the static model.
- 4) Perform simulation on fluid/dynamic model.
- 5) Run simulation with various conditions/parameters including;
  - CO<sub>2</sub> technology (CO<sub>2</sub> flooding, WAG)
  - CO<sub>2</sub> injection rate (0.2, 0.4 and 0.8 MMSCF/day)
  - Water injection rate (300 and 500 STB/day)
  - Operating pressure (80 and 90% of fracture pressure)
- 6) Evaluate the results.
- 7) Discuss the results.
- 8) Conclude the performance evaluation of CO<sub>2</sub> flooding and WAG.

The parameters of this study are using 2 technologies of CO<sub>2</sub>EOR including CO<sub>2</sub> flooding and WAG. These technologies are controlled by 2 parameters including CO<sub>2</sub> injection rate (0.2, 0.4 and 0.8 MMSCF/day), water injection rate (300 and 500 STB/day) and operating pressures at 80% and 90% of fracture pressure. These 2 parameters are monitored and evaluated to get the optimal value for performance evaluation as well as recovery factor. The parameters of this study are assigned and presented in Table 3.4

Table 3.4 The studied parameter

Technology	Injection rate (MMSCF/D - For CO <sub>2</sub> ), (STB/D - for water)	Operating pressure (% of fracture pressure) (psi)
CO <sub>2</sub> flooding (6 cases)	case 1: 0.2 case 2: 0.2 case 3: 0.4 case 4: 0.4 case 5: 0.8 case 6: 0.8	case 1: 80% case 2: 90% case 3: 80% case 4: 90% case 5: 80% case 6: 90%
WAG (8 cases)	case 7: 0.4 and 300 case 8: 0.4 and 300 case 9: 0.4 and 500 case 10: 0.4 and 500 case 11: 0.8 and 300 case 12: 0.8 and 300 case 13: 0.8 and 500 case 14: 0.8 and 500	case 7: 80% case 8: 90% case 9: 80% case 10: 90% case 11: 80% case 12: 90% case 13: 80% case 14: 90%
Injection period	20 years	

Because the rate of CO<sub>2</sub> producing in some areas in the Gulf of Thailand is around 1 MMSCF/day, the rates of CO<sub>2</sub> injection are set to be less than the CO<sub>2</sub> production in that area as an assumption. Therefore, 0.8 MMSCF/day rate is assigned in this study. For the rest of CO<sub>2</sub> injection rate are at 0.4 and 0.2 MMSCF/day due to the recovery factor checking in case of half reduction of the injection rate. For the water injection rate, the less injection of water is assigned at 300 and 500 STB due to the challenging of CO<sub>2</sub> utilization and for the storage purpose in the future.

The basic methodology of this study for both 2 technologies CO<sub>2</sub> flooding and WAG in the heterogeneous reservoir model are illustrated in Figure 3.6.



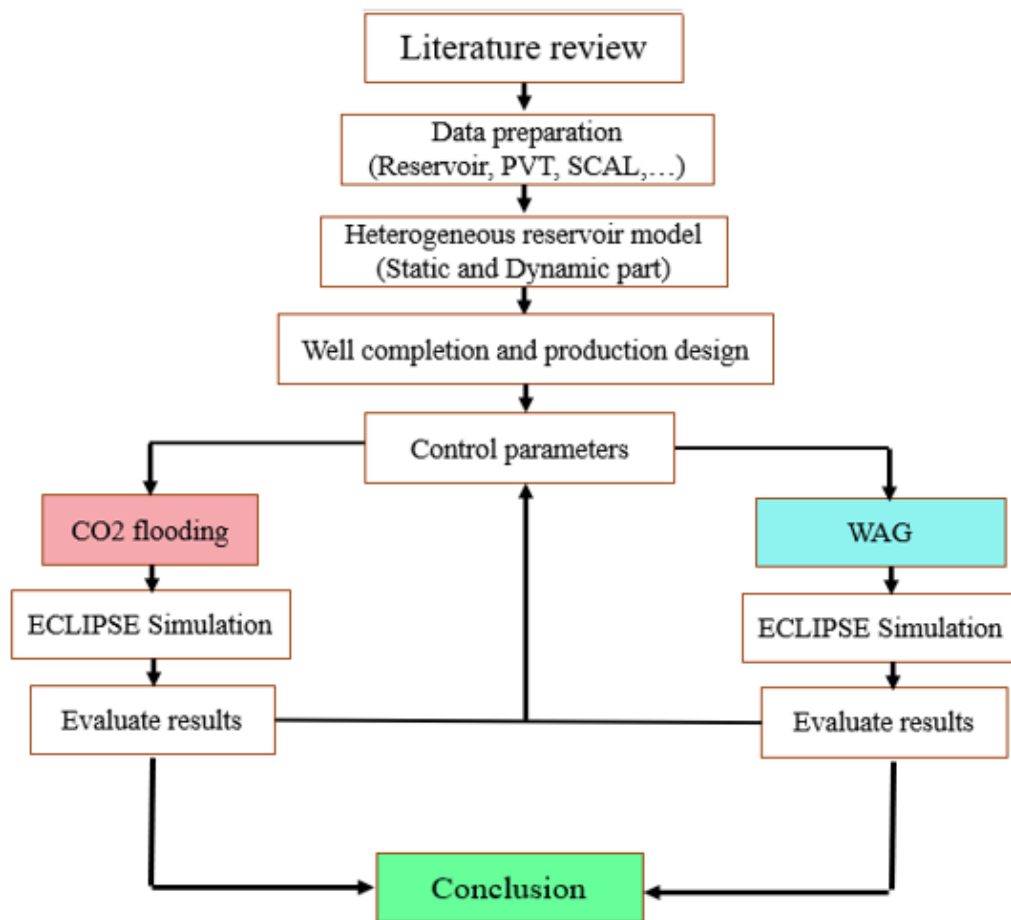


Figure 3.6 Working flow chart of methodology of this study



## CHAPTER 4

### RESULTS AND DISCUSSION

Data preparation part is in the beginning part of methodology. The heterogeneous reservoir model is constructed based on the actual data from offshore area in the Gulf of Thailand. Likewise, the fluid properties and relative permeability data are also added into the reservoir model. Furthermore, the reservoir pressure will be monitored to prevent the fracture of the formation.

The results and discussion in this chapter are obtained from the reservoir heterogeneous model with studied parameters in Table 3.3 by ECLIPSE 300 simulation and based on primary recovery around 4 years and 20 years of CO<sub>2</sub>EOR including CO<sub>2</sub> flooding and WAG. All studied cases end at 24 years. The heterogeneous reservoir model in this study has 1,143,508 STB of total original oil in place (OOIP). The varied operating parameters of both CO<sub>2</sub> flooding and WAG technologies are simulated by ECLIPSE 300. Finally, the results of each studied parameters and technology will be discussed in this chapter. After the primary production, the oil in place will be 1,071,821 STB. The total original oil in place is represented in Figure 4.1.

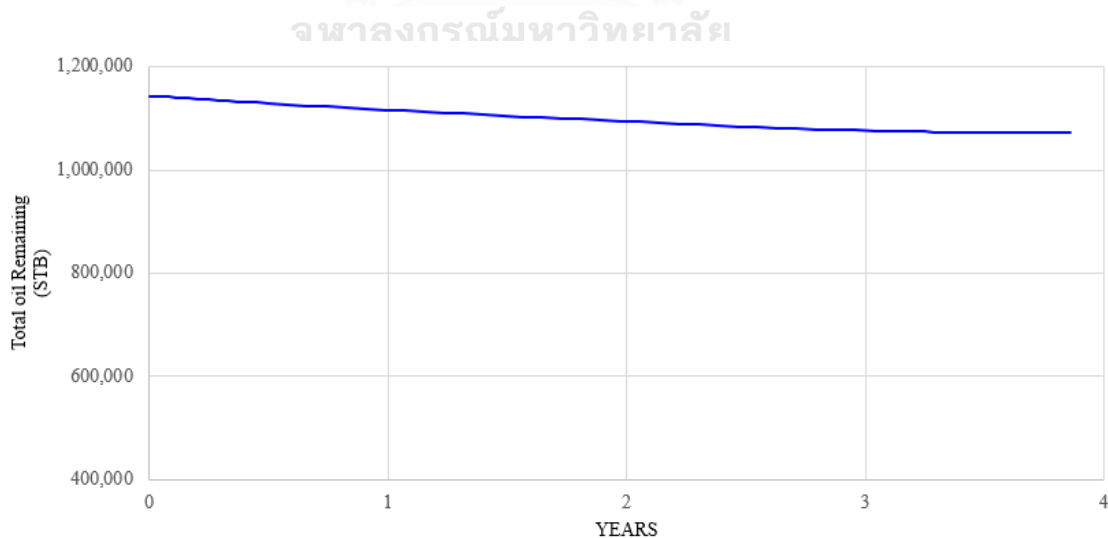


Figure 4.1 Total original oil in place in this study

#### 4.1 Reservoir depletion

Since the heterogeneous reservoir model is completed, the reservoir is produced by natural drive with artificial lift in order to reservoir depletion. The recognized initial pressure is 3,023 psi before starting production. At the depletion stage, the reservoir pressure is lowered to 840 psi which is an initial pressure of CO<sub>2</sub>EOR. The reservoir depletion is produced around 4 years until insufficient energy support. The pressure profile is represented in Figure 4.2.

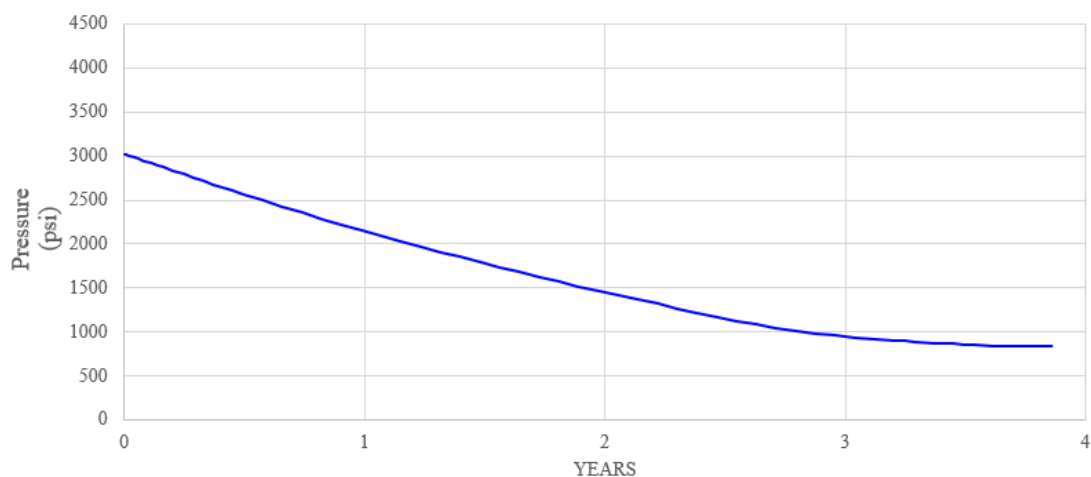


Figure 4.2 Profile of reservoir pressure

To observe the natural drive performance of primary recovery stage, the total oil production and recovery factor are the key results. The total production and recovery factor are 0.07 MMSTB. and 6.3%, respectively. Due to the calculation of the bubble point pressure or  $P_b$  from crude component in PVTi program is around 300 psi and the depletion drive without the aquifer support as shown in the water cut curve causes the low recovery factor in the primary recovery stage. Figure 4.3 and 4.4 represent the total production and recovery factor in primary recovery stage respectively. Furthermore, Figure 4.5 – 4.7 represent the oil production rate per day, water production rate and water cut in primary recovery stage, respectively. The results of oil production and production data at the end of depletion stage or natural drive stage of this study are presented in Table 4.1 and 4.2, respectively.

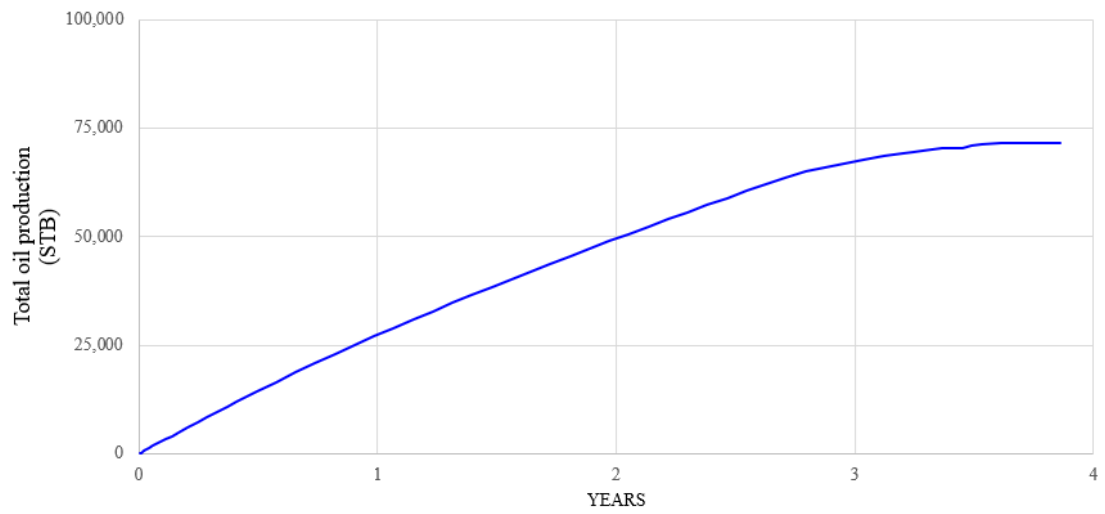


Figure 4.3 Total oil production in primary recovery stage

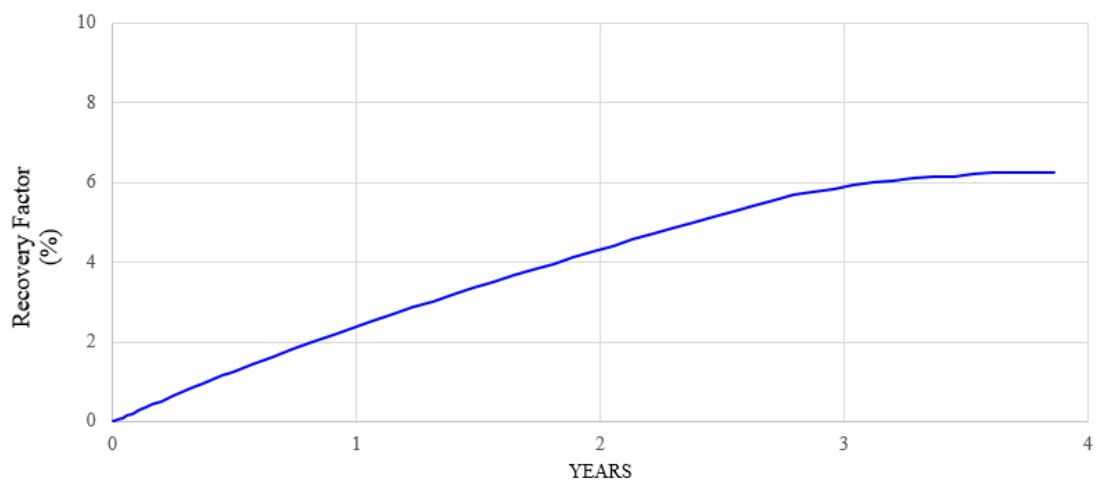


Figure 4.4 Recovery factor in primary recovery stage

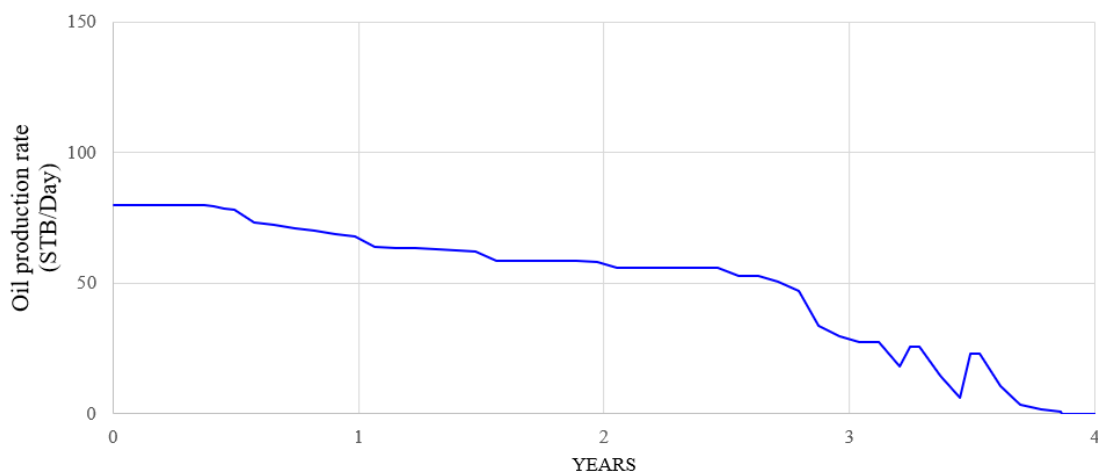


Figure 4.5 Oil production rate per day in primary recovery stage



Figure 4.6 Water production rate per day in primary recovery stage

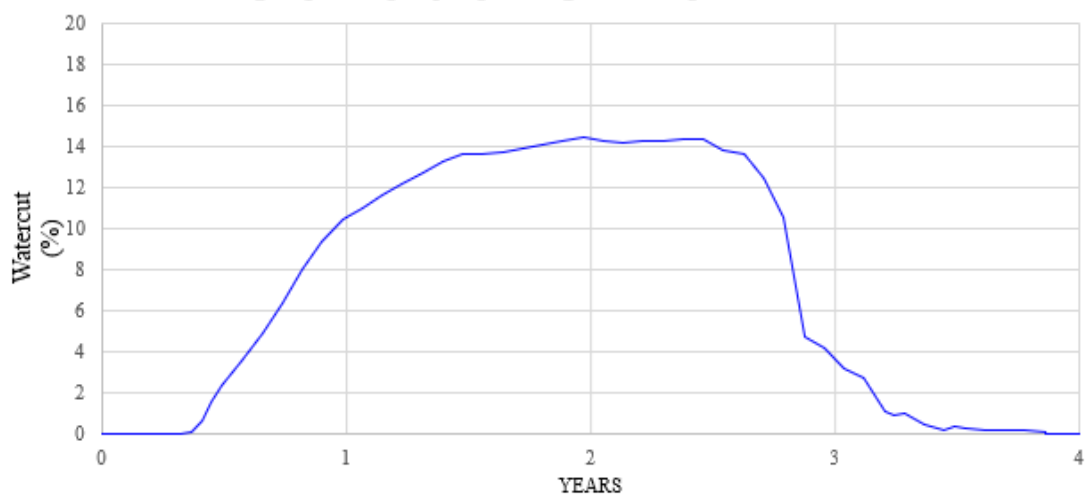


Figure 4.7 The water cut in primary recovery stage

Table 4.1 Results of oil production at the end of primary production

<b>Result</b>	<b>Initial value</b>	<b>Final value</b>	<b>Unit</b>
Oil in place	1,143,508	1,071,821	STB
Total oil production	0	71,687	STB
Total water production	0	7,058	STB
Recovery factor	0	6.3	%
Reservoir pressure	3,023	840	psi

Table 4.2 Production data at the end of primary production

<b>Statistic information</b>	<b>Min</b>	<b>Max</b>	<b>AVG</b>	<b>Unit</b>
Oil production rate/day	0	80	55	STB
Water production rate/day	0	10	4	STB
Water cut	0	14	6	%

## 4.2 Simulation results of CO<sub>2</sub>EOR

In this study, there are 2 technologies of CO<sub>2</sub>EOR with various designed injection rates of CO<sub>2</sub> and water as well as operating pressure. Consequently, there are 14 total cases which includes 6 cases of CO<sub>2</sub> flooding and 8 cases of WAG. Table 4.3 represents all cases in this study. For every case, the CO<sub>2</sub> injection starts after the reservoir depletion (around 4 years) to increase reservoir pressure and continuously injects CO<sub>2</sub> for 20 years to produce remaining oil. Reservoir pressure is one of parameters to be monitored. All case results include total oil production, recovery factor, remaining oil in place, reservoir pressure, oil and water production rate, water cut, total CO<sub>2</sub> and water injection and gas oil ratio are presented in term of curves.

Table 4.3 Studied cases

Study case	Technology	Injection rate (MMSCF/D - For CO <sub>2</sub> ), (STB/D - for water)	Operating pressure (% of fracture pressure) (psi)
1	CO <sub>2</sub> flooding	CO <sub>2</sub> : 0.2	80%
2	CO <sub>2</sub> flooding	CO <sub>2</sub> : 0.2	90%
3	CO <sub>2</sub> flooding	CO <sub>2</sub> : 0.4	80%
4	CO <sub>2</sub> flooding	CO <sub>2</sub> : 0.4	90%
5	CO <sub>2</sub> flooding	CO <sub>2</sub> : 0.8	80%
6	CO <sub>2</sub> flooding	CO <sub>2</sub> : 0.8	90%
7	WAG	CO <sub>2</sub> : 0.4, Water : 300	80%
8	WAG	CO <sub>2</sub> : 0.4, Water : 300	90%
9	WAG	CO <sub>2</sub> : 0.4, Water : 500	80%
10	WAG	CO <sub>2</sub> : 0.4, Water : 500	90%
11	WAG	CO <sub>2</sub> : 0.8, Water : 300	80%
12	WAG	CO <sub>2</sub> : 0.8, Water : 300	90%
13	WAG	CO <sub>2</sub> : 0.8, Water : 500	80%
14	WAG	CO <sub>2</sub> : 0.8, Water : 500	90%

The performance of CO<sub>2</sub>EOR process is continually monitored by analyzing all the aspects of process; performance of oil production, gas oil ratio (GOR) and water cut to support for improving of recovery factor (Verma, 2015).

#### 4.2.1 Results of CO<sub>2</sub> flooding technology

Case 1 to Case 6 are designed to simulate CO<sub>2</sub> flooding technology with varied CO<sub>2</sub> injection rates and operating pressures. The designed CO<sub>2</sub> injection rate are set in the assumption that CO<sub>2</sub> supply from daily produced CO<sub>2</sub> in a wellhead platform. There are 3 rates of injection including 0.2 MMSCF/day, 0.4 MMSCF/day and 0.8 MMSCF/day. Then, each rate is separated into 2 cases by operating pressure in order to preventing rock fracture. Table 4.4 represents all cases of CO<sub>2</sub> flooding.

Table 4.4 CO<sub>2</sub> flooding technology cases

Study case	Technology	Injection rate (MMSCF/D - For CO <sub>2</sub> ), (STB/D - for water)	Operating pressure (% of fracture pressure) (psi)
1	CO <sub>2</sub> flooding	CO <sub>2</sub> : 0.2	80%
2	CO <sub>2</sub> flooding	CO <sub>2</sub> : 0.2	90%
3	CO <sub>2</sub> flooding	CO <sub>2</sub> : 0.4	80%
4	CO <sub>2</sub> flooding	CO <sub>2</sub> : 0.4	90%
5	CO <sub>2</sub> flooding	CO <sub>2</sub> : 0.8	80%
6	CO <sub>2</sub> flooding	CO <sub>2</sub> : 0.8	90%

The results from case 1 to case 6 simulations are represented in the plotted curves from Figure 4.8 to Figure 4.16 and Table 4.5 to Table 4.7. Table 4.5 represents the total oil production and recovery factor of all CO<sub>2</sub> flooding cases at the end of 24 years since first oil production with natural drive and Figure 4.8, Figure 4.9 and Figure 4.10 illustrate the total oil production, recovery factor, remaining oil in place of CO<sub>2</sub> flooding for Case 1 to 6, respectively.

Table 4.5 Total oil production and recovery factor at the end of simulation of CO<sub>2</sub> flooding for 24 years

Study case	Technology	Injection rate (MMSCF/D - For CO <sub>2</sub> ), (STB/D - for water)	Operating pressure (% of fracture pressure) (psi)	Total production volume (STB)	Recovery factor (%)
1	CO <sub>2</sub> flooding	CO <sub>2</sub> : 0.2	80%	331,634	29.0
2	CO <sub>2</sub> flooding	CO <sub>2</sub> : 0.2	90%	342,955	30.0
3	CO <sub>2</sub> flooding	CO <sub>2</sub> : 0.4	80%	402,359	35.2
4	CO <sub>2</sub> flooding	CO <sub>2</sub> : 0.4	90%	407,550	35.6
5	CO <sub>2</sub> flooding	CO <sub>2</sub> : 0.8	80%	490,196	42.9
6	CO <sub>2</sub> flooding	CO <sub>2</sub> : 0.8	90%	492,893	43.1

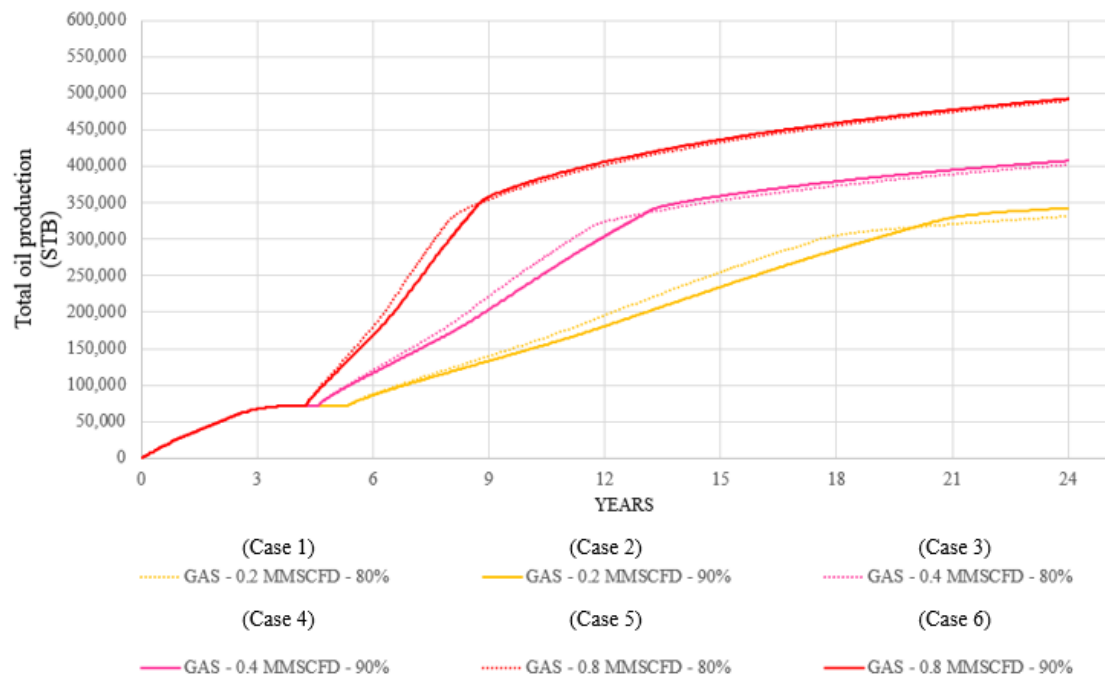


Figure 4.8 Total oil production of CO<sub>2</sub> flooding for case 1 to 6

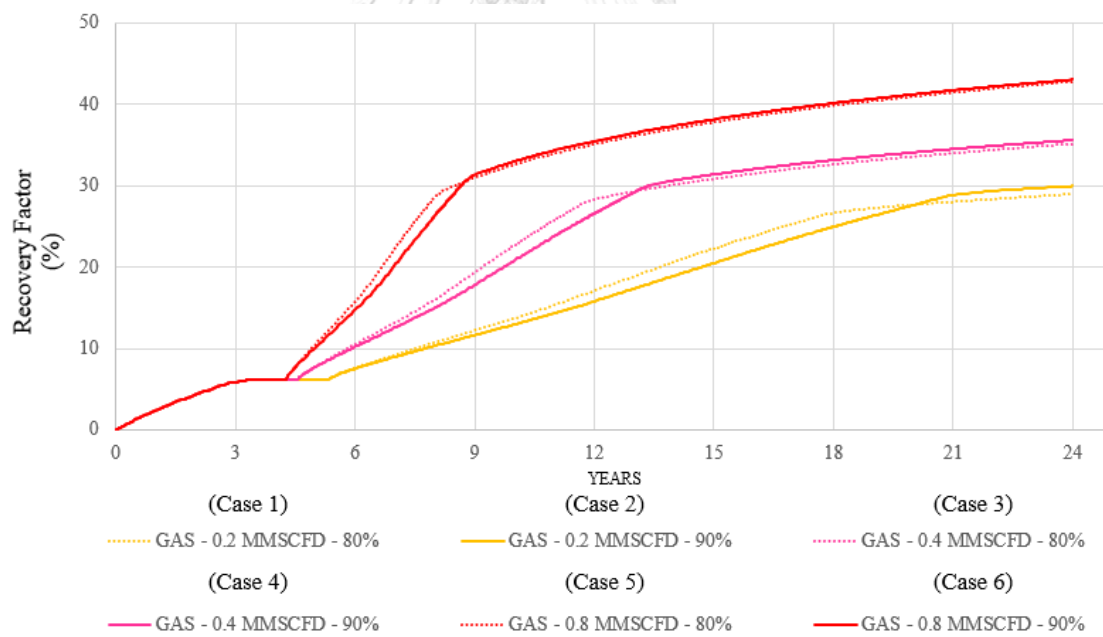


Figure 4.9 Recovery factor of CO<sub>2</sub> flooding for Case 1 to 6



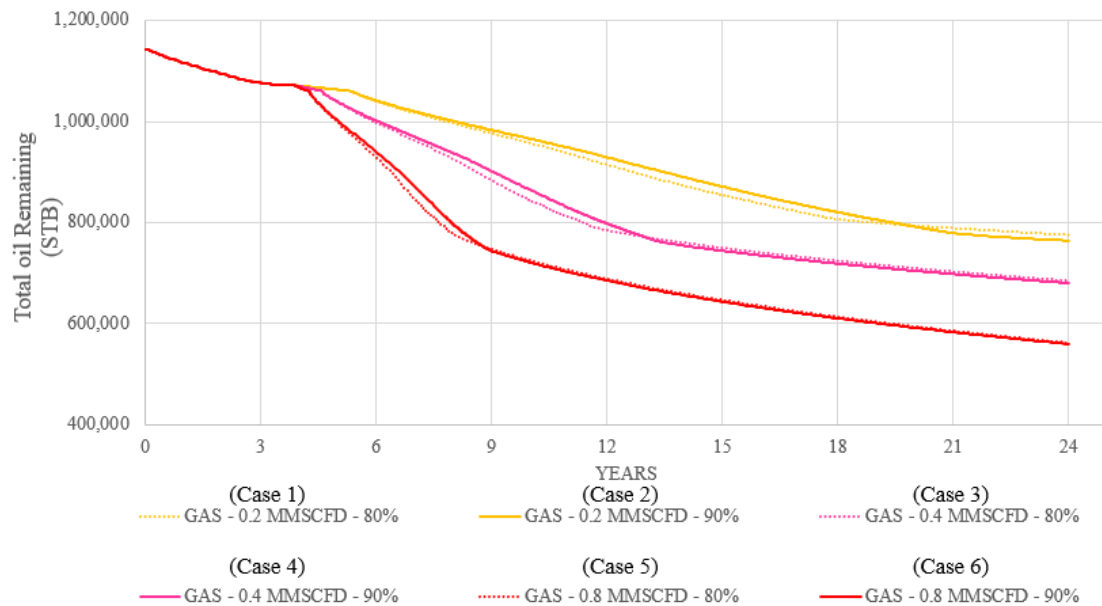


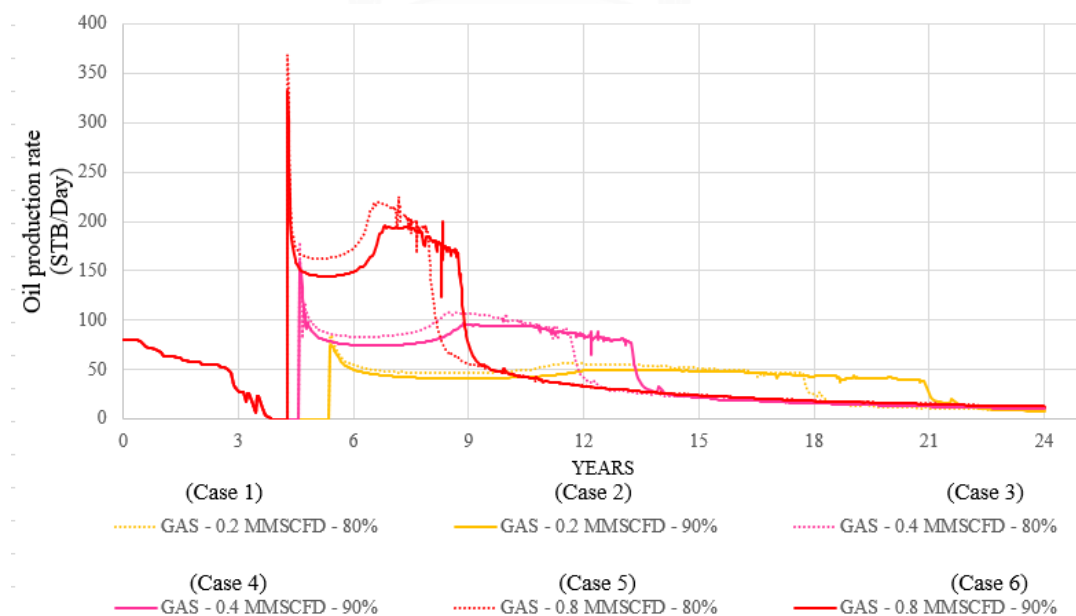
Figure 294.10 Remaining oil in place of CO<sub>2</sub> flooding for Case 1 to 6

From Table 4.5 and Figure 4.8 and 4.9, the results from the 6 cases of CO<sub>2</sub> flooding, which presented in Table 4.5 and Figure 4.8 – 4.10, Case 6 (injection rate of CO<sub>2</sub> at 0.8 MMSCF/day with 90% operating pressure of fracture pressure) has the highest total oil production at 492,900 STB as well as the recovery factor at 43.1%. Consequently, the remaining oil in place is around 559,400 STB. The worst case of CO<sub>2</sub> flooding is Case 1 (injection rate of CO<sub>2</sub> at 0.2 MMSCF/day with 80% operating pressure of fracture pressure) which has the lowest total oil production at 331,600 STB and the recovery factor at 29%. Therefore, the remaining oil in place is around 775,600 STB. Although, the recoveries of the individual reservoirs differ from each other, they all show a similar trend of oil recoveries that increase with injection volume of CO<sub>2</sub> rate (Verma, 2015; Azzolina et. al., 2014). Not only the higher rate of injection causes the increase in oil recovery, but also the higher operating pressure gives the higher oil production because of ability of miscible CO<sub>2</sub> which is nearly MMP (Mansour, 2018) and maintaining the reservoir pressure and the drive mechanism. The remaining oil in place represents in Table 4.6

Table 4.6 Remaining oil in place from CO<sub>2</sub> flooding case

Study case	Technology	Injection rate (MMSCF/D - For CO <sub>2</sub> ), (STB/D - for water)	Operating pressure (% of fracture pressure) (psi)	Remaining oil in place (STB)
1	CO <sub>2</sub> flooding	CO <sub>2</sub> : 0.2	80%	775,559
2	CO <sub>2</sub> flooding	CO <sub>2</sub> : 0.2	90%	764,076
3	CO <sub>2</sub> flooding	CO <sub>2</sub> : 0.4	80%	684,786
4	CO <sub>2</sub> flooding	CO <sub>2</sub> : 0.4	90%	680,241
5	CO <sub>2</sub> flooding	CO <sub>2</sub> : 0.8	80%	561,765
6	CO <sub>2</sub> flooding	CO <sub>2</sub> : 0.8	90%	559,357

Furthermore, the oil and water production rates per day are represented in Figure 4.11 and Figure 4.12, respectively. To compare between oil and water production, the water cut curve is represented in Figure 4.13. Due to the controlling of operating pressure by managing the production rate, the higher production rate is set for the lower operating pressure. From Figure 4.11 and Figure 4.12, the oil and water production rate of 80% are higher than that of 90% of fracture pressure cases at the early stage of CO<sub>2</sub> flooding of every cases. The highest of production rate gives the highest water cut which 58%, 52% and 48% (injection rate at 0.8, 0.4 and 0.2 MMSCF/day), respectively. The trend of produced water decreases with time which presented in Figure 4.13.

Figure 4.11 Oil production rate of CO<sub>2</sub> flooding for Case 1 to 6

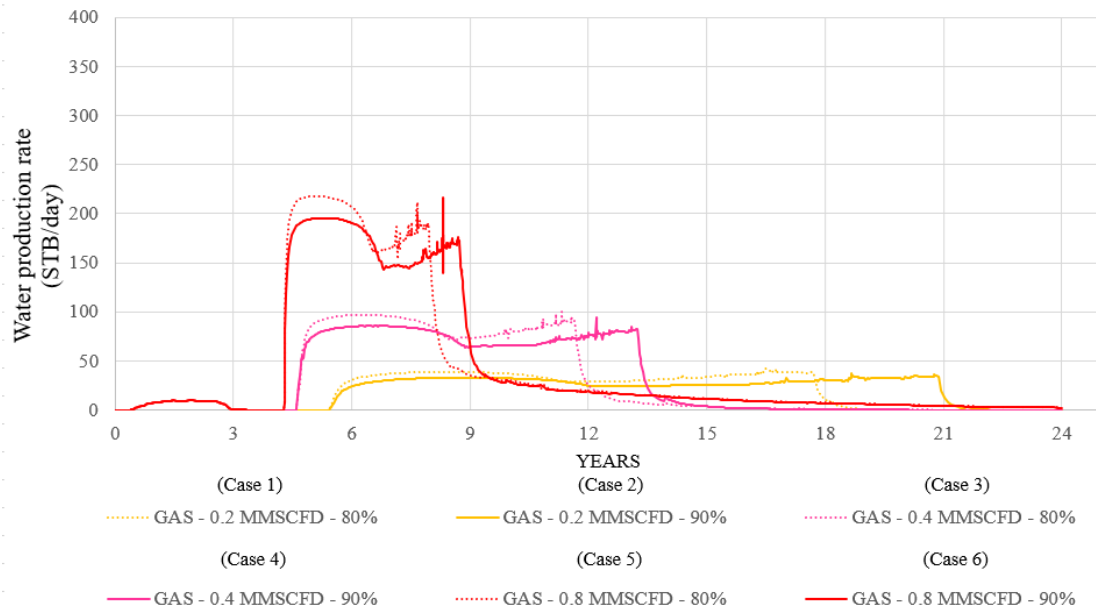


Figure 4.12 Water production rate of CO<sub>2</sub> flooding for Case 1 to 6

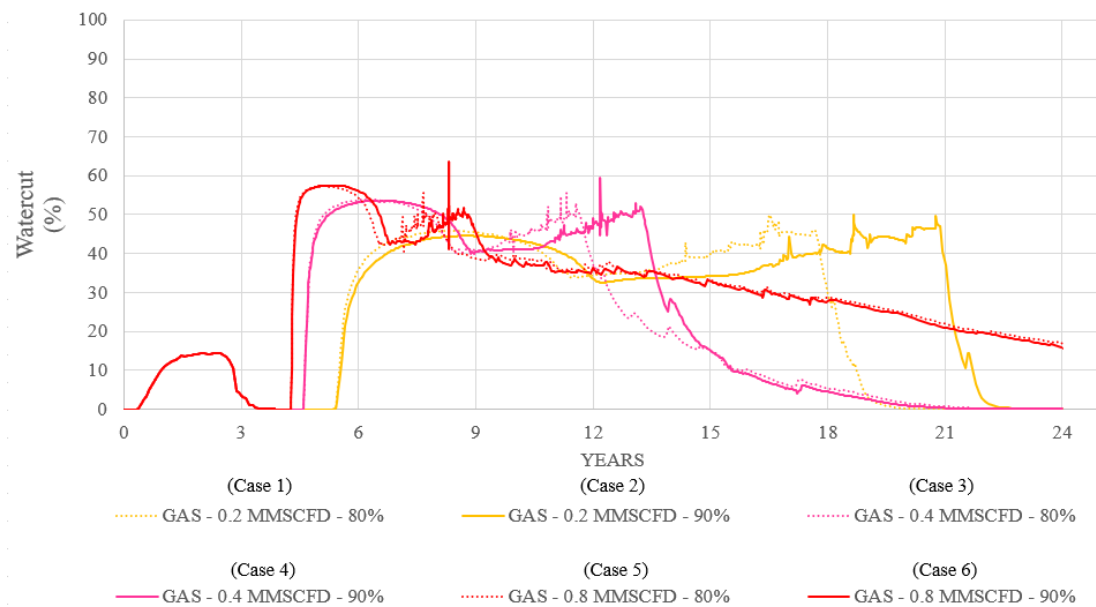


Figure 4.13 Water cut of CO<sub>2</sub> flooding for Case 1 to 6

To control the operating pressure, the oil production rate is adjusted to apply for each individual case. The operating pressures are 80% and 90% of fracture pressure. The operating pressure is illustrated in Figure 4.14, the solid curves and the dash curve represent 90% and 80% of fracture pressure respectively. Pressure for all CO<sub>2</sub> flooding cases is lower than the calculated fracture pressure at 4,414 psi (purple

curve). When the injected CO<sub>2</sub> breakthroughs from the injection well to the production well, the reservoir pressure decreases until it hits equilibrium stage.

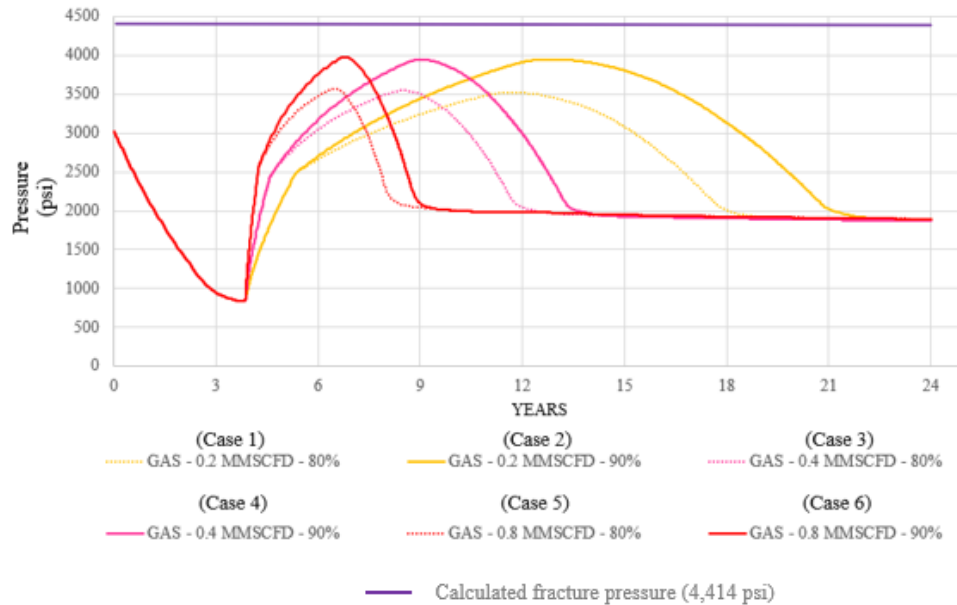
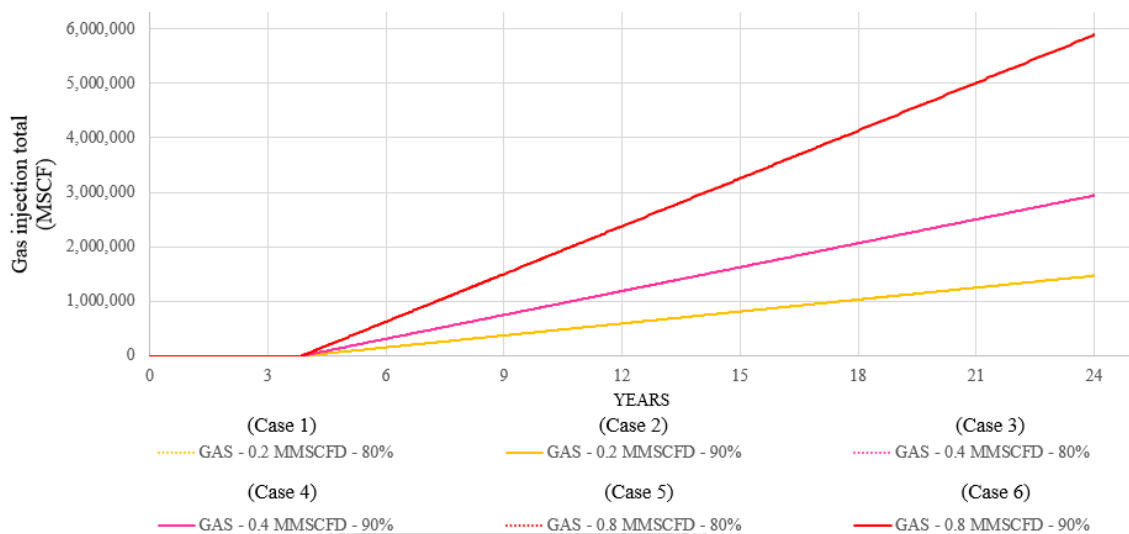


Figure 4.14 Reservoir pressure of CO<sub>2</sub> flooding (case 1 to 6)

In the case of total CO<sub>2</sub> injection, the results of total CO<sub>2</sub> injection are represented in Table 4.7 and illustrated in Figure 4.15. The highest total CO<sub>2</sub> injection are the case that CO<sub>2</sub> is injected with highest rate which are 0.8 MMSCF/day for Case 5 and 6. The higher injection rate of both 80% and 90% of fracture pressure result in the higher total of CO<sub>2</sub> injection. Due to the same injection rate, the total injection is equal, despite of the difference of operating pressure. The total CO<sub>2</sub> injection rates at 0.8 MMSCF/day of both 80% and 90% are 5,903,000 MSCF which is the highest value and decreasing of the injection rate give the lower of total CO<sub>2</sub> injection.

Table 4.7 Total CO<sub>2</sub> injection volume of CO<sub>2</sub> flooding cases

Case	Injection rate (MMSCF/D - For CO <sub>2</sub> )	Operating pressure (% of fracture pressure) (psi)	Total CO <sub>2</sub> injection volume (MSCF)
1	CO <sub>2</sub> : 0.2	80%	1,474,400
2	CO <sub>2</sub> : 0.2	90%	1,474,400
3	CO <sub>2</sub> : 0.4	80%	2,946,600
4	CO <sub>2</sub> : 0.4	90%	2,946,600
5	CO <sub>2</sub> : 0.8	80%	5,902,800
6	CO <sub>2</sub> : 0.8	90%	5,902,800

Figure 4.15 Total CO<sub>2</sub> injection of CO<sub>2</sub> flooding cases

Besides, the performance of oil production, and water cut to support for improving of recovery factor, Gas oil ratios (GOR) is another factor to be monitored (Verma, 2015). GORs of these cases are illustrated in Figure 4.16. In this result, the highest rate of injection has the fastest CO<sub>2</sub> breakthrough due to the amount of injection and the displacing fluid viscosity (CO<sub>2</sub>) (Thomas, 2008). Consequently, the 0.8 MMSCF/day of 80% of injection is the fastest CO<sub>2</sub> breakthrough because of (1) the amount of CO<sub>2</sub> injection rate and (2) set up production rate due to the controlling of operating pressure. The rest of cases give the same result with the same reasons. Finally, for all cases at some states of production period, the GOR of the higher operating pressure is higher than that of the lower operating pressure due to the increase in the total oil production at the time with the same gas production after the gas breakthrough.

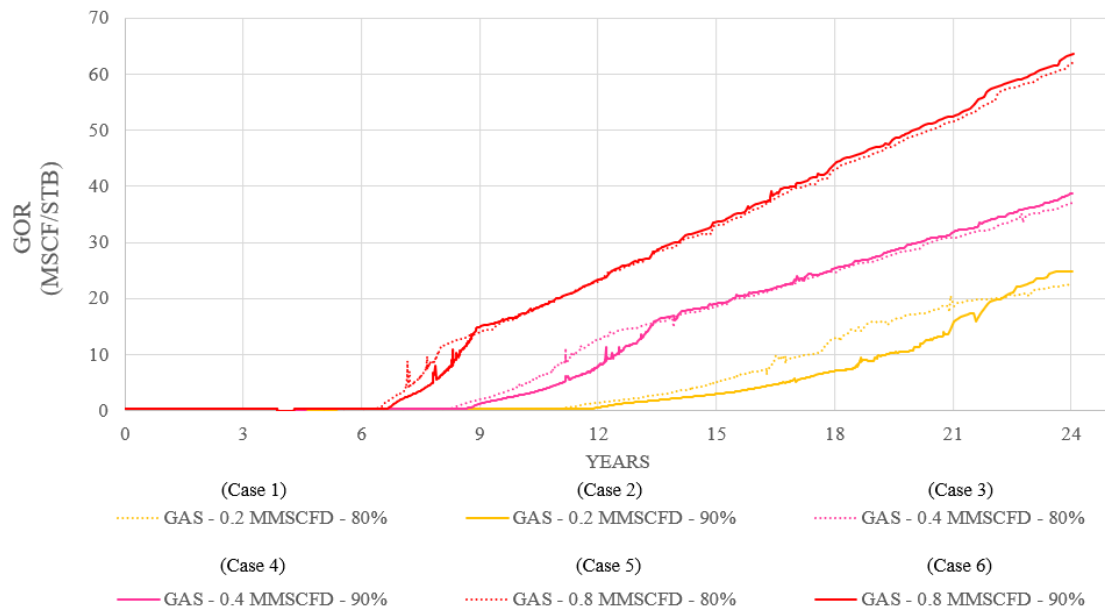


Figure 4.16 Gas oil ratio (GORs) of CO<sub>2</sub> flooding cases

At the end of production of CO<sub>2</sub> flooding cases, the injection of 0.8 MMSCF/day with 90% of fracture pressure or Case 6 has the highest total oil production and recovery factor at 492,893 STB and 43.1%, respectively. The remaining oil in place is 559,357 STB. The maximum of water cut of all CO<sub>2</sub> flooding cases is in range of 40 – 60% and the oil and water production rate declines through the end of production. Case 6 has the highest 57.5% of water cut. In case of reservoir pressure, the pressure of reservoir continuously increases since the first day of CO<sub>2</sub> injection until the CO<sub>2</sub> breakthrough. Therefore, the pressure suddenly drops to the equilibrium pressure. The gas oil ratio (GOR) can indicate the breakthrough time, in case of the higher rate of injection and the higher rate of production, the breakthrough time becomes faster. The CO<sub>2</sub> injection at injection rate of 0.8 MMSCF/day with 80% of fracture pressure or Case 5 is the fastest of the breakthrough time due to the rate of production and the rate of injection. The highest of total CO<sub>2</sub> injection are Case 5 and Case 6 at 5,903,000 MSCF. Consequently, because of the special property of CO<sub>2</sub>, CO<sub>2</sub> improves the total oil production and oil recovery by lowering the interfacial tension, oil swelling, reducing oil viscosity and mobilizing the lighter components of the oil (Verma, 2015). Therefore, MMP and amount of CO<sub>2</sub> are necessary parameters for the enhanced oil recovery process.

#### 4.2.2 Result of water alternating gas (WAG) technology

Case 7 to Case 14 are designed to simulate the application of water alternating gas (CO<sub>2</sub>) (WAG) technology with varied CO<sub>2</sub> – water injection and operating pressure. The designed CO<sub>2</sub> injection rate on the CO<sub>2</sub> flooding technology result in the previous section. The 0.8 MMSCF/day and 0.4 MMSCF/day rate of CO<sub>2</sub> injection are designed for the injection rate of CO<sub>2</sub>. Water injection rate at 300 BBL/day and 500 BBL/day are applied with two CO<sub>2</sub> injection rates. The operating pressures at 80% and 90% of fracture pressure are the one of control parameters in order to preventing rock fracture. Table 4.8 represents all cases of WAG.

Table 4.8 WAG technology cases

Study case	Technology	Injection rate (MMSCF/D - For CO <sub>2</sub> ), (STB/D - for water)	Operating pressure (% of fracture pressure) (psi)
7	WAG	CO <sub>2</sub> : 0.4, Water : 300	80%
8	WAG	CO <sub>2</sub> : 0.4, Water : 300	90%
9	WAG	CO <sub>2</sub> : 0.4, Water : 500	80%
10	WAG	CO <sub>2</sub> : 0.4, Water : 500	90%
11	WAG	CO <sub>2</sub> : 0.8, Water : 300	80%
12	WAG	CO <sub>2</sub> : 0.8, Water : 300	90%
13	WAG	CO <sub>2</sub> : 0.8, Water : 500	80%
14	WAG	CO <sub>2</sub> : 0.8, Water : 500	90%

The result from Case 7 to Case 14 simulations are reported in Figure 4.17 to Figure 4.26 and Table 4.8 to Table 4.11. Table 4.9 represents the total production and recovery factor of all WAG cases at the end of 24 years since the first oil production with natural drive and Figure 4.17, Figure 4.18 and Figure 4.19 illustrate the total oil production, recovery factor and remaining oil in place of WAG for Case 7 to Case 14, respectively.

Table 4.9 Total production and recovery factor at the end of simulation of WAG for 24 years

Study case	Technology	Injection rate (MMSCF/D - For CO <sub>2</sub> ), (STB/D - for water)	Operating pressure (% of fracture pressure) (psi)	Total production volume (STB)	Recovery factor (%)
7	WAG	CO <sub>2</sub> : 0.4, Water : 300	80%	503,944	44.1
8	WAG	CO <sub>2</sub> : 0.4, Water : 300	90%	509,116	44.5
9	WAG	CO <sub>2</sub> : 0.4, Water : 500	80%	532,345	46.6
10	WAG	CO <sub>2</sub> : 0.4, Water : 500	90%	537,685	47.0
11	WAG	CO <sub>2</sub> : 0.8, Water : 300	80%	537,036	47.0
12	WAG	CO <sub>2</sub> : 0.8, Water : 300	90%	541,525	47.4
13	WAG	CO <sub>2</sub> : 0.8, Water : 500	80%	544,924	47.7
14	WAG	CO <sub>2</sub> : 0.8, Water : 500	90%	550,496	48.1

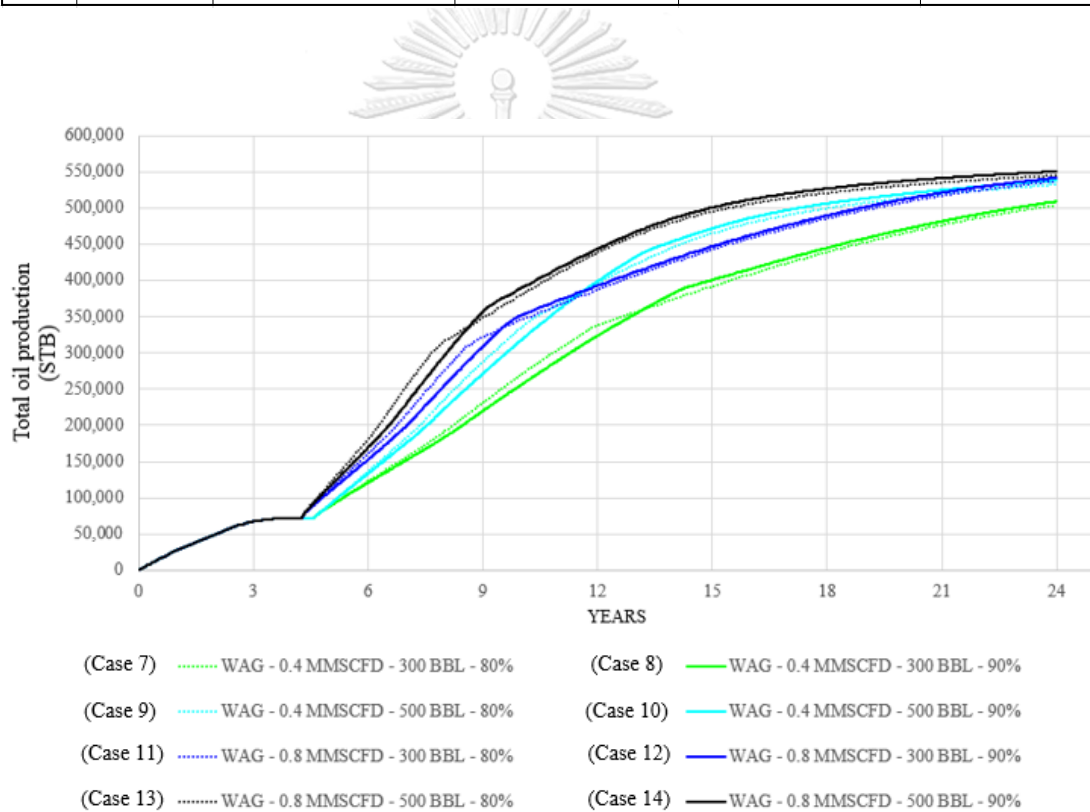


Figure 4.17 Total oil production of WAG for Case 7 to 14



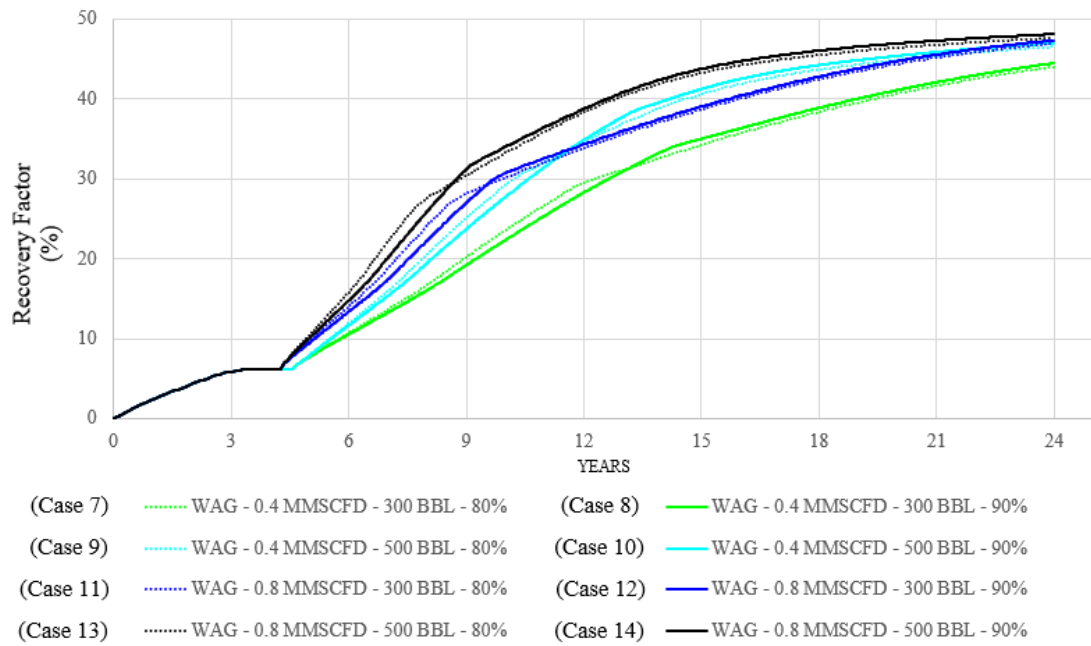


Figure 4.18 Recovery factor of WAG for Case 7 to 14

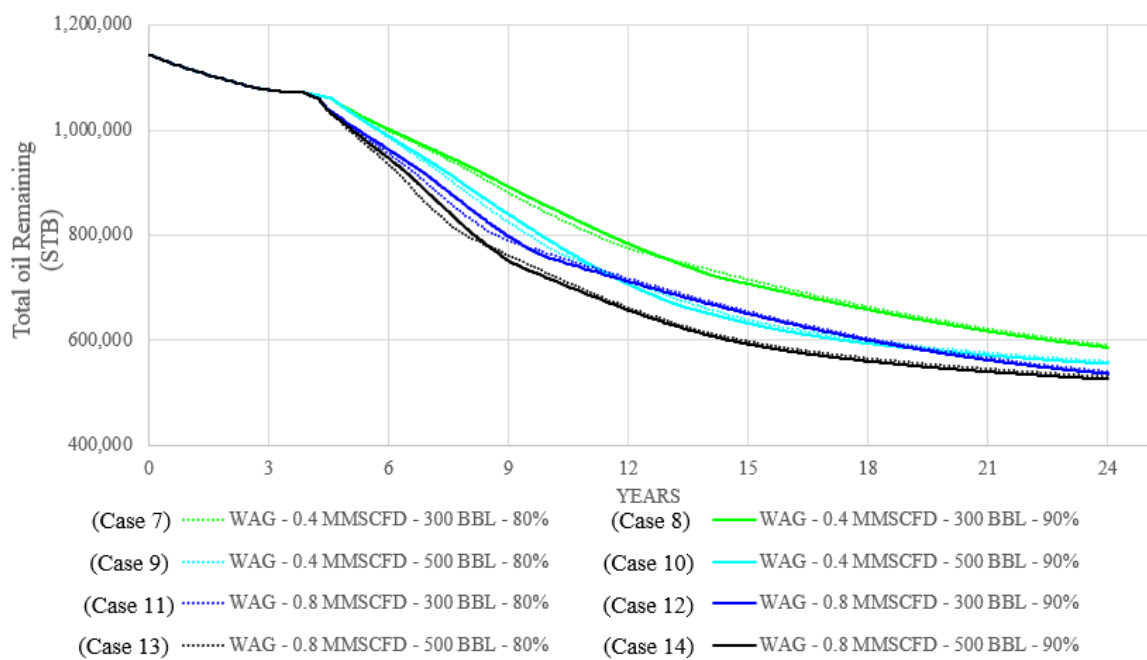


Figure 4.19 Remaining oil in place of WAG for Case 7 to 14

The results from 8 cases of WAG, which presented in Table 4.9 and Figure 4.17 to Figure 4.19, Case 14 (injection rate of CO<sub>2</sub> at 0.8 MMSCF/day and injection rate of water at 500 STB/day with 90% operating pressure of fracture pressure) has the highest total oil production at 550,500 STB as well as recovery factor at 48.1%. Consequently, the remaining oil in place will be around 526,300 STB. The worst case of WAG is Case 7 (injection rate of CO<sub>2</sub> at 0.4 MMSCF/day and injection rate of water at 300 STB/day with 80% operating pressure of fracture pressure) which has the lowest total oil production at 503,900 STB and recovery factor at 44.1%. Consequently, the remaining oil in place is around 591,200 STB. WAG technology improves the total recovery factor because water provides the mobility control of water and gas phases, better sweep control (Bhatia et. al., 2014). Furthermore, the higher rate of injection can cause an increase in production (Verma, 2015; Azzolina et. al., 2014). Lastly, not only the higher rate of injection causes the increasing in oil recovery, but also the higher operating pressure give the higher oil production because of the ability of miscible CO<sub>2</sub> which is nearly MMP (Mansour, 2018) and maintaining the reservoir pressure and the drive mechanism. The remaining oil in place represents is shown in Table 4.9.

Table 4.10 Remaining oil in place volume of WAG case

Study case	Technology	Injection rate (MMSCF/D - For CO <sub>2</sub> ), (STB/D - for water)	Operating pressure (% of fracture pressure) (psi)	Remaining oil in place (STB)
7	WAG	CO <sub>2</sub> : 0.4, Water : 300	80%	591,209
8	WAG	CO <sub>2</sub> : 0.4, Water : 300	90%	586,333
9	WAG	CO <sub>2</sub> : 0.4, Water : 500	80%	560,250
10	WAG	CO <sub>2</sub> : 0.4, Water : 500	90%	555,632
11	WAG	CO <sub>2</sub> : 0.8, Water : 300	80%	541,031
12	WAG	CO <sub>2</sub> : 0.8, Water : 300	90%	536,683
13	WAG	CO <sub>2</sub> : 0.8, Water : 500	80%	531,570
14	WAG	CO <sub>2</sub> : 0.8, Water : 500	90%	526,262

Furthermore, the oil and water production rates per day are represented in Figure 4.20 and Figure 4.21, respectively. To compare between oil and water production, the water cut curve is represented in Figure 4.22. Due to controlling of the operating pressure by managing the production rate, the higher production rate is set for the

lower operating pressure. From Figure 4.20 and Figure 4.21, oil and water production rates of 80% are higher than that of 90% of fracture pressure at the early stage of CO<sub>2</sub> flooding of every cases. Moreover, water is applied into WAG technology. The produced water trend increases along with an accumulative of total water injection. The results of WAG technology demonstrate that the higher injection rate of water gives the highest water cut which 98%, 95%, 90% and 85% ((1) injection rate of CO<sub>2</sub> at 0.8 MMSCF/day and water at 500 STB/day, (2) injection rate of CO<sub>2</sub> at 0.4 MMSCF/day and water at 500 STB/day, (3) injection rate of CO<sub>2</sub> at 0.8 MMSCF/day and 300 STB/day and (4) injection rate of CO<sub>2</sub> at 0.4 MMSCF/day and 300 STB/day). Also at the same rate of water injection, the higher CO<sub>2</sub> rate gives the higher water cut.

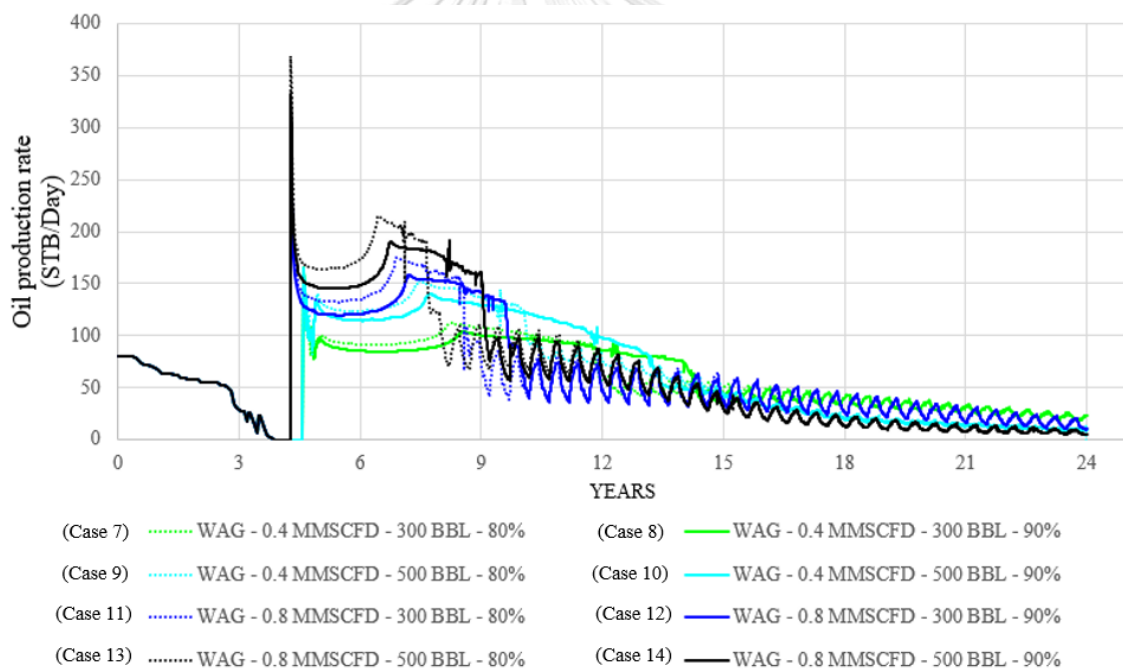


Figure 4.20 Oil production rate of WAG for Case 7 to 14

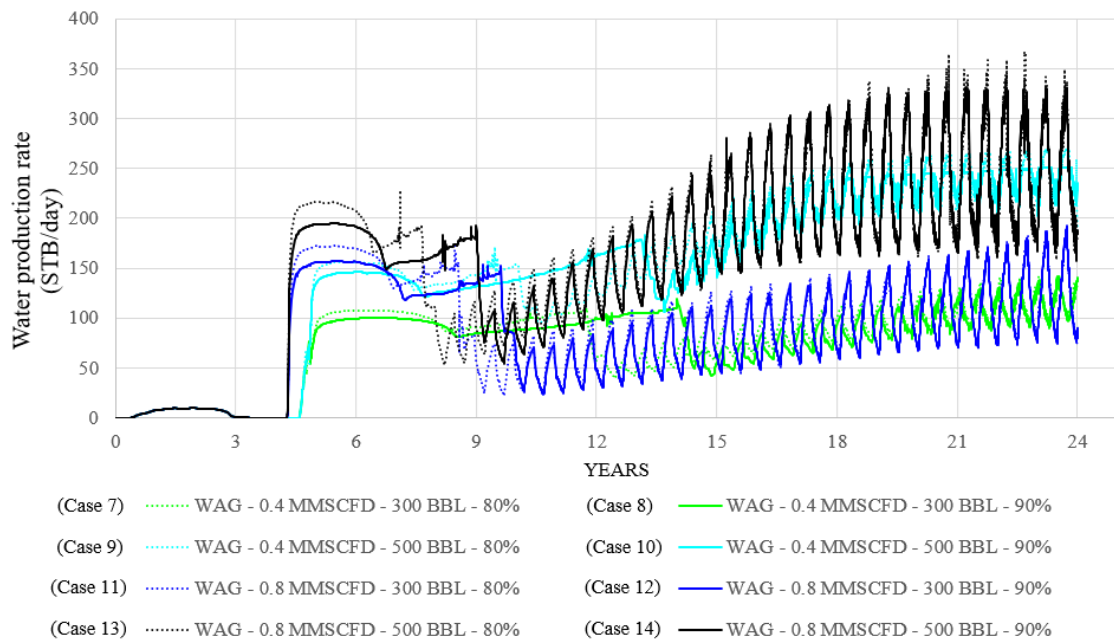


Figure 4.21 Water production rate of WAG for Case 7 to 14

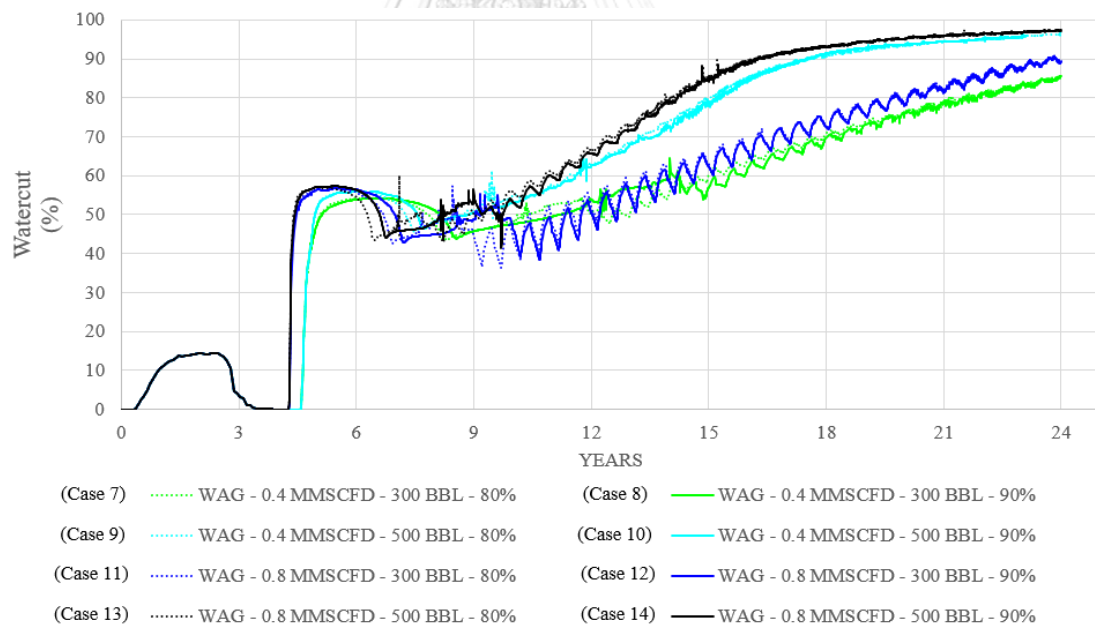


Figure 4.22 Water cut of WAG for Case 7 to 14

To control the operating pressure, the oil production rate is adjusted to apply for each individual case. The operating pressures are 80% and 90% of fracture pressure. The operating pressure is illustrated in Figure 4.23, the solid curves and the dash curve represent 90% and 80% of fracture pressure respectively. Pressure for all CO<sub>2</sub>

flooding cases is lower than that of the calculated fracture pressure at 4,414 psi (purple curve). When the injected CO<sub>2</sub> breakthroughs from the injection well to production well, the reservoir pressure decreases until it hits to equilibrium stage.

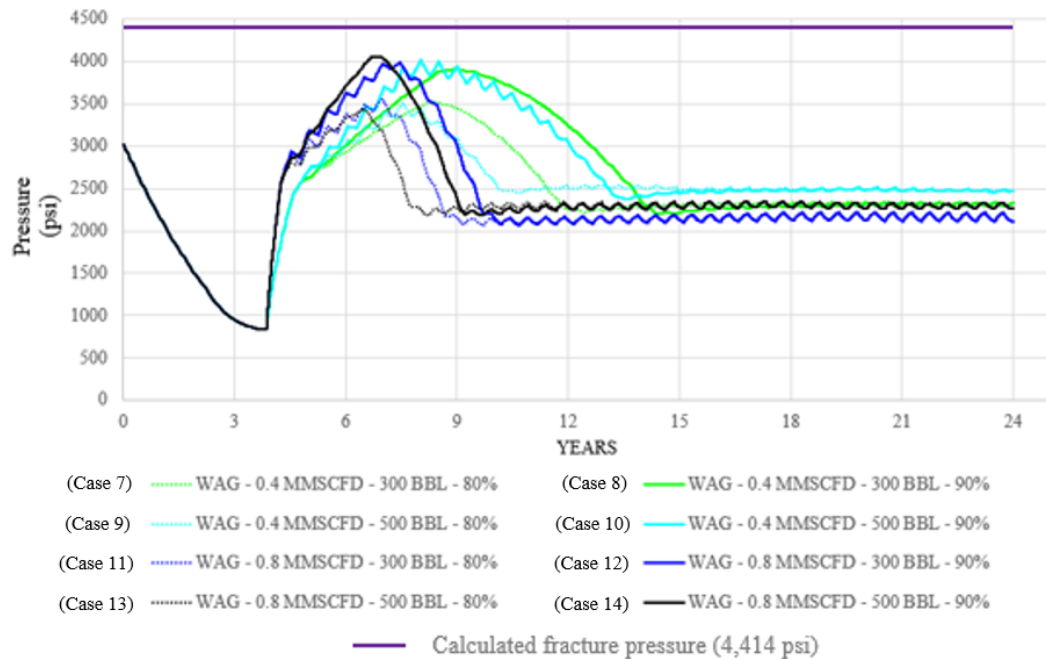


Figure 4.23 Reservoir pressure of WAG for Case 7 to 14

In the case of total CO<sub>2</sub> injection, the results of total CO<sub>2</sub> injection are represented in Table 4.8 and illustrated in Figure 4.24 and Figure 4.25. The highest total CO<sub>2</sub> injection are the case that CO<sub>2</sub> is injected with highest rate which are 0.8 MMSCF/day for Case 11, Case 12, Case 13 and Case 14. The higher injection rates of both 80% and 90% of fracture pressure result in the higher total of injection. Due to the same injection rate, the total CO<sub>2</sub> injection is equal, despite of the difference of operating pressure. The total CO<sub>2</sub> injection rate at 0.8 MMSCF/day of both 80% and 90% of operating pressure is 3,005,000 MSCF which is the highest value and decrease in the injection rate give the lower of total CO<sub>2</sub> injection (CO<sub>2</sub> injection rate at 0.4 MMSCF/day of both 80% and 90% of operating pressure). Not only the total CO<sub>2</sub> injection is monitored, but also the total water injection. The result of the higher rate of water injection has the higher total water injection. The highest total injection rate of water at 1,800,000 STB is the case of water injection at 500 STB/day with CO<sub>2</sub> injection at 0.8 MMSCF/day and the lowest total injection rate of water at 1,053,000

STB is the case of water injection at 300 STB/day with CO<sub>2</sub> injection at 0.4 MMSCF/day.

Table 4.11 The total CO<sub>2</sub> and water injection volume of WAG cases

Case	Injection rate (MMSCF/D - For CO <sub>2</sub> ), (STB/D - For WAG)	Operating pressure (% of fracture pressure) (psi)	Total CO <sub>2</sub> injection volume (MSCF)	Total water injection volume (STB)
7	CO <sub>2</sub> : 0.4, Water : 300	80%	1,538,600	1,053,000
8	CO <sub>2</sub> : 0.4, Water : 300	90%	1,538,600	1,053,000
9	CO <sub>2</sub> : 0.4, Water : 500	80%	1,538,600	1,755,000
10	CO <sub>2</sub> : 0.4, Water : 500	90%	1,538,600	1,755,000
11	CO <sub>2</sub> : 0.8, Water : 300	80%	3,005,000	1,080,000
12	CO <sub>2</sub> : 0.8, Water : 300	90%	3,005,000	1,080,000
13	CO <sub>2</sub> : 0.8, Water : 500	80%	3,005,000	1,800,000
14	CO <sub>2</sub> : 0.8, Water : 500	90%	3,005,000	1,800,000

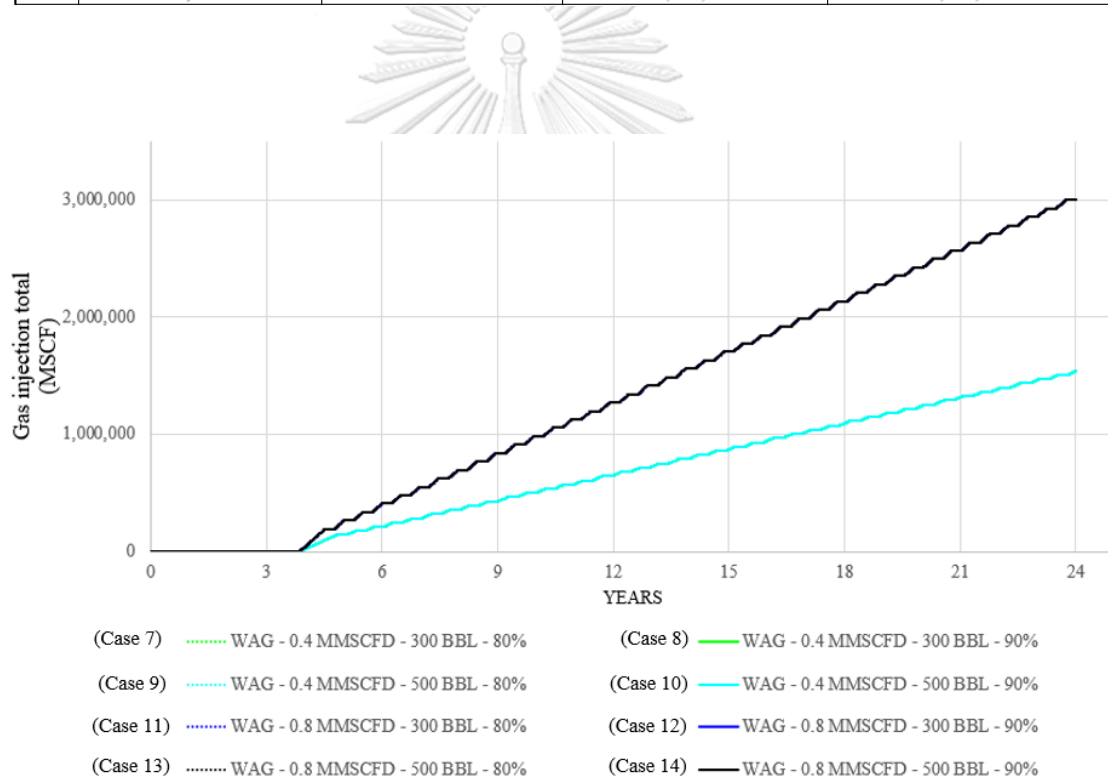


Figure 4.24 Total CO<sub>2</sub> injection of WAG cases

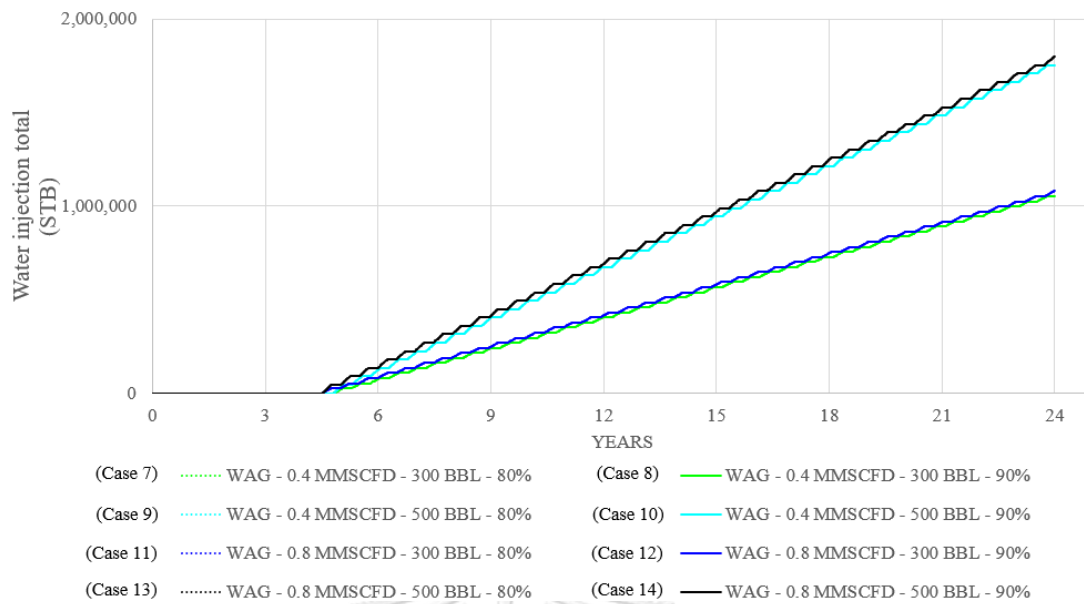


Figure 4.25 Total water injection of WAG cases

In addition to the performance of oil production, and water cut to support for improving of recovery factor and the project economics, gas oil ratios (GOR) is another factor to be monitor (Verma, 2015). GORs of these cases are illustrated in Figure 4.26. In this result, the highest rate of injection has the fastest CO<sub>2</sub> breakthrough due to the amount of injection and the displacing fluid viscosity (CO<sub>2</sub>) (Thomas, 2008). Consequently, the 0.8 MMSCF/day alternating with water at 500 STB/day of 80% of injection is the fastest CO<sub>2</sub> breakthrough because of (1) the amount of CO<sub>2</sub> injection rate and (2) set up production rate due to the controlling of operating pressure. The rest of cases gives the same result with the same reasons. Finally, for all cases at some states of production period, the GOR of the higher operating pressure is higher than that of the lower operating pressure due to an increase in total oil production at the time with the same gas production after the gas breakthrough.



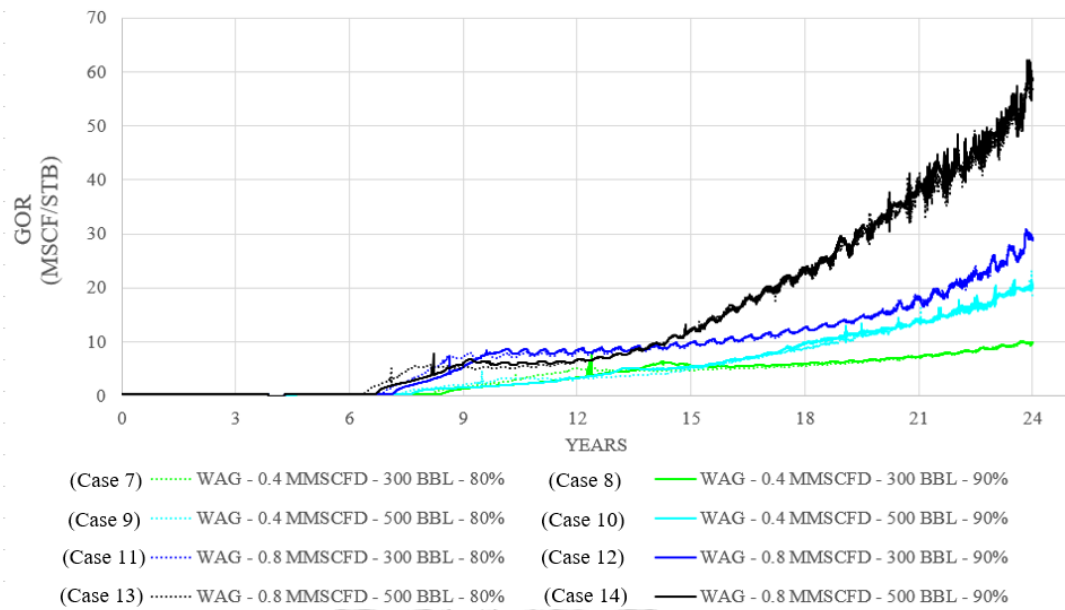


Figure 4.26 Gas oil ratio (GOR) of WAG cases

At the end of production of WAG cases, the injection of 0.8 MMSCF/day alternating water at 500 STB/day and 90% of fracture pressure or Case 14 has the highest total oil production and recovery factor at 550,496 STB and 48.1%, respectively. The remaining oil in place is 526,262 STB. The trend of water cut of all WAG cases is an increase in the percent of water cut and heading to 100% and the oil production rate declines through the end of production but the produced water inclines through the end of the production period. Case 13 and Case 14 have the highest 98% of water cut. In case of reservoir pressure, the pressure of reservoir continuously increases since the first day of CO<sub>2</sub> injection until the CO<sub>2</sub> breakthrough. Therefore, the pressure suddenly drops to the equilibrium pressure. The gas oil ratio (GOR) can indicate the breakthrough time, in case of the higher rate of injection and the higher rate of production, the breakthrough time becomes faster. The injection of CO<sub>2</sub> at injection rate of 0.8 MMSCF/day alternating with water at 500 STB/day and with 80% of fracture pressure or Case 13 is the fastest of the breakthrough time due to the rate of production and the rate of injection. The highest of total CO<sub>2</sub> injection are Case 11, Case 12, Case 13 and Case 14 at 3,005,000 MSCF and the highest of total water injection are Case 13 and Case 14 at 1,800,000 STB. Consequently, because of the special property of CO<sub>2</sub>, CO<sub>2</sub> improves the total oil production and oil recovery by lowering the interfacial tension, oil swelling, reducing oil viscosity and mobilizing the



lighter components of the oil (Verma, 2015). Therefore, MMP and amount of CO<sub>2</sub> are necessary parameters for the enhanced oil recovery process.

#### 4.2.3 CO<sub>2</sub> flooding and WAG comparison

Since the total oil production and recovery factor are the main considerable factors for all cases. The top 3 ranks are from WAG technology with the highest injection rate of both CO<sub>2</sub> and water although the lower operating pressures give the higher rate of production. When after the gas breakthrough for some period of time the rate of production of the higher operating pressure can overcome the lower operating pressure. At the beginning of the injection state of CO<sub>2</sub> flooding cases at the same rate of CO<sub>2</sub> injection of WAG, the total oil production and recovery factor are increasing with the same slope of WAG. Since the gas breakthrough occurs, the oil production significantly drops which causes the flat of the slope of total oil production and recovery factor. All cases are ranked by those parameters and presented in Table 4.12. Figure 4.27 presents the top 3 ranking of all studied parameters including the best case of CO<sub>2</sub> flooding in term of recovery factor.

Table 4.12 Total oil production and recovery factor

Rank	Study case	Technology	Injection rate (MMSCF/D - For CO <sub>2</sub> ), (STB/D - for water)	Operating pressure (% of fracture pressure) (psi)	Total production volume (STB)	Recovery factor (%)
1	14	WAG	CO <sub>2</sub> : 0.8, Water : 500	90%	550,496	48.1
2	13	WAG	CO <sub>2</sub> : 0.8, Water : 500	80%	544,924	47.7
3	12	WAG	CO <sub>2</sub> : 0.8, Water : 300	90%	541,525	47.4
4	10	WAG	CO <sub>2</sub> : 0.4, Water : 500	90%	537,685	47.0
5	11	WAG	CO <sub>2</sub> : 0.8, Water : 300	80%	537,036	47.0
6	9	WAG	CO <sub>2</sub> : 0.4, Water : 500	80%	532,345	46.6
7	8	WAG	CO <sub>2</sub> : 0.4, Water : 300	90%	509,116	44.5
8	7	WAG	CO <sub>2</sub> : 0.4, Water : 300	80%	503,944	44.1
9	6	CO <sub>2</sub> flooding	CO <sub>2</sub> : 0.8	90%	492,893	43.1
10	5	CO <sub>2</sub> flooding	CO <sub>2</sub> : 0.8	80%	490,196	42.9
11	4	CO <sub>2</sub> flooding	CO <sub>2</sub> : 0.4	90%	407,550	35.6
12	3	CO <sub>2</sub> flooding	CO <sub>2</sub> : 0.4	80%	402,359	35.2
13	2	CO <sub>2</sub> flooding	CO <sub>2</sub> : 0.2	90%	342,955	30.0
14	1	CO <sub>2</sub> flooding	CO <sub>2</sub> : 0.2	80%	331,634	29.0

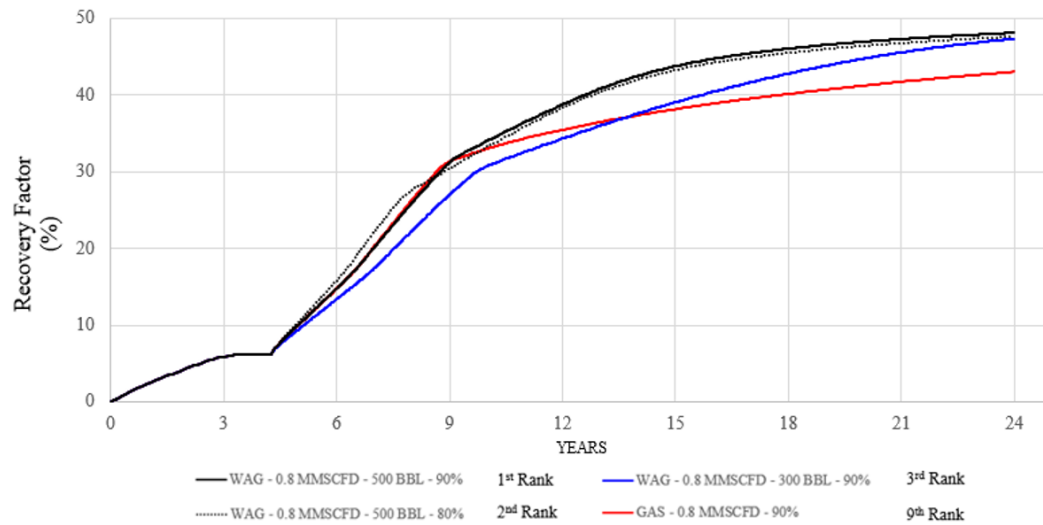


Figure 4.27 Top 3 ranking in recovery factor term including the best case of CO<sub>2</sub> flooding

The oil and water production rates of the top 3 ranking in total oil production term are also observed as well as water cut. For oil production, the beginning state of injection both CO<sub>2</sub> flooding and WAG has the same oil production profile with little difference in the production rate. Due to the CO<sub>2</sub> breakthrough, all cases have the sudden drop of the production rate and decline until the end of designed production time for 24 years. However, the WAG has a higher rate of production than that of CO<sub>2</sub> flooding due to the support of the water sweep efficiency to sweep more the remaining oil in the lower part of reservoir. For water production, the significant increase in water production starts at the beginning of both CO<sub>2</sub> flooding and WAG due to the significantly higher production rate which are individually applied in each case because of the controlling of the operating pressure. The trends of water production are heading in different direction for CO<sub>2</sub> flooding and WAG technology. The produced water suddenly declines after the CO<sub>2</sub> breakthrough. The declining trend is then smooth when the reservoir pressure is in equilibrium. For the WAG technology, the produced water suddenly declines after the CO<sub>2</sub> breakthrough. However, produced water increases the higher rate of water injection. The oil and water production rate are illustrated in Figure 4.28 and Figure 4.29, respectively. The fluctuation of the curves of WAG technology are observed on Figure 4.28 and Figure 4.29 due to the fluid phase difference of liquid and gas. While water is injected, the

produced water increases along with the increasing amount of water. When the process alternates to CO<sub>2</sub> injection, the produced water rate significantly decreases.

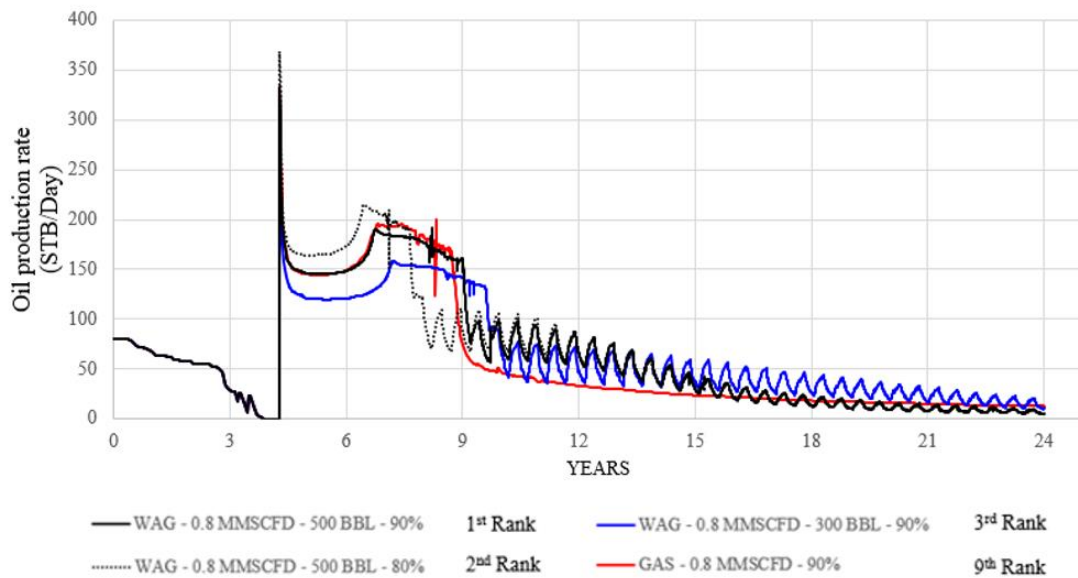


Figure 4.28 Oil production rate of top 3 rank of recovery factor

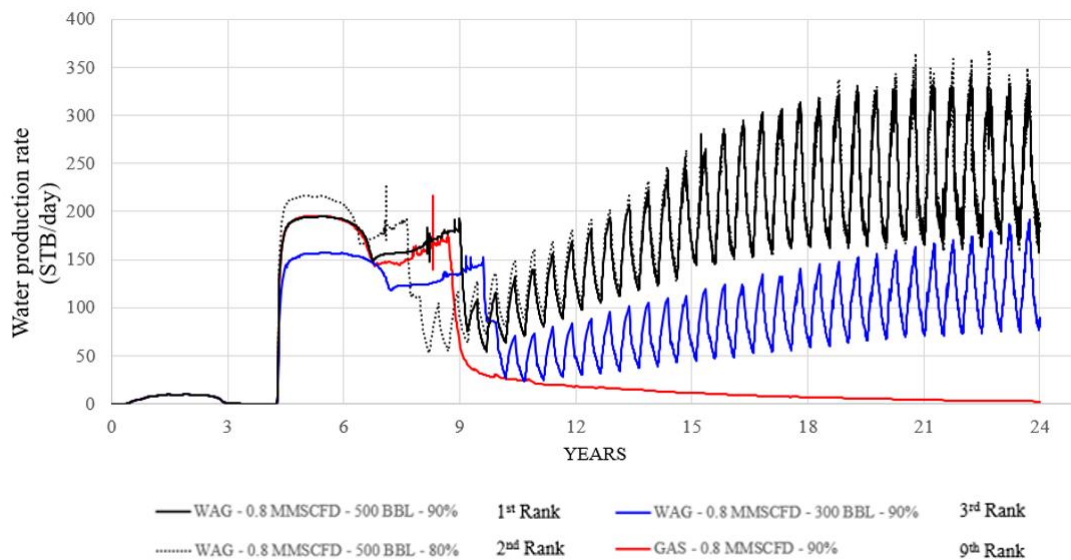


Figure 4.29 Water production rate of top 3 rank of recovery factor

In addition, water cut of the top 3 ranking in term of recovery factor including the best CO<sub>2</sub> flooding case are illustrated in Figure 4.30. In the graph, the top 1<sup>st</sup> and 2<sup>nd</sup> ranks in term of recovery factor hits 90% of water cut at year 16 production. However, the top 3<sup>rd</sup> rank in term of recovery factor hits the 90% of water cut at the

end of production at year 24. For the CO<sub>2</sub> flooding technology, the water cut has downward trend since the 9<sup>th</sup> year of production, but the increasing trend in the term of gas production is observed. And also, the curves of WAG technology are fluctuated due to the difference of injected fluids.

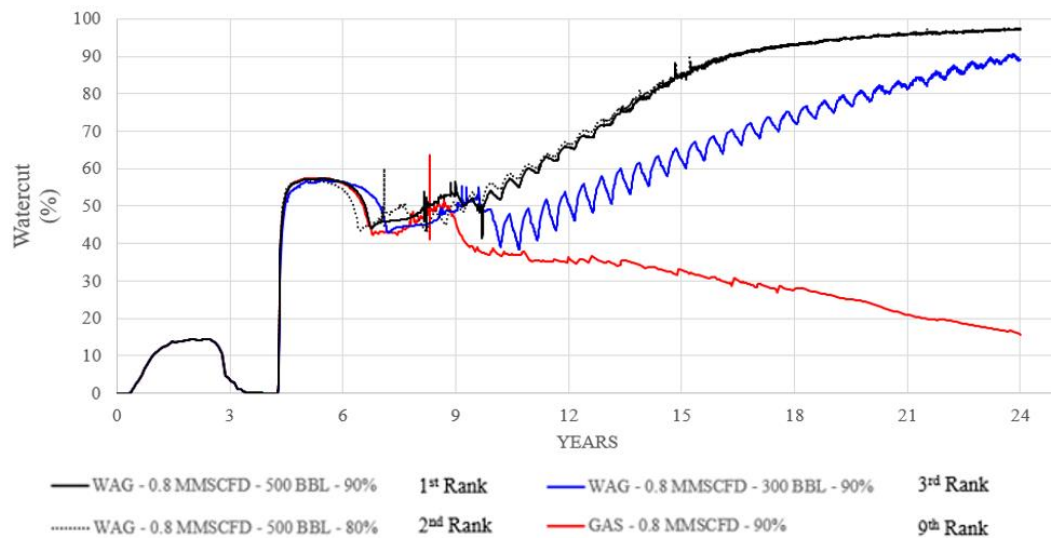


Figure 4.30 Water cut of top 3 rank of recovery factor

Besides, the fluctuation of production rate is observed for all of WAG cases due to the two different of injection fluids (CO<sub>2</sub> and water), this can be also found in reservoir pressure profile in Figure 4.31. The fluctuated curves are observed since the conducting of displacing fluid at around 4<sup>th</sup> year of production until the end of production period for 24 years. And the smooth curve of the CO<sub>2</sub> flooding is easily observed.

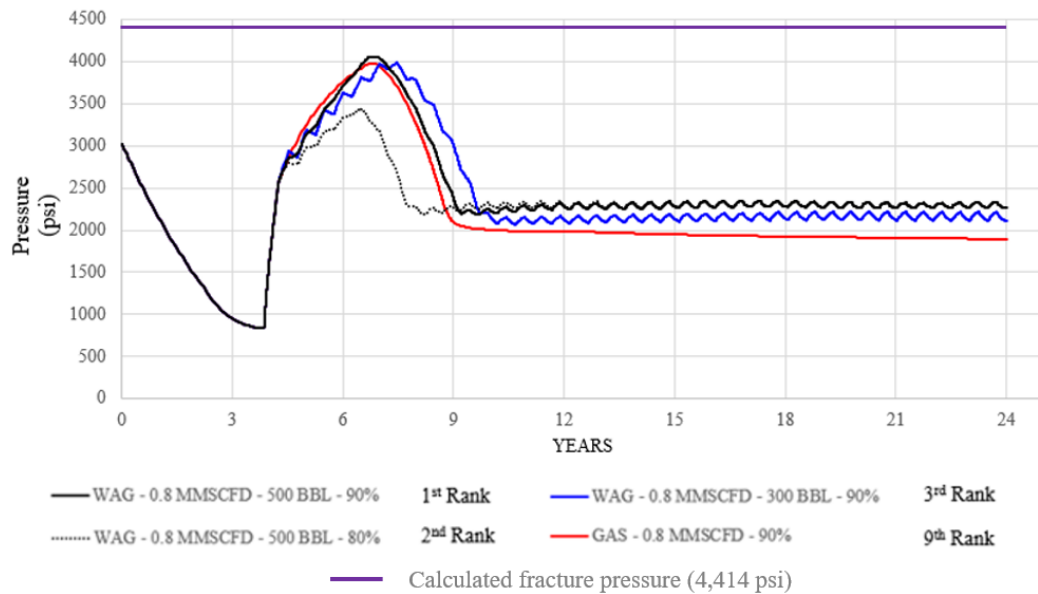


Figure 4.31 Reservoir pressure profile of top 3 rank of recovery factor

### 4.3 Fluid movement in heterogeneous reservoir

#### 4.3.1 The results in on 2-D cross-section

Besides the previous simulation results, the representative of 2 technologies includes CO<sub>2</sub> flooding at 0.8 MMSCF/day with 90% of fracture pressure (Case 6 – 9<sup>th</sup> Rank) and WAG at 0.8 MMSCF/day of CO<sub>2</sub> and 500 BBL/day of water with 90% of fracture pressure (Case 14 – 1<sup>st</sup> Rank) which are presented in 2-D cross section for being observed in Figure 4.32 to Figure 4.33.

The cross section is cut between the injection well and the production well. CO<sub>2</sub> movement is observed in the CO<sub>2</sub> flooding case and the CO<sub>2</sub> and water are presented in WAG. The blue color is represented as a non-hydrocarbon which can be water and gas (CO<sub>2</sub>) and the red color is the maximum oil saturation in this reservoir model which represents hydrocarbon or crude oil. The 2-D cross section is separated into 4 parts.

The 1<sup>st</sup> part is at starting time of this study.

The 2<sup>nd</sup> part is at 5 years since starting production.

The 3<sup>rd</sup> part is at 10 years since starting production.

The 4<sup>th</sup> part is at 24 years since starting production (at the end of production).

Figure 4.32 and Figure 4.33 illustrates the CO<sub>2</sub> movement from the top view of reservoir and CO<sub>2</sub> movement in the side view of 2-D cross-section of CO<sub>2</sub> flooding at 0.8 MMSCF/day with 90% of fracture pressure case (Case 6 – 9<sup>th</sup> Rank), respectively.

For Figure 4.32, the 1<sup>st</sup> part presented at the starting time of this study locates on top left of the figure. The 2<sup>nd</sup> part presented at 5 years since the starting production locates on top right of the figure. Also, the 3<sup>rd</sup> part presented at 10 years since the starting production locates on the below left of the figure and the 4<sup>th</sup> part at 24 years since starting production (at the end of production) locates on the below right of the figure. The co-ordinate of (0.0) is the injection well location and the co-ordinate of (1160, -1160) is the production well location. The distance between 2 well or well spacing is 1,640 ft.

At the beginning, the top part of the heterogeneous reservoir model is full of hydrocarbon represented in red color. After the injection has been performed for 5 years, the non-hydrocarbon (CO<sub>2</sub>) movement is observed in blue color. The CO<sub>2</sub> move overrides of the hydrocarbon and the CO<sub>2</sub> breakthrough to the production well is around 6.3 years since the first oil production. Consequently, the non-hydrocarbon (CO<sub>2</sub>) or blue color is found on the top of reservoir model at 10 years and 24 years and the remaining hydrocarbon is found at around the production well as shown in green color.



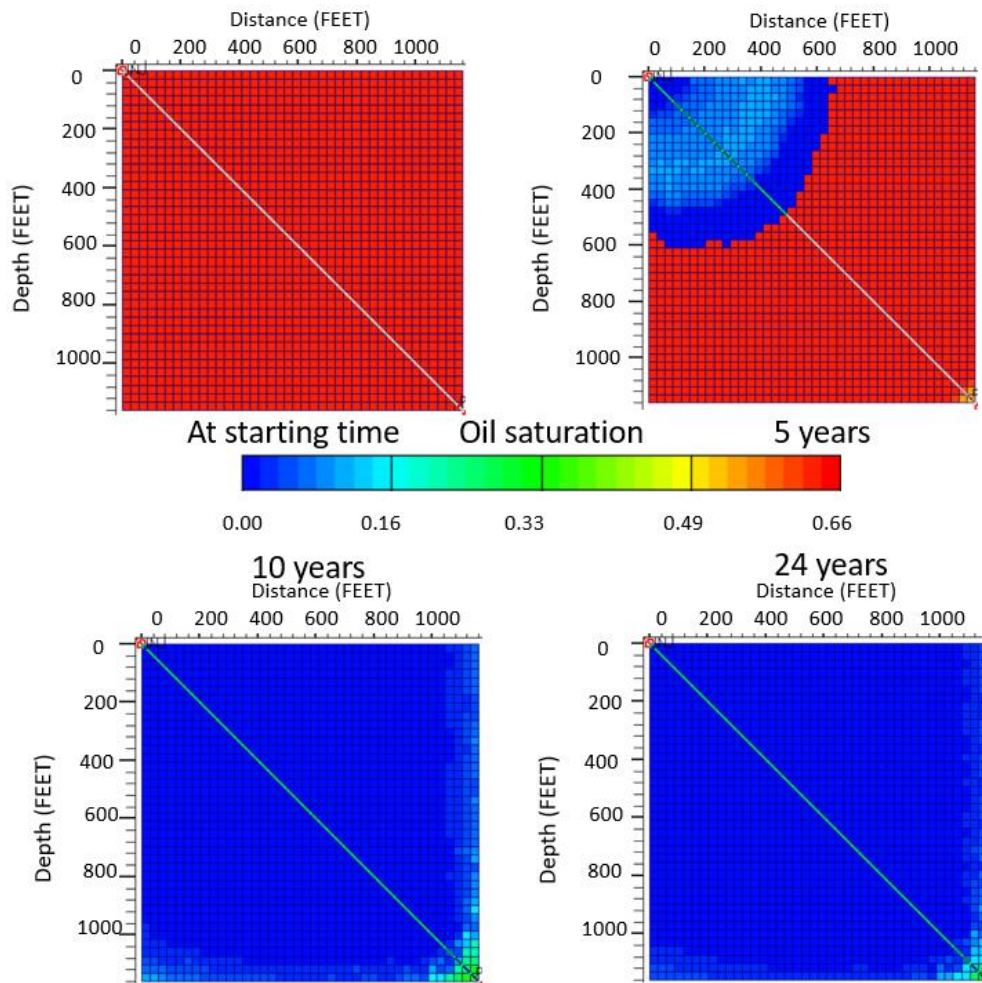


Figure 4.32 CO<sub>2</sub> movement on top view of reservoir of the CO<sub>2</sub> flooding for Case 6

For Figure 4.33, the 1<sup>st</sup> at the starting time, 2<sup>nd</sup> at 5 years, 3<sup>rd</sup> at 10 years and 4<sup>th</sup> at 24 years presented in this study are located on top left, top right, below left and below right of the figure, respectively. X-axis represents the depth of reservoir and Y-axis represents the distance between injector and production well (1,640 ft. or 500 m.) The left side of each sub figure is the location of injection well and the right side of each sub-figure is the location of production well. Like the same as presented in the previous section, the red represents hydrocarbon or crude oil at the higher oil saturation ( $S_o = 0.66$ ) and the blue represents the non-hydrocarbon ( $S_o = 0$ ). When, the displacing fluid or CO<sub>2</sub> is injected, the CO<sub>2</sub> is partially miscible with light part of crude oil causes the reduction of IFT, reduction of oil viscosity and oil swelling (Mansour, 2018). The top part of reservoir is swept through the production well. The CO<sub>2</sub> overrides top of the reservoir model due to the effect of gravity (Nurafiqah and

Hasan, 2021) and the crude oil is displaced and moves into the lower zone of the reservoir model. When the CO<sub>2</sub> breakthroughs the production well, the gas moves easier than before due to the gas moving path, causing the high remaining oil left below.

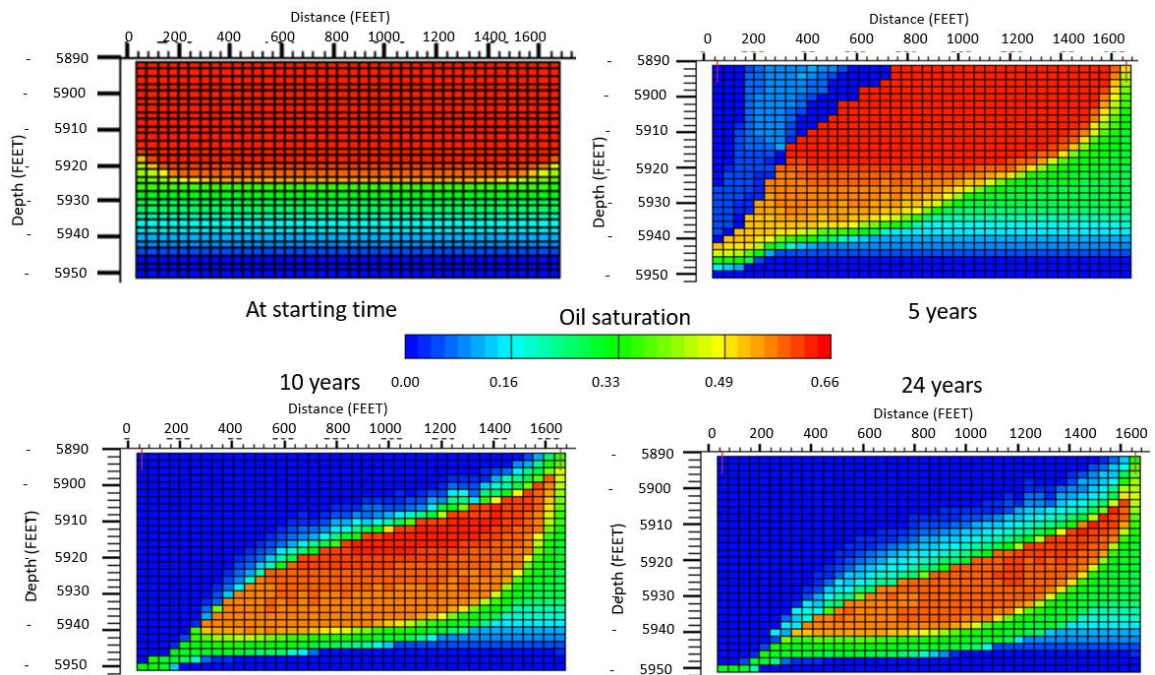


Figure 4.33 CO<sub>2</sub> movement inside view in 2-D cross-section of CO<sub>2</sub> flooding for Case 6

Figure 4.34 and Figure 4.35 illustrates the CO<sub>2</sub> movement from the top view of reservoir and CO<sub>2</sub> movement in the side view of 2-D cross-section of CO<sub>2</sub> flooding at 0.8 MMSCF/day and 500 STB/day with 90% of fracture pressure case (Case 14 – 1<sup>st</sup> Rank), respectively.

At the beginning, the top part of the heterogeneous reservoir model is full of hydrocarbon in red color. After the injection has been performed for 5 years, the non-hydrocarbon (CO<sub>2</sub>) movement is observed in blue color. The CO<sub>2</sub> movement overrides of the hydrocarbon, CO<sub>2</sub> breakthrough to the production well is around 6.5 years since the first oil production. The breakthrough time is little longer than that of the CO<sub>2</sub> flooding at 0.8 MMSCF/day with 90% of fracture pressure or Case 6 (9<sup>th</sup> Rank) due to the injected water with higher viscosity and denser than gas. The



injected water slows down the gas breakthrough (Nurafiqah and Hasan, 2021). The same results of the CO<sub>2</sub> flooding cases are observed. The non-hydrocarbon (CO<sub>2</sub>) or blue color is found on the top of reservoir model at 10 years and 24 years and the remaining hydrocarbon is found with a little higher than CO<sub>2</sub> flooding cases at around the production well as shown in green color.

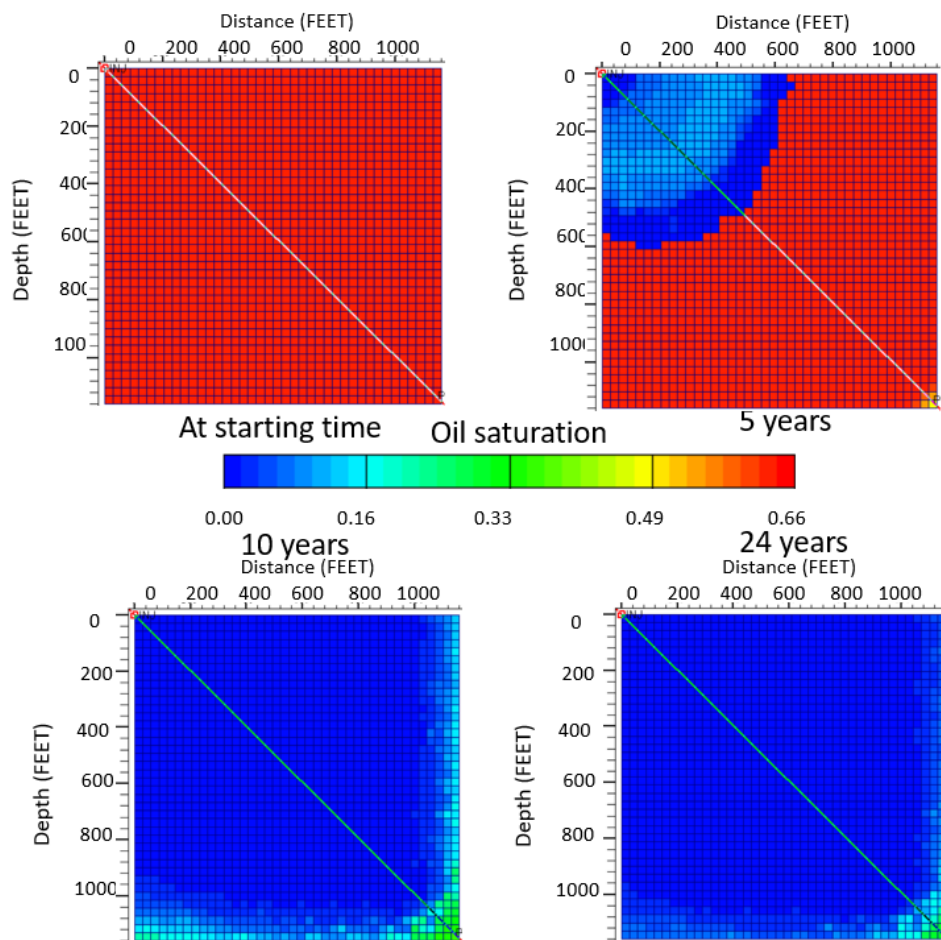


Figure 4.34 CO<sub>2</sub> movement on top view of reservoir of the WAG for Case 14

As presented in Figure 4.35, the left side of each sub-figure is the location of injection well and the right side of each sub-figure is the location of production well. The red zone represents hydrocarbon or crude oil at the higher oil saturation ( $S_o = 0.66$ ) and the blue area represents the non-hydrocarbon ( $S_o = 0$ ). When, the displacing fluids (CO<sub>2</sub> and water) are alternately injected, the CO<sub>2</sub> is partially miscible with light part of crude oil causing the reduction of IFT, reduction of oil viscosity and oil swelling (Mansour, 2018). The CO<sub>2</sub> moves to the top of reservoir and dense water

tends to migrate to the bottom of the reservoir due to the gravity difference. Consequently, the oil in the upper part of reservoir may be contacted by the injected CO<sub>2</sub> and injected water push the miscible slug. This process increases the small efficiency because the unswept crude in the reservoir model will be smaller. Less remaining oil will remain in the reservoir and thus improving the oil recovery as well as the fluid composition variation and a decrease in the residual oil saturation resulting from the flow of 3 phases. (Nurafiqah and Hasan, 2021)

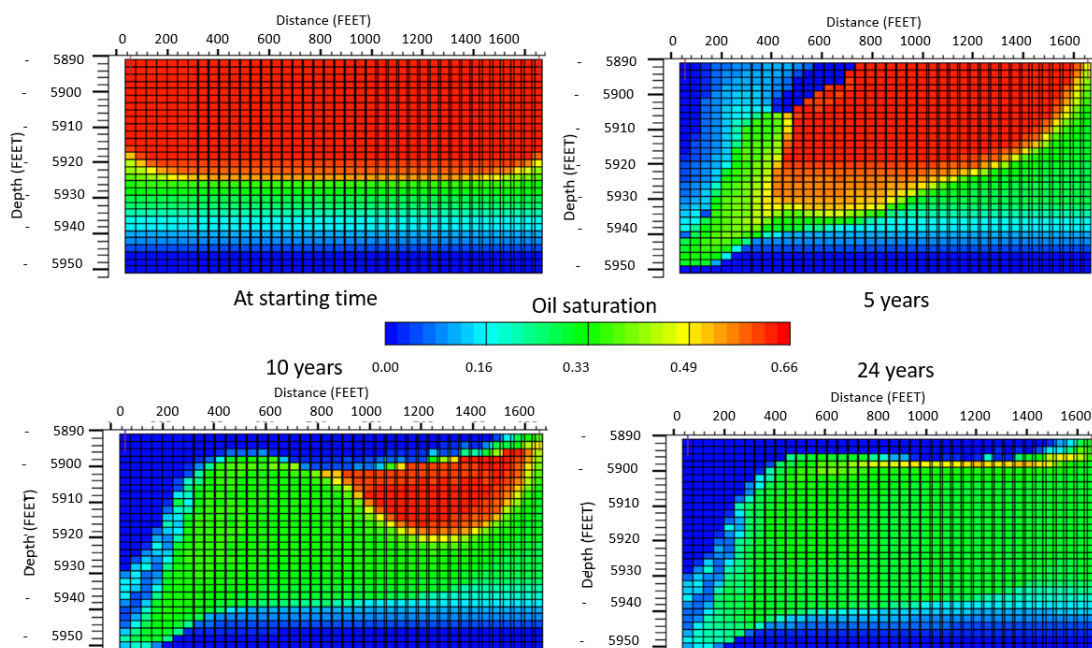


Figure 4.35 CO<sub>2</sub> and water movement inside view in 2-D cross-section of WAG for Case 14

From the results of both cases, CO<sub>2</sub> movement moves up due to plume migration of CO<sub>2</sub> underneath caprock. Since CO<sub>2</sub> is injected into the reservoir, the injected CO<sub>2</sub> migrates to the upper-part of the reservoir due to its gravity and buoyancy. Although the CO<sub>2</sub> injection is stopped, the injected CO<sub>2</sub> continuously migrates as well as the changing of saturation (Mackay, 2013). The CO<sub>2</sub> migrates faster in the higher permeability section. Consequently, CO<sub>2</sub> movement on both CO<sub>2</sub> flooding and WAG is the same in the top view of reservoir. In case of WAG technology, CO<sub>2</sub> displaces the upper zone of reservoir and the dense water displaces the lower zone of reservoir due to the gravity different during the continuous injection and it reduces the

remaining oil in place as well the as oil saturation (Nurafiqah and Hasan, 2021) which are represented in Figure 4.35.

#### 4.3.2 The results on 3-D reservoir model

For more clarification of the observation, 3-D reservoir model of both representative cases which are CO<sub>2</sub> flooding case (Case 6) and WAG case (Case 14) are illustrated in Figure 4.36 and Figure 4.37, respectively. The injecting well locates on the left conner and the production well locates on the right of the 3-D reservoir model. The oil saturation is used to represent the hydrocarbon in the reservoir. The injected CO<sub>2</sub> migrates on the top of the reservoir due to its gravity for both cases. The CO<sub>2</sub> displaced the light oil components by partially miscible process and gas drive mechanism. The heavier components are displaced into the lower zone of the reservoir. The unswept zone is larger than WAG and the CO<sub>2</sub> remains on the top of reservoir at the end of the production period.

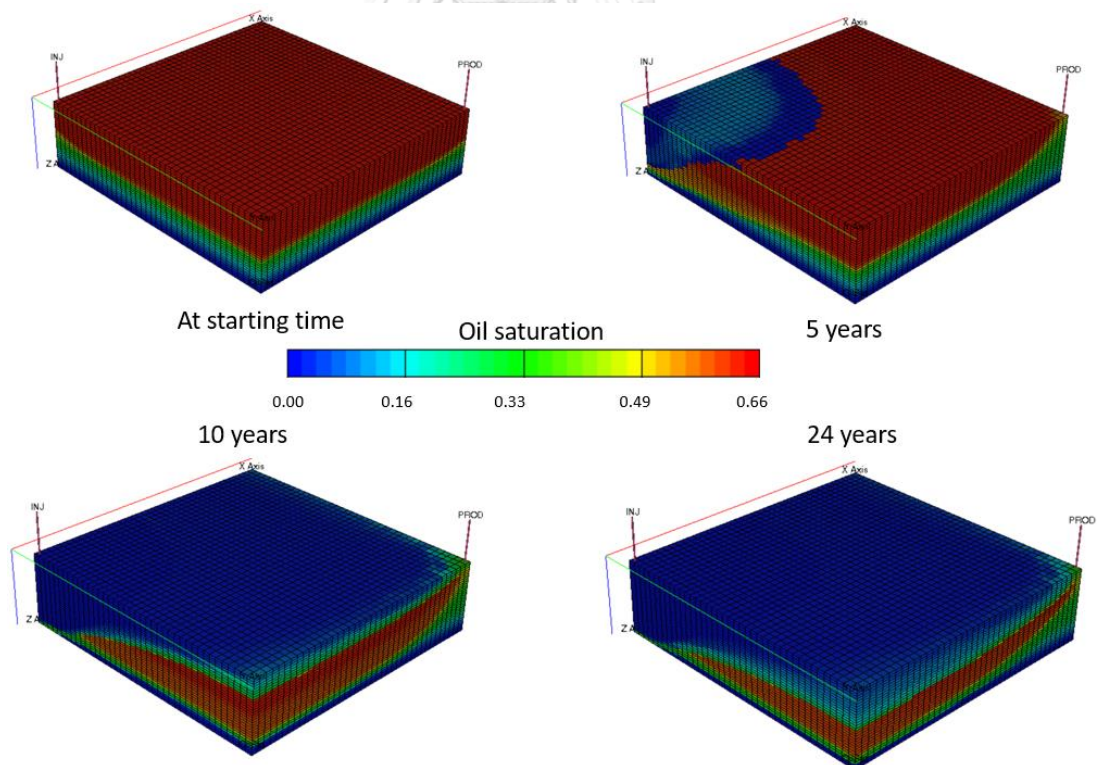


Figure 4.36 CO<sub>2</sub> movement in 3-D reservoir model CO<sub>2</sub> flooding case 6

Not only the injection of CO<sub>2</sub> is applied in the WAG technology but also using water is used to increase the sweep efficiency. The displacing water is injected in the reservoir via injection well at the left corner of the reservoir. The injected CO<sub>2</sub> and water migrate to the top and bottom of reservoir. Therefore, the crude oil on the bottom part is swept up to the upper zone and the crude oil on the top part is partially miscible and displaced down to the below zone, causing the lesser residual oil in term of oil saturation of WAG presented in Figure 4.37 at the end of production at 24 years. In addition, because of water, CO<sub>2</sub> breakthrough of Case 14 is slower than that of Case 6 which are 6.5 years and 6.3 years, respectively.

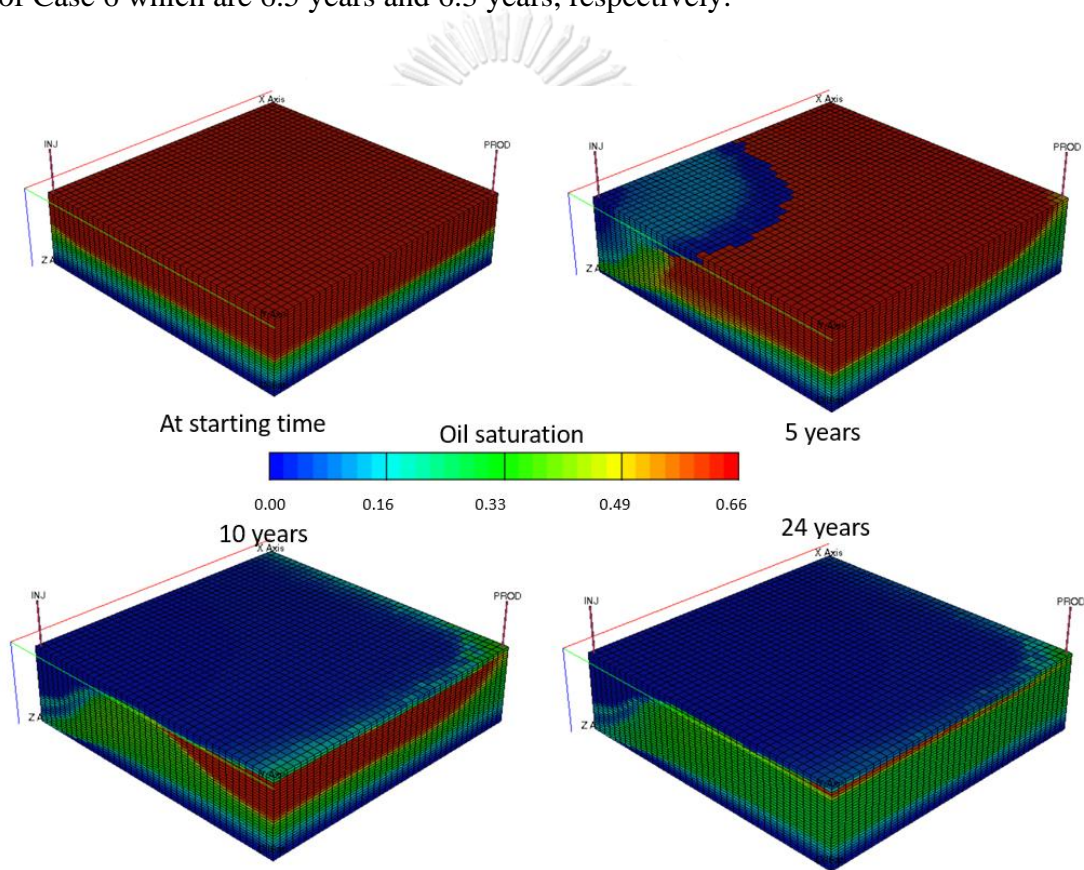


Figure 4.37 CO<sub>2</sub> and water movement in 3-D reservoir model WAG case 14

From the results of both cases, the WAG case has CO<sub>2</sub> and water displacement on both upper zone and lower zone, respectively. Since CO<sub>2</sub> has the breakthrough from injection well to production well, CO<sub>2</sub> keep overrides on the top of and water displaces the remaining oil at lower part. The water helps to lift the remaining oil to upper zone due to its gravity. Therefore, the crude oil on the bottom part is displaced by water and moves to the upper zone and the crude oil on the top part is partially

miscible and displaced down to the lower zone by CO<sub>2</sub>. This causes the lesser residual oil in term of oil saturation (Nurafiqah and Hasan, 2021). The WAG injection is used to improve the sweep efficiency, to maintain nearly initial high pressure, to slow down the CO<sub>2</sub> breakthrough and to reduce viscosity of oil. Owing to water, CO<sub>2</sub> breakthrough of Case 14 is slower than that of Case 6 which are 6.5 years and 6.3 years, respectively.

The three phases interaction of CO<sub>2</sub>, water, crude oil cause complicated coupling behaviors, for instance, dissolution, migration, nucleation and mixing of multiple fluids with the fluctuation of the formation pressure and the multiphase distribution. The migration process also changes accordingly. The fluctuation on the curves of WAG occurs from the CO<sub>2</sub> saturated oil displaced by CO<sub>2</sub> and water. Also, the injected water forms a favored migration passage under both wet conditions. The pore throat structure does not essentially hinder the waterfront edge in water wet. But the oil wet pore throat provides the extra capillary restriction and the flow needs further accumulation of higher pressure to curst and migrate downstream, resulting in the maximum velocity in the oil wet favor passage three times larger than the water wet condition. The water eventually breaks through the oil phase blocked at throats and pushes part of the oil phase encapsulating CO<sub>2</sub> bubble to flow downstream, where a new water favor migration passage is formed (Lu, et. al., 2021).

CO<sub>2</sub>, water, oil three phase migration in porous structures is affected significantly by supercritical CO<sub>2</sub> exsolution and expansion. The multiphase migration process is under different wettability, in water wet condition and the aqueous phase can still migrate downstream through the water film between the CO<sub>2</sub> and oil and the wall, unable to further drive CO<sub>2</sub> and oil downstream. Whilst, in oil wet condition, the aqueous phase ultimately breaks through the oil phase blocked at throats and forms a new favor migration passage pushing the part of the oil phase encapsulating CO<sub>2</sub> bubble downstream (Lu, et. al., 2021).



## CHAPTER 5

### CONCLUSIONS AND RECOMMENDATION

This chapter concludes the results of the performance evaluation of CO<sub>2</sub> flooding and WAG technology with various of injection rates of CO<sub>2</sub> for CO<sub>2</sub> flooding and CO<sub>2</sub> and water for WAG in heterogeneous reservoir model including operating pressures. Furthermore, recommendation is provided for future study.

#### 5.1 Conclusions

In this study, the porosity is in range from 0.21 – 0.29 and the permeability from 76 – 717 mD are used to set up the heterogeneous reservoir model. The conclusions of this study are presented as follow:

1. WAG technology gives the better sweep efficiency, mobility control of water and gas phases and improve recovery factor.

2. The rate of injections both CO<sub>2</sub> and water affect the total oil production and recovery factor from reservoir model. The results show that the higher both CO<sub>2</sub> and water injection, the higher the increment of the total oil production as well as recovery factor. The 1<sup>st</sup> rank in term of total oil production is the highest rate of both CO<sub>2</sub> and water and has been noticed as 48.1% of RF which is Case 14 with the injection of CO<sub>2</sub> at 0.8 MMSCF/day and 500 STB/day water.

3. The higher operating pressure affects the total oil production and recovery factor from the reservoir model. The results present that the higher the operating pressure at the same injection rate for both technologies, the higher the increment of the total oil production and recovery factor. Because the CO<sub>2</sub> injection does not only give the miscible benefit but also maintain the reservoir pressure and the drive mechanism.

4. Although the WAG technology gives the highest total oil production and recovery factor, the WAG technology also comes with the highest water production as presented in the result of water cut.

5. The fluctuation of the curves from the WAG technology is observed due to three phase process under different wettability, in water wet condition, the aqueous phase can still migrate downstream through the water film between the CO<sub>2</sub> and oil

and the wall is unable to further drive CO<sub>2</sub> and oil downstream. Whilst, in oil wet condition, the aqueous phase ultimately breaks through the oil phase blocked at throats and forms a new favor migration passage to push part of the oil phase encapsulating CO<sub>2</sub> bubble downstream. Consequently, the fluctuation occurs from the different phase of injection fluid.

## 5.2 Recommendation

Some recommendation is suggested for the future studies in this particular field after simulation results as follows:

1. Other gases such as methane nitrogen as well as LPG could be applied with the studied rate.
2. In this study, the WAG technology has better total oil production and recovery factor than that CO<sub>2</sub> flooding significantly but the different rate of water injection has little difference of total oil production and recovery factor.
3. Because the perforating zone of this study is located on the top of reservoir, CO<sub>2</sub> movement overrides on the hydrocarbon in the reservoir and displaces the hydrocarbon to the lower part of the reservoir. Another method to overcome of CO<sub>2</sub> overriding is the change of the perforating zone from the top part of the reservoir to the lower part of the reservoir instead.
4. Geomechanic experimental results and/or geochemical model as well as the fracture of rock path of individual reservoir should be added in the model for more accuracy.
5. The surface facilities as well as economic factors should be considered for WAG cases due to the high total water production.
6. In term of economic, CO<sub>2</sub> is an expensive resource and operation, the WAG is a better method when compare to CO<sub>2</sub> flooding and water flooding due to less amount of injected CO<sub>2</sub> in continuous CO<sub>2</sub> injection.

## REFERENCES



จุฬาลงกรณ์มหาวิทยาลัย  
**CHULALONGKORN UNIVERSITY**



- Abeydeera, Lebune Hewage Udara Willhelm, Hayantha Wadu Mesthrige and Tharushi Imalka Samarasinghalage. (2019). Global research on carbon emissions: A Scientometric review. *Sustainability (Switzerland)*, 11(14), 3972.  
<https://doi.org/10.3390/su11143972>
- Akinlotan, Oladapo, Byami Jolly, Okwudiri Anyiam. (2018). Hydrocarbon Generation Potentials of Cenozoic Lacustrine Source Rocks: Gulf of Thailand, Southeast Asia. *International Journal of Geology and Earth Sciences*, 4(4):35-55  
<http://10.32937/IJGES.4.4.2018.35-55>
- Attavittkamthorn, Vitsarut, Javier Valcaez and Kozo Sato. (2013). Metnamodeling of Gas Flooding EOR in Pattani Basin, Thailand. *Journal of the Japanese Association for Petroleum Technology*, 78(6):508  
<https://doi:10.3720/japt.78.508>
- Bashu, S. (2003). Screening and ranking of sedimentary basins for sequestration of CO<sub>2</sub> in geological media in response to climate change. *Environental Geology*, 44(3), 227-289  
<http://10.1007/s00254-003-0762-9>
- Basry, A. Al, S. Al Hajeri, H. Saadiwi, F. Al Aryani, A. Obeidi, S. Negahban and G. Al Yafei (2013). Lessons Learned from the First Miscible CO<sub>2</sub>-EOR Pilot Project in Heterogeneous Carbonate Oil Reservoir in Abu Dhabi, UAE. *SPE*, SPE142665  
<https://doi:10.2118/142665-MS>
- Becker, Sylvain, Tatiana Bouzdine-Chameeva and Anicia Jaegler. (2020). The carbon neutrality principle: A case study in the French spirits sector. *Cleaner Production*, 274, 122739.  
<https://doi.org/10.1016/j.jclepro.2020.122739>
- Bhatia, Jagar, J.P. Srivastava, Abhay Sharma, Hitendra S. Sangwai. (2014). Production Performance of Water Alternate Gas Injection Techniques for Enhanced Oil Recovery: Effect of WAG ratio, Number of WAG Cycles and The Type of injection gas. *International Journal of Oil Gas and Coal Technology*. 7(2):132 – 151  
<http://doi:10.1504/ijogct.2014.059323>

- Bourgoyne, Adam T., K.K. Millheim, M.E. Chenevert, F.S. Young (1986). Applied drilling engineering, *International Journal of Rock Mechanics and Mining Sciences & Geomechanics Abstracts*, 24(4), P.149  
[http://doi: 10.1016/0148-9062\(87\)90345-7](http://doi:10.1016/0148-9062(87)90345-7)
- Brennan, Sean T., Robert C. Burruss, Matthew D. Merrill, Philip A. Freeman and Leslie F. Ruppert. (2009). A Probabilistic Assessment Methodology for the Evaluation of Geologic Carbon Dioxide Storage. *USGS (U.S. Geological Survey)*, Open-File Report 2010–1127  
<https://pubs.usgs.gov/of/2010/1127/ofr2010-1127.pdf>
- Buchanan, Rex and Timothy R. Carr. (2008). Geologic Sequestration of Carbon Dioxide in Kansas. *Kansas Geological Survey*, Public Information Circular 27. Retrieved from  
[https://www.kgs.ku.edu/Publications/PIC/PIC27\\_2011.pdf](https://www.kgs.ku.edu/Publications/PIC/PIC27_2011.pdf)
- Budisa, Nediljko and Dirk Schulze-Makuch. (2014). Supercritical Carbon Dioxide and Its Potential as a Life-Sustaining Solvent in a Planetary Environment. *Life*, 4, 331-340  
[http:// doi:10.3390/life4030331](http://doi:10.3390/life4030331)
- Charusiri, Punya and Somchai Pum-Im. (2009). Cenozoic Tectonic Evolution of Major Sedimentary Basins in Central, Northern, and the Gulf of Thailand. *BEST 2009*, Vol.2, No1&2, p.40-62
- EPA. (2022), Retrieved from  
<https://www.epa.gov/ghgemissions/global-greenhouse-gas-emissions-data>
- FanChi, John. (2010). Integrated Reservoir asset Management. Chapter 4, Pages 49-69.  
<https://doi.org/10.1016/B978-0-12-382088-4.00004-9>
- Fitch, Peter, Sarah Davies, Mike Lovell and Tim Pritchard. (2013). Reservoir Quality and Reservoir Heterogeneity: Petrophysical Application of the Lorenz Coefficient. *Petrophysics*. SPWA-2013-v54n5-A5, Volume 54, No.5 Pages 465-474
- Freund, P. (2013). Anthropogenic climate change and the role of CO<sub>2</sub> Capture and storage (CCS). *Geoscience, Technologies, Environmental Aspects and Legal Frameworks*, Pages 3-25

<https://doi.org/10.1533/9780857097279.1.3>

Hill, Bruce, Xiao Chun Li, Ning Wei.(2020). CO<sub>2</sub>-EOR in China: A comparative review. *International Journal of Greenhouse Gas Control*, 103:103173

<https://doi.org/10.1016/j.ijggc.2020.103173>

Huang Feng, Huang Haidong, Wang Yanqing, Ren Jianfeng, Zhang Liang, Ren Bo, Hassan Butt, Ren Shaoran and Chen Guoli. (2016). Assessment of Miscibility Effect for CO<sub>2</sub> Flooding EOR in a Low Permeability Reservoir. *Journal of Petroleum Science and Engineering*. Volume 145, Pages 328-335

<https://doi.org/10.1016/j.petrol.2016.05.040>

IPCC. Bert Metz, Ogunlade Davidson, Heleen de Coninck, Manuela Loos, Leo Meyer (2005). IPCC Special Report on Carbon Dioxide Capture and Storage. *Intergovernmental Panel on Climate Change 2005*. Retrieved from

<https://www.ipcc.ch/report/carbon-dioxide-capture-and-storage/>

IEA. (2022). CO<sub>2</sub> Emissions in 2021. *IEA Global Energy Review publication (France)*. Retrieved from

<https://iea.blob.core.windows.net/assets/c3086240-732b-4f6a-89d7-db01be018f5e/GlobalEnergyReviewCO2Emissionsin2021.pdf>

Kananithikorn, Nardthida and Teerarat Songsaeng. (2021). Pre-Drilled ECD Design by Using Fracture Pressure Model in Satun-Funan Fields, Pattani Basin, Gulf of Thailand. *International Petroleum Technology Conference*. IPTC-21368-MS.

<https://doi.org/10.2523/IPTC-21368-MS>

Khazam M., Arebi T, Mahnoudi T. and Froja M. (2016). A New Simple CO<sub>2</sub> Minimum Miscibility Pressure Correlation. *Oil Gas Res.*2:3

<https://doi.org/10.4172/2472-0518.1000120>

Li, Ding, Shuixiang Xie, Xiangliang Li, Yinghua Zhang, Heng Zhang and Shiling Yuan. (2021). Determination of Minimum Miscibility Pressure of CO<sub>2</sub>-Oil System: A Molecular Dynamics Study. *Molecules* 2021. 26, 4983.

<https://doi.org/10.3390/molecules26164983>

Lu, Haowei, Feng Huang, Peixue Jaing, Ruina Xu. (2021). Exsolution effects in CO<sub>2</sub> huff-n-puff enhanced oil recovery: Water-Oil-CO<sub>2</sub> three phase flow visualization and measurements by micro-PIV in micromodel. *International Journal of Greenhouse Gas Control* 2023. Volume 111, 103445.

<https://doi.org/10.1016/j.ijggc.2021.103445>

Mackay, Eric James (2013). Modelling the injectivity, migration and trapping of CO<sub>2</sub> in carbon capture and storage (CCS), Geological Storage of Carbon Dioxide (CO<sub>2</sub>): Geoscience, Technologies, Environmental Aspects and Legal Frameworks. *Woodhead Publishing Limited 2013*. pp. 45-67, Volume 54.

<https://doi.org/10.1533/9780857097279.1.45>

Mansour, E.M., A.M. Al-Sabagh, S.M. Desouky, F.M. Zawawy, M. Ramzi. (2018). A new estimating method of minimum miscibility pressure as a key parameter in designing CO<sub>2</sub> gas injection process. *Egyptian Journal of Petroleum*. Volume 27, Issue 4. Pages 801-810.

<https://doi.org/10.1016/j.ejpe.2017.12.002>

Mansour, Eman Mohamed Ibrahim. (2022). Carbon Dioxide-Oil Minimum Miscibility Pressure Methods Overview. *Enhanced Oil Recovery selected Topics*.

<https://doi.org/10.5772/intechopen.106637>

Meyer, James. (2007). Summary of Carbon Dioxide Enhanced Oil Recovery (CO<sub>2</sub> EOR) Injection Well Technology. *Background report for the American Petroleum Institute*. Retrieved from

<https://www.api.org/~media/files/ehs/climate-change/summary-carbon-dioxide-enhanced-oil-recovery-well-tech.pdf>

Moghadasi, Ramin, Alireza Rostami and Abdolhossein Hemmati-Srapar deh. (2018). Enhanced Oil Recovery Using CO<sub>2</sub>. *Fundamentals of Enhanced Oil and Gas Recovery from Conventional and Unconventional Reservoirs*. Chapter Three – Enhanced Oil Recovery Using CO<sub>2</sub>, pages 61 – 99.

<https://doi.org/10.1016/B978-0-12-813027-8.00003-5>

Nasa. (2022). Retrieved from

<https://climate.nasa.gov/vital-signs/carbon-dioxide/>

NETL (National Energy Technology Laboratory). (2011). Retrieve from

<https://www.netl.doe.gov/research/coal/energy-systems/gasification/gasificationpedia/eor>

- NETL (National Energy Technology Laboratory). (2010). Carbon Dioxide Enhanced Oil Recovery: Untapped Domestic Energy Supply and Long Term Carbon Storage Solution. Retrieve from [https://www.netl.doe.gov/sites/default/files/netl-file/NETL\\_CO2-EOR-Primer.pdf](https://www.netl.doe.gov/sites/default/files/netl-file/NETL_CO2-EOR-Primer.pdf)
- Nghiem, L., V. Shrivastava, B. Kohse, M. Hassam, C. Yang. (2009). Simulation of Trapping Processes for CO<sub>2</sub> Storage in Saline Aquifers. *Petroleum Society Journal*, PETSOC-2009-156  
[https:// doi.org/10.2118/2009-156](https://doi.org/10.2118/2009-156)
- Nunez-Lopez, Vanessa and Emily Moskal. (2019). Potential of CO<sub>2</sub>-EOR for Near-Term Decarbonization. *Frontiers in Climate*, Vol 1 Article 5.  
<http://doi:10.3389/fclim.2019.00005>
- Nurafiqah Abdullah, Nurul Hasan. (2021). The implementation of Water Alternating (WAG) injection to obtain optimum recovery in Cornea Field, Australia. *Journal of Petroleum Exploration and Production (2021)*. 11:1475-1485.  
<https://doi.org/10.1007/s13202-021-01103-7>
- Pickup, G. E. (2013). CO<sub>2</sub> storage capacity calculation using static and dynamic modelling, *Geological Storage of Carbon Dioxide (CO<sub>2</sub>): Geoscience, Technologies, Environmental Aspects and Legal Frameworks*. Woodhead Publishing Limited.  
[https://doi: 10.1533/9780857097279.1.26](https://doi:10.1533/9780857097279.1.26)
- Sabine, C.L., R.A. Feely. (2013). Carbon Dioxide. *Encyclopedia of Atmospheric Science*, Pages 335-343  
<https://doi.org/10.1016/B0-12-227090-8/00095-6>
- Schlumberger. (2020). ECLIPSE Industry-Reference Reservoir Simulator. Retrieved from <https://www.solfware.slb.com/products/eclipse>
- Thomas, S. (2008). Enhanced Oil Recovery-An Overview. *Oil & Gas Science and Technology*, Vol. 63, No. 1, pp. 9-19  
[https:// doi: 10.2516/ogst:2007060](https://doi:10.2516/ogst:2007060)
- United Nations. (2021). Climate Change. *Glasgow Climate Change Conference (October/November 2021)*. Retrieved from

- <https://unfccc.int/documents/367046>
- United States Environmental Protection Agency (EPA). (2022). Retrieved from <https://www.epa.gov/ghgemissions/global-greenhouse-gas-emissions-data>
- Van der Meer, L.G.H. (Bert), Ferhat Yavuz. (2009). CO<sub>2</sub> storage capacity calculations for the Dutch subsurface. *Energy Procedia*, Volume 1, Issue 1, Pages 2615-2622  
<https://doi.org/10.1016/j.egypro.2009.02.028>
- Verma, Mahendra K. (2015). Fundamentals of Carbon Dioxide-Enhanced Oil Recovery (CO<sub>2</sub>-EOR): A Supporting Document of The Assessment Methodology for Hydrocarbon Recovery Using CO<sub>2</sub>-EOR Associated with Carbon Sequestration. *USGS (2015). Open-File Report 2015–1071*  
<https://doi.org/10.3133/ofr20151071>
- Vishnyakov, Vladimir, Baghir Suleimanov, Ahmad Salmanov and Eldar Zeynalov. (2020). Chapter 10 – Gas flooding. *Primer on Enhanced Oil Recovery 2020*. Pages 95 – 125.  
<https://doi.org/10.1016/B978-0-12-817632-0.00010-4>
- Voormeij, Danae, and George J. Simandl. (2003). Geological and Mineral CO<sub>2</sub> Sequestration Options: A Technical Review. *Geological Fieldwork 2002*, Paper 2003-1  
<https://www.researchgate.net/publication/246314679>
- Whittaker, Steve, Ernie Perkins. (2013). Technical Aspects of CO<sub>2</sub> Enhanced Oil Recovery and Associated Carbon Storage. *GLOBAL CCS INSTITUTE*. Retrieve from <https://www.globalccsinstitute.com/archive/hub/publications/118946/technical-aspects-co2-enhanced-oil-recovery-and-associated-carbon-sto.pdf>
- Yong, Wen Pin, Ahmad Ismail Azahree, Siti Syareena M Ali, Farhana Jaafar Azuddin and Sharadah M Amin. (2019). A New Modelling Approach to Simulate CO<sub>2</sub> Movement and Containment Coupled with Geochemical Reactions and Geomechanical Effects for an Offshore CO<sub>2</sub> Storage in Malaysia. *SPE*, SPE-195432-MS  
<https://doi.org/10.2118/195432-MS>

Zhong, Zhi, Siyan Liu, Timothy R. Carr, Ali Takbiri-Borujeni, Mohammad Kazemi, Qinwen Fu. (2018). Numerical simulation of Water-Alternating-Gas Process for Optimizing EOR and Carbon Storage. *Energy Procedia*, 158:6079-6086  
<https://10.1016/j.egypro.2019.01.50>



## VITA

<b>NAME</b>	Pariwat Wongsriraksa
<b>DATE OF BIRTH</b>	09 Oct 1985
<b>PLACE OF BIRTH</b>	Udonthani
<b>INSTITUTIONS ATTENDED</b>	Department of Electrical and Computer Engineering, Faculty of Engineering, Thammasat university, Bachelor degree (2004 – 2008).
<b>HOME ADDRESS</b>	351/140, Condo Supalai Loft Yaek Fai Chay, Bangkhunsi, Bangkoknoi, Bangkok, Thailand
<b>PUBLICATION</b>	The 5th International Conference on Clean Energy and Electrical Systems held in Tokyo, Japan on April 1-4, 2023.
<b>AWARD RECEIVED</b>	-

